GENETIC AND MECHANISTIC ANALYSES OF TYPE I INTERFERON-DRIVEN LYME ARTHRITIS

by

Jacqueline Kaylah Paquette

A dissertation submitted to the faculty of
The University of Utah
in partial fulfillment of the requirements for the degree of

Doctor of Philosophy

in

Microbiology and Immunology

Department of Pathology

The University of Utah

August 2017

The University of Utah Graduate School

STATEMENT OF DISSERTATION APPROVAL

The dissertation of **Jacqueline Kaylah Paquette**

has been approved by the following supervisory committee members:

Janis J. Weis	, Chair	**05/23/2017** Date Approved
Xiao He	, Member	**05/23/2017** Date Approved
Daniel Leung	, Member	**05/23/2017** Date Approved
Ryan O'Connell	, Member	**05/23/2017** Date Approved
Matthew Williams	, Member	**05/23/2017** Date Approved

and by **Peter E. Jensen**, Chair/Dean of

the Department/College/School of **Pathology**

and by David B. Kieda, Dean of The Graduate School.

ABSTRACT

B6 and C3H mice develop opposite Lyme arthritis phenotypes in response to the same *Borrelia burgdorferi* infection, providing a unique opportunity to use unbiased genetic approaches to identify host genes modulating pathogenic responses. Previously, gene expression profiling in joint tissue revealed a robust type I IFN profile in C3H mice that was formally linked to arthritis severity through IFNAR1 mAb blockade and genetic ablation. Independently, forward genetics identified a QTL, termed *Borrelia burgdorferi* arthritis-associated locus 1 (*Bbaa1*), which regulates Lyme arthritis severity and includes the type I IFN gene cluster. Here, interval specific congenic lines on B6 and C3H backgrounds were generated to mechanistically analyze the role of *Bbaa1* as a regulator of Lyme arthritis severity.

B6 mice congenic for the C3H *Bbaa1* allele (B6.C3-*Bbaa1*) developed more severe Lyme arthritis than parental B6, which was correctable by IFNAR1 mAb blockade. *Bbaa1* also regulated the magnitude of interferon-stimulated gene expression in BMDMs. Extensive analysis on phagocytic uptake, bacterial sensing and trafficking pathways, and IFN-responsive states further established that genes within *Bbaa1* intrinsically control the differential IFN response. B6.C3-*Bbaa1* mice also developed more severe K/B×N serum transfer arthritis through dysregulated type I IFN, establishing shared pathological processes in models of Lyme and rheumatoid arthritis.

Refined, interval specific recombinant congenic lines further highlighted the

contribution of C3H type I IFN genes to Lyme arthritis. Specific mAb blockade identified IFN-β (and not IFN-α) as the proarthritogenic type I IFN in B6.C3-*Bbaa1* mice, and IFN-β was solely responsible for interferon-stimulated gene expression and feed-forward amplification in BMDMs. Reciprocal radiation chimeras between B6.C3-*Bbaa1* and B6 mice illuminated a critical "pass off" in joint tissue, where radiation-sensitive cells initiate arthritis (likely through internalization-dependent initiation of IFN-β) and radiation-resistant joint resident cells choreograph arthritis development through myostatin upregulation. Together, these findings suggest tantalizing new options for therapeutic intervention in Lyme arthritic patients: (1) blockade of IFN-β to only partially suppress the antiviral response, and (2) blockade of myostatin to correct dysregulated inflammation without interfering with conventional inflammatory pathways.

To Andrew and Isabelle

TABLE OF CONTENTS

LIST OF FIGURES

ACKNOWLEDGEMENTS

The work presented in this dissertation would not have been possible without the support of many individuals. First, I would like to thank Dr. Janis Weis for investing in me as a student in her lab. In addition to fostering my scientific development, she continually encouraged me to persevere through graduate school, allowed me to explore postgraduate career options, and accommodated my childcare needs. I will always be grateful for her unwavering commitment to my personal and professional success.

Next, I thank Ying Ma for her endless help with experiments and friendship. It has been a privilege to learn from and work with the legendary Ying, and her camaraderie was critical to my success. Thank you also to Colleen Fisher and Jinze Li for being reliable, motivated lab mates, and for providing critical assistance with various aspects of my project. Dr. John Weis was also a major inspiration to me, and his authenticity and passion for science will always be in my memory.

I would also like to thank the members of my thesis committee: Drs. Xiao He, Daniel Leung, Ryan O'Connell, and Matthew Williams. Each of these brilliant scientists provided thoughtful suggestions and guidance that inspired me and helped shape the direction of this work. And thank you to all of the faculty in the Pathology department for asking stimulating questions during presentations that helped sharpen my critical thinking and communication skills. It has been a blessing to be a part of this elite, collaborative, and friendly community.

Most of all, I am thankful to my husband, Andrew, for being my ultimate supporter, teammate, and best friend. We have had the privilege and challenge of working toward our PhD degrees at the same time, and I could not have asked for a better life partner. We also grew our family during graduate school, and I am thankful to our precious daughter, Isabelle, for continually being a breath of fresh air. It is because of my beloved family, friends, and Savior that I have completed this journey.

CHAPTER 1

INTRODUCTION

Lyme Disease

Lyme disease is a multistage, multisystem inflammatory disorder triggered by infection with a tick-borne bacteria belonging to the genus *Borrelia* (1, 2). Lyme disease is rampant in the United States, Europe, and Asia, specifically in regions amenable to the life cycle of the *Ixodes sps* tick vector (3). The three primary disease-causing species of *Borrelia* are *B. burgdorferi, B. afzelii,* and *B. garnii,* but *B. bavariensis* has also been identified in a small percentage of cases (4–6). *Borrelia burgdorferi* is the only species found in the United States and causes approximately 300,000 cases of Lyme disease each year, making this the most common vector-borne disease in the U.S. (7). Unfortunately, Lyme disease incidence is expected to increase internationally as *Ixodes* populations are rapidly expanding due to many man-made changes to the environment (8). Thus, Lyme disease is a major global public health concern with an urgent need for preventative measures.

Lyme disease begins with a localized dermal infection at the site of the tick bite. Infection with *B. burgdorferi* usually manifests as a painless bulls-eye rash called an erythema migrans (which is diagnostic of infection) accompanied by flu-like symptoms including fever, headache, and fatigue (2, 9). Weeks to months after infection, *B. burgdorferi* disseminates (possibly through the bloodstream, lymphatic system, or direct penetration of tissues (10)) to distal sites of the body, typically the joint synovial fluid, nervous system, or heart (2). Thus, patients with disseminated infection may experience intermittent attacks of arthritis, neuropathies, or carditis, the latter of which can be deadly (7, 9, 11, 12). Early administration of oral antibiotics, including doxycycline, amoxicillin, or cefuroxime azetil, usually promotes a full recovery, while more severe neurological

and cardiac forms of illness require intravenous treatment with ceftriaxone or penicillin and have a worse prognosis (7). A subset of patients experience post-treatment Lyme disease syndrome (PTLDS) with continued fatigue, pain, or joint and muscle aches after antibiotic therapy (7). Although the exact cause of PTLDS is unknown (with hypotheses of infection-induced autoimmunity (13), persistence of nonviable bacterial antigens (14) or drug-tolerant persister cells (15)), long-term antibiotic therapy is clearly not effective (7) and these patients are currently underserved.

Lyme Arthritis

Lyme arthritis is the most common late disease manifestation, affecting up to 60% of untreated patients and persisting in 10% of patients after antibiotic therapy (16, 17). Lyme arthritis is characterized by edema, synovial hyperplasia, and neutrophil infiltration, and usually develops asymmetrically in the knee joint, though multiple joints may be affected throughout the course of infection (16, 18). A spectrum of Lyme arthritis severity exists among patients, ranging from acute-episodic to chronic-persistent (16, 19), and has been broadly attributed to the genetic composition of the host (involving genes of the immune response) as well as the infecting *B. burgdorferi* isolate (involving genes aiding dissemination and immune evasion) (20).

The mouse model of Lyme arthritis has provided invaluable insight into all aspects of the host-pathogen interplay, particularly with regard to the genetic contribution of the host. Mice are reservoir hosts for *B. burgdorferi* infection in the wild (21), and inbred laboratory strains display a reproducible spectrum of arthritis severity in their rear ankle joints, with clinical features similar to human Lyme arthritis (22). Thus, in addition

to the plethora of laboratory tools and reagents available for mouse studies, the inherent genetic differences among mice has allowed the impact of host genes on pathogenic responses to be systematically explored in a natural model of *B. burgdorferi* infection.

Accordingly, Weis *et al.* initiated a forward genetics approach over twenty years ago whereby C3H mice (which develop severe Lyme arthritis) were bred with C57BL/6 (B6) mice (which develop mild Lyme arthritis), and identified six quantitative trait loci (QTL) associated with *Borrelia burgdorferi* arthritis development, termed *Bbaa1-6* (23, 24). Further analysis of the *Bbaa2* mouse congenic line led to the identification of *Gusb* as a novel arthritis susceptibility gene (25) and validated the utility of this rigorous and unbiased approach. Importantly, the Weis group also conducted an unbiased screen using microarray technology to identify gene expression differences in C3H and B6 joint tissue that promote arthritis development (26). This thesis shows that these two independent approaches have converged on the identification of a pathologic type I IFN response, which is further elaborated below.

The Interferon Family

Interferons (IFNs) are a major family of cytokines first identified for their ability to interfere with viral replication (27). IFNs are divided into three classes (type I, II, or III) based on the receptors in which they interact (IFNAR1/2, IFNGR1/2, or IFNLR1/IL-10R2, respectively) (28, 29). Type I IFN is the largest class, consisting of IFN-α, β, ε, κ, ω, or ζ (*aka* limitin) proteins, and is further expanded by numerous IFN-α subtypes (13 in humans and 14 in mice, not including pseudogenes) (30–32). Type II IFN consists of a single IFN-γ protein (33), and type III IFN is represented by four IFN-λ subtypes (29).

Although the IFN classes (as well as members) have distinct upstream triggers, downstream IFN-stimulated gene (ISG) profiles, and may be cell type or tissue-restricted, each plays a vital role in immunomodulation—with balanced regulation being key to their antimicrobial success (29, 33–35).

Pathologic Type I Interferon in Lyme Disease

Soon after the protective role of IFNs was established, their dichotomous ability to promote pathogenesis became evident (28, 33, 36). In the case of *Borrelia burgdorferi* infection, IFN pathogenicity was first suspected when an unbiased microarray analysis identified a preclinical IFN profile in the joint tissue of Lyme arthritis susceptible C3H mice that was absent in Lyme arthritis resistant B6 mice (26). Although the ISGs identified by the microarray could have been induced by type I or II IFNs (26), IFN-γ had already been shown to be dispensable for Lyme arthritis development in C3H mice (37). Thus, the contribution of type I IFN was assessed by IFNAR1 mAb blockade (38) and genetic ablation (39) and revealed a significant (and equivalent) reduction in Lyme arthritis severity in C3H mice, formally linking pathologic production of type I IFN to arthritogenesis. Intriguingly, an independent forward genetics approach also revealed the type I IFN gene cluster in the *Borrelia burgdorferi* arthritis-associated locus 1 (*Bbaa1*), a QTL regulating arthritis severity (23, 24). Further analysis of *Bbaa1* is the subject of Chapters 2 and 3.

The surprising finding that *B. burgdorferi,* an extracellular pathogen, induces type I IFN production in mice has also been observed in humans (40, 41), and multiple studies have been conducted in both human and murine cells in order to better understand the

mechanism of *B. burgdorferi*-triggered IFN-induction. Specifically, *B. burgdorferi* factors capable of inducing a type I IFN profile include the surface lipoprotein OspA, various secreted non-nucleic acid ligands, RNA, linear plasmid 36, and other dissemination factors (42–46). Host pattern recognition receptors (PRRs) involved in IFN-induction in response to *B. burgdorferi* include NOD2 (47), TLR2 (48, 49), TLR8 (in human monocytes) (43, 50), TLR7 and TLR9 (in human peripheral blood mononuclear cells (51) and dendritic cells (44)), and there seems to be a MyD88- and TRIF-independent pathway (52) but details remain to be elucidated. In regard to the initiating cell type, there is a unique requirement for phagocytosis and degradation of *B. burgdorferi* (38, 47, 49, 50). This was corroborated by the finding that $CD45^+$ cells harvested from a naïve mouse joint are capable of generating an IFN profile upon *B. burgdorferi* stimulation, whereas $CD45^-$ cells are only capable of responding to exogenous IFN-β protein (39).

Undoubtedly, IFN-induction in response to *B. burgdorferi* is complex, but the empirical identification of a differential type I IFN response between B6 and C3H mice (26, 38, 39) that was also suggested by forward genetics (23, 24) has provided a unique platform to uncover novel genetic mechanisms of type I IFN regulation.

Pathologic Type I Interferon in Other Diseases

There are additional links between arthritis and type I IFN in other diseases. Specifically, arthritis is a documented side effect of hepatitis C (53) and multiple sclerosis (54) patients treated with type I IFN. Arthritis is also a common symptom of systemic lupus erythematosus patients, who, for still unclear etiological reasons,

aberrantly produce type I IFN (55). And, a subset of rheumatoid arthritis patients, particularly those who fail to respond to TNF-α blockade, display an IFN signature (56) and will require novel treatment strategies (57).

Moreover, a number of viral infections including human immunodeficiency virus (58), hepatitis C virus (59), and persistent lymphocytic choriomeningitis virus (60) induce a type I IFN profile that has been correlated with disease severity. Other bacteria that have been reported to use type I IFN to their advantage include *Listeria monocytogenes, Francisella tularensis,* and *Mycobacterium tuberculosis* (28). Other autoimmune diseases that have been associated with dysregulated type I IFN include Sjögren's syndrome (61), scleroderma (62), type I diabetes (63), and systemic sclerosis (64). Thus, pathologic production of type I IFN is highly relevant to a plethora of human diseases, and insights gleaned from our model may transcend Lyme disease.

Preview of Dissertation Research

This dissertation focuses on examining the role of *Bbaa1* (the QTL that harbors the type I IFN locus (23, 24)) in modulating Lyme arthritis severity. In Chapter 2, we developed *Bbaa1* interval specific congenic lines on the B6 and C3H backgrounds and tested the hypothesis that type I IFN within *Bbaa1* drives Lyme arthritis severity. In Chapter 3, we assessed the specific contributions of IFN-α and IFN-β to Lyme arthritis severity, refined the *Bbaa1* congenic line, and utilized RNA-seq to elucidate the mechanism of *Bbaa1*-directed Lyme arthritis development. In addition to the novel findings presented herein, this work will provide the foundation for uncovering novel genetic mechanisms of type I IFN regulation, with vast potential to impact human

disease.

References

1. Burgdorfer, W., A. Barbour, S. Hayes, J. Benach, E. Grunwaldt, and J. Davis. 1982. Lyme disease- a tick-borne spirochetosis? *Science* 216: 1317–1319.

2. Steere, A. C., J. Coburn, and L. Glickstein. 2004. The emergence of Lyme disease. *J Clin Invest* 113: 1093–1101.

3. Radolf, J. D., M. J. Caimano, B. Stevenson, and L. T. Hu. 2012. Of ticks, mice and men: understanding the dual-host lifestyle of Lyme disease spirochaetes. *Nat Rev Microbiol* 10: 87–99.

4. Margos, G., S. A. Vollmer, M. Cornet, M. Garnier, V. Fingerle, B. Wilske, A. Bormane, L. Vitorino, M. Collares-Pereira, M. Drancourt, and K. Kurtenbach. 2009. A new *Borrelia* species defined by multilocus sequence analysis of housekeeping genes. *Appl Environ Microbiol* 75: 5410–5416.

5. O'Rourke, M., A. Traweger, L. Lusa, D. Stupica, V. Maraspin, P. N. Barrett, F. Strle, and I. Livey. 2013. Quantitative detection of *Borrelia burgdorferi sensu lato* in erythema migrans skin lesions using internally controlled duplex real time PCR. *PLoS One* 8: 1–9.

6. Brandt, F. C., B. Ertas, T. M. Falk, D. Metze, and A. Boer-Auer. 2014. Genotyping of *Borrelia* from formalin-fixed paraffin-embedded skin biopsies of cutaneous borreliosis and tick bite reactions by assays targeting the intergenic spacer region, ospA and ospC genes. *Br J Dermatol* 171: 528–543.

7. CDC (2016) Available from: http://www.cdc.gov. .

8. Hofmeester, T. R., E. C. Coipan, S. E. Wieren, H. H. T. Prins, W. Takken, and H. Sprong. 2016. Few vertebrate species dominate the *Borrelia burgdorferi s.l.* life cycle. *Env Res Lett* 11: 1–16.

9. Hu, L. T. 2012. Lyme disease in the clinic. *Ann Intern Med* 1–16.

10. Hyde, J. A. 2017. *Borrelia burgdorferi* keeps moving and carries on: a review of Borrelial dissemination and invasion. *Front Immunol* 8: 1–16.

11. Yoon, E. C., E. Vail, G. Kleinman, P. a. Lento, S. Li, G. Wang, R. Limberger, and J. T. Fallon. 2015. Lyme disease: a case report of a 17-year-old male with fatal Lyme carditis. *Cardiovasc Pathol* 2–6.

12. Kuehn, B. M. 2013. CDC estimates 300,000 US cases of Lyme disease annually. *JAMA* 310: 1110.

13. Drouin, E. E., R. J. Seward, K. Strle, G. McHugh, K. Katchar, D. Londono, C. Yao, C. E. Costello, and A. C. Steere. 2013. A novel human autoantigen, endothelial cell growth factor, is a target of T and B cell responses in patients with Lyme disease. *Arthritis Rheum* 65: 186–196.

14. Bockenstedt, L. K., J. Mao, E. Hodzic, S. W. Barthold, and D. Fish. 2002. Detection of attenuated, noninfectious spirochetes in *Borrelia burgdorferi* – infected mice after antibiotic treatment. *J Infect Dis* 186: 1430–1437.

15. Sharma, B., A. V. Brown, N. E. Matluck, L. T. Hu, and K. Lewis. 2015. *Borrelia burgdorferi*, the causative agent of Lyme disease, forms drug-tolerant persister cells. *Antimicrob Agents Chemother* 59: 4616–4624.

16. Steere, A. C., and L. Glickstein. 2004. Elucidation of Lyme arthritis. *Nat. Rev. Immunol.* 4: 143–152.

17. 17. Borchers, A., C. Keen, A. Huntley, and M. E. Gershwin. 2015. Lyme disease: a rigorous review of diagnostic criteria and treatment. *J. Autoimmun.* 57: 82–115.

18. Steere, A. C., R. T. Schoen, and E. Taylor. 1987. The clinical evolution of Lyme arthritis. *Ann Intern Med* 107: 725–731.

19. Steere, A. C., and S. M. Angelis. 2006. Therapy for Lyme arthritis, strategies for the treatment of antibiotic-refractory arthritis. *Arthritis Rheum* 54: 3079–3086.

20. Petzke, M., and I. Schwartz. 2015. *Borrelia burgdorferi* pathogenesis and the immune response. *Clin Lab Med* 35: 745–764.

21. Tracey, K. E., and N. Baumgarth. 2017. *Borrelia burgdorferi* manipulates innate and adaptive immunity to establish persistence in rodent reservoir hosts. *Front Immunol* 8: 1–11.

22. Barthold, S. W., D. S. Beck, G. M. Hansen, G. A. Terwilliger, S. The, I. Diseases, N. Jul, S. W. Barthold, D. S. Beck, G. M. Hansen, G. A. Terwilliger, and K. D. Moody. 1990. Lyme borreliosis in selected strains and ages of laboratory mice. *J Infect Dis* 162: 133–138.

23. Weis, J. J., B. A. McCracken, Y. Ma, D. Fairbairn, R. J. Roper, T. B. Morrison, J. H. Weis, J. F. Zachary, R. W. Doerge, and C. Teuscher. 1999. Identification of quantitative trait loci governing arthritis severity and humoral responses in the murine model of Lyme disease. *J Immunol* 162: 948–956.

24. Ma, Y., J. C. Miller, H. Crandall, E. T. Larsen, D. M. Dunn, R. B. Weiss, M.

Subramanian, J. H. Weis, J. F. Zachary, C. Teuscher, and J. J. Weis. 2009. Interval-specific congenic lines reveal quantitative trait loci with penetrant Lyme arthritis phenotypes on chromosomes 5, 11, and 12. *Infect Immun* 77: 3302–3311.

25. Bramwell, K. K. C., Y. Ma, J. H. Weis, X. Chen, J. F. Zachary, C. Teuscher, and J. J. Weis. 2014. Lysosomal β-glucuronidase regulates Lyme and rheumatoid arthritis severity. *J Clin Invest* 124: 311–320.

26. Crandall, H., D. M. Dunn, Y. Ma, R. M. Wooten, J. F. Zachary, J. H. Weis, R. B. Weiss, and J. J. Weis. 2006. Gene expression profiling reveals unique pathways associated with differential severity of Lyme arthritis. *J Immunol* 177: 7930–7942.

27. Isaacs, A., and J. Lindenmann. 1957. Pillars article: Virus interference. I . The interferon. *Proc R Soc L. B Biol Sci* 147: 258–267.

28. Trinchieri, G. 2010. Type I interferon: friend or foe? *J Exp Med* 207: 2053–2063.

29. Lasfar, A., A. Zioza, A. de la Torre, and K. A. Cohen-Solal. 2016. IFN-λ: a new inducer of local immunity against cancer and infections. *Front Immunol* 7: 1–7.

30. Pesch, V. Van, H. Lanaya, J. Renauld, and T. Michiels. 2004. Characterization of the murine alpha interferon gene family. *J Virol* 78: 8219–8228.

31. Oritani, K., and Y. Kanakura. 2005. IFN- ζ/ limitin: a member of type I IFN with mild lympho-myelosuppression. *J Cell Mol Med* 9: 244–254.

32. Moll, H. P., T. Maier, A. Zommer, T. Lavoie, and C. Brostjan. 2010. The differential activity of interferon-α subtypes is consistent among distinct target genes and cell types. *Cytokine* 53: 52–59.

33. Billiau, A., and P. Matthys. 2009. Interferon-γ: a historical perspective. *Cytokine Growth Factor Rev* 20: 97–113.

34. Ivashkiv, L. B., and L. T. Donlin. 2014. Regulation of type I interferon responses. *Nat Rev Immunol* 14: 36–49.

35. Schneider, W. M., M. D. Chevillotte, and C. M. Rice. 2014. Interferon-stimulated genes: a complex web of host defenses. *Annu Rev Immunol* 32: 513–545.

36. Vilcek, J. 2006. Fifty years of interferon research: aiming at a moving target. *Immunity* 25: 343–348.

37. Brown, C. R., and S. L. Reiner. 1999. Experimental Lyme arthritis in the absence of interleukin-4 or gamma interferon. *Infect Immun* 67: 3329–3333.

38. Miller, J. C., Y. Ma, J. Bian, K. C. F. Sheehan, J. F. Zachary, J. H. Weis, R. D.

Schreiber, and J. J. Weis. 2008. A critical role for type I IFN in arthritis development following *Borrelia burgdorferi* infection of mice. *J Immunol* 181: 8492–8503.

39. Lochhead, R. B., F. L. Sonderegger, Y. Ma, E. Brewster, D. Cornwall, H. Maylor-Hagen, J. C. Miller, J. F. Zachary, J. H. Weis, and J. J. Weis. 2012. Endothelial cells and fibroblasts amplify the arthritogenic type I IFN response in murine Lyme disease and are major sources of chemokines in *Borrelia burgdorferi*-infected joint tissue. *J Immunol* 189: 2488–2501.

40. Salazar, J. C., C. D. Pope, T. J. Sellati, H. M. Feder Jr, M. J. Caimano, J. G. Pope, P. J. Krause, and J. D. Radolf. 2003. Coevolution of markers of innate and adaptive immunity in skin and peripheral blood of patients with erythema migrans. *J Immunol* 171: 2660–2670.

41. Jacek, E., B. A. Fallon, A. Chandra, M. K. Crow, G. P. Wormser, and A. Alaedini. 2013. Increased IFNα activity and differential antibody response in patients with a history of Lyme disease and persistent cognitive deficits. *J Neuroimmunol* 255: 85–91.

42. Miller, J. C., H. Maylor-hagen, Y. Ma, H. John, J. J. Weis, J. C. Miller, H. Maylor-hagen, Y. Ma, J. H. Weis, and J. J. Weis. 2010. The Lyme disease spirochete *Borrelia burgdorferi* utilizes multiple ligands, including RNA, for interferon regulatory factor 3-dependent induction of type I interferon-responsive genes. *Infect Immun* 78: 3144–3153.

43. Cervantes, J. L., C. J. La Vake, B. Weinerman, S. Luu, C. O. Connell, P. H. Verardi, and J. C. Salazar. 2013. Human TLR8 is activated upon recognition of *Borrelia burgdorferi* RNA in the phagosome of human monocytes. *J Leukoc Biol* 94: 1231–1241.

44. Love, A. C., I. Schwartz, and M. M. Petzke. 2014. *Borrelia burgdorferi* RNA induces type I and III interferons via toll-like receptor 7 and contributes to production of NF-kB-dependent cytokines. *Infect Immun* 82: 2405–2416.

45. Krupna-Gaylord, M. A., D. Liveris, A. C. Love, G. P. Wormser, I. Schwartz, and M. M. Petzke. 2014. Induction of type I and type III interferons by *Borrelia burgdorferi* correlates with pathogenesis and requires linear plasmid 36. *PLoS One* 9: 1–14.

46. Petzke, M. M., R. Iyer, A. C. Love, Z. Spieler, A. Brooks, and I. Schwartz. 2016. *Borrelia burgdorferi* induces a type I interferon response during early stages of disseminated infection in mice. *BMC Microbiol* 16: 1–13.

47. Petnicki-Ocwieja, T., A. S. Defrancesco, E. Chung, C. T. Darcy, R. T. Bronson, K. S. Kobayashi, and L. T. Hu. 2011. Nod2 suppresses *Borrelia burgdorferi* mediated murine Lyme arthritis and carditis through the induction of tolerance. *PLoS One* 6: 1–13.

48. Salazar, J. C., S. Duhnam-Ems, C. La Vake, A. R. Cruz, M. W. Moore, M. J. Caimano, L. Velez-Climent, J. Shupe, W. Krueger, and J. D. Radolf. 2009. Activation of human monocytes by live *Borrelia burgdorferi* generates TLR2-dependent and independent responses which include induction of IFN-β. *PLoS Pathog* 5: 1–21.

49. Petnicki-Ocwieja, T., E. Chung, D. I. Acosta, L. T. Ramos, O. S. Shin, S. Ghosh, L. Kobzik, X. Li, and L. T. Hu. 2013. TRIF mediates toll-like receptor 2-dependent inflammatory responses to *Borrelia burgdorferi*. *Infect Immun* 81: 402–410.

50. Cervantes, J. L., S. M. Dunham-Ems, C. J. La Vake, M. M. Petzke, B. Sahay, T. J. Sellati, J. D. Radolf, and J. C. Salazar. 2011. Phagosomal signaling by *Borrelia burgdorferi* in human monocytes involves Toll-like receptor (TLR) 2 and TLR8 cooperativity and TLR8-mediated induction of IFN-β. *Proc Natl Acad Sci USA* 108: 3683–3688.

51. Petzke, M. M., A. Brooks, M. A. Krupna, D. Mordue, and I. Schwartz. 2009. Recognition of *Borrelia burgdorferi*, the Lyme disease spirochete, by TLR7 and TLR9 induces a type I IFN response by human immune cells. *J Immunol* 183: 5279–5292.

52. Hastey, C. J., J. Ochoa, K. J. Olsen, S. W. Barthold, and N. Baumgarth. 2014. MyD88- and TRIF-independent induction of type I interferon drives naive B cell accumulation but not loss of lymph node architecture. *Infect Immun* 82: 1548–1558.

53. Wilson, L. E., D. Widman, S. H. Dikman, and P. D. Gorevic. 2002. Autoimmune disease complicating antiviral therapy for hepatitis C virus infection. *Semin Arthritis Rheum* 32: 163–173.

54. Strueby, L., B. Nair, and A. Kirk. 2005. Arthritis and bursitis in multiple sclerosis patients treated with interferon-beta. *Scand J Rheumatol* 34: 485–488.

55. Luo, S., Y. Wang, M. Zhao, and Q. Lu. 2016. The important roles of type I interferon and interferon-inducible genes in systemic lupus erythematosus. *Int J Immunopharmacol* 40: 542–549.

56. van der Pouw Kraan, T. C. T. M., C. A. Wijbrandts, L. G. M. van Baarsen, A. E. Voskuyl, F. Rustenburg, J. M. Baggen, S. M. Ibrahim, M. Fero, B. A. C. Dijkmans, P. P. Tak, and C. L. Verweij. 2007. Rheumatoid arthritis subtypes identified by genomic profiling of peripheral blood cells: assignment of a type I interferon signature in a subpopulation of patients. *Ann Rheum Dis* 66: 1008–1014.

57. Muskardin, T. W., P. Vashisht, J. M. Dorschner, M. A. Jensen, B. S. Chrabot, M. Kern, J. R. Curtis, M. I. Danila, S. S. Co, N. Shadick, P. A. Nigrovic, E. W. St Clair, C. O. Bingham III, R. Furie, W. Robinson, M. Genovese, C. C. Striebich, J. R. O. Dell, G. M. Thiele, L. W. Moreland, M. Levesque, S. L. Bridges Jr, P. K. Gregersen, and T. B. Niewold. 2016. Increased pretreatment serum IFN-β/α ratio predicts non-

response to tumour necrosis factor α inhibition in rheumatoid arthritis. *Ann Rheum Dis* 75: 1757–1762.

58. Hardy, G. A. D., S. Sieg, B. Rodriguez, D. Anthony, R. Asaad, W. Jiang, J. Mudd, T. Schacker, N. T. Funderburg, H. A. Pilch-Cooper, R. Debernardo, R. L. Rabin, M. M. Lederman, and C. V Harding. 2013. Interferon-α is the primary plasma type-I IFN in HIV-1 infection and correlates with immune activation and disease markers. *PLoS One* 8: 1–9.

59. Bolen, C. R., M. D. Robek, L. Brodsky, V. Schulz, J. K. Lim, M. W. Taylor, and S. H. Kleinstein. 2013. The blood transcriptional signature of chronic hepatitis C virus is consistent with an ongoing interferon-mediated antiviral response. *J Interf Cytokine Res* 33: 15–23.

60. Ng, C. T., B. M. Sullivan, J. R. Teijaro, A. M. Lee, M. Welch, S. Rice, K. C. F. Sheehan, R. D. Schreiber, and M. B. A. Oldstone. 2015. Blockade of interferon beta, but not interferon alpha, signaling controls persistent viral infection. *Cell Host Microbe* 17: 653–661.

61. Emamian, E. S., J. M. Leon, C. J. Lessard, M. Grandits, E. C. Baechler, P. M. Gaffney, and B. Segal. 2009. Peripheral blood gene expression profiling in Sjogren's syndrome. *Genes Immun* 10: 285–296.

62. Higgs, B. W., Z. Liu, B. White, W. Zhu, W. I. White, C. Morehouse, P. Brohawn, P. A. Kiener, L. Richman, D. Fiorentino, S. A. Greenberg, B. Jallal, and Y. Yao. 2011. Patients with systemic lupus erythematosus, myositis, rheumatoid arthritis and scleroderma share activation of a common type I interferon pathway. *Ann Rheum Dis* 70: 2029–2036.

63. Ferreira, R. C., H. Guo, R. M. R. Coulson, D. J. Smyth, M. L. Pekalski, O. S. Burren, A. J. Cutler, J. D. Doecke, S. Flint, E. F. Mckinney, P. A. Lyons, K. G. C. Smith, P. Achenbach, A. Beyerlein, D. B. Dunger, D. G. Clayton, L. S. Wicker, J. A. Todd, E. Bonifacio, C. Wallace, and A.-G. Ziegler. 2014. Transcriptional signature precedes autoimmunity in children genetically at risk for type 1 diabetes. *Diabetes* 63: 2538–2550.

64. Guo, X., B. W. Higgs, A. C. Bay-jensen, M. A. Karsdal, Y. Yao, L. K. Roskos, and W. I. White. 2015. Suppression of T cell activation and collagen accumulation by an anti-IFNAR1 mAb, anifrolumab, in adult patients with systemic sclerosis. *J Invest Dermatol* 135: 2402–2409.

CHAPTER 2

BORRELIA BURGDORFERI ARTHRITIS-ASSOCIATED LOCUS *BBAA1* REGULATES LYME ARTHRITIS AND K/B×N SERUM TRANSFER ARTHRITIS THROUGH INTRINSIC CONTROL OF TYPE I IFN PRODUCTION

Originally published in *The Journal of Immunology*. Ying Ma, Kenneth K.C. Bramwell, Robert B. Lochhead, Jackie K. Paquette, James F. Zachary, John H. Weis, Cory Teuscher and Janis J. Weis. 2014. *Borrelia burgdorferi* Arthritis-Associated Locus *Bbaa1* Regulates Lyme Arthritis and K/B×N Serum Transfer Arthritis through Intrinsic Control of Type I IFN Production. *J Immunol* 193:6050-6060.

The Journal of Immunology

Borrelia burgdorferi Arthritis–Associated Locus *Bbaa1* Regulates Lyme Arthritis and K/B×N Serum Transfer Arthritis through Intrinsic Control of Type I IFN Production

Ying Ma,* Kenneth K. C. Bramwell,* Robert B. Lochhead,* Jackie K. Paquette,* James F. Zachary,† John H. Weis,* Cory Teuscher,‡ and Janis J. Weis*

Localized upregulation of type I IFN was previously implicated in development of *Borrelia burgdorferi*–induced arthritis in C3H mice, and was remarkable due to its absence in the mildly arthritic C57BL/6 (B6) mice. Independently, forward genetics analysis identified a quantitative trait locus on Chr4, termed *B. burgdorferi*–associated locus 1 (*Bbaa1*), that regulates Lyme arthritis severity and includes the 15 type I IFN genes. Involvement of *Bbaa1* in arthritis development was confirmed in B6 mice congenic for the C3H allele of *Bbaa1* (B6.C3-*Bbaa1*), which developed more severe Lyme arthritis and K/B×N model of rheumatoid arthritis (RA) than did parental B6 mice. Administration of a type I IFN receptor blocking mAb reduced the severity of both Lyme arthritis and RA in B6.C3-*Bbaa1* mice, formally linking genetic elements within *Bbaa1* to pathological production of type I IFN. Bone marrow–derived macrophages from *Bbaa1* congenic mice implicated this locus as a regulator of type I IFN induction and downstream target gene expression. *Bbaa1*-mediated regulation of IFN-inducible genes was upstream of IFN receptor–dependent amplification; however, the overall magnitude of the response was dependent on autocrine/paracrine responses to IFN-β. In addition, the *Bbaa1* locus modulated the functional phenotype ascribed to bone marrow–derived macrophages: the B6 allele promoted expression of M2 markers, whereas the C3H allele promoted induction of M1 responses. This report identifies a genetic locus physically and functionally linked to type I IFN that contributes to the pathogenesis of both Lyme and RA. *The Journal of Immunology*, 2014, 193: 6050–6060.

Lyme disease is caused by infection with the tick-borne spirochete, *Borrelia burgdorferi*, and is associated with a spectrum of disease symptoms and severity (1, 2). A localized skin lesion at the site of the tick bite is found in 70% of infected individuals, and can progress to disseminated infection resulting in skin lesions, peripheral neuropathies, inflammation of the CNS, carditis, and accompanying fatigue (3). Arthritis occurs in 30–60% of patients and is often identified by effusive swelling and tendonitis in the knee (4). The variability in clinical symptoms reflects a number of factors including invasive potential of the infecting genotype of *B. burgdorferi* and inherent variances in the host response to infection (5, 6). Patient studies have identified multiple components of the innate and adaptive immune response that contribute to host defense, disease resolution, and arthritis pathogenesis (7–14). Much of the analysis of the varied spectrum of disease in patients has focused on a comparison between those whose disease resolves readily after antibiotic treatment and those whose symptoms persist for months after treatment, and suggests that failure to suppress the inflammatory response and/or initiation of an autoimmune response are important in chronic disease (15, 16).

Barthold et al. (6) made the seminal observation that different inbred strains of mice consistently display a spectrum of disease severity postinfection with *B. burgdorferi*, thus demonstrating host factors inherent to different strains of mice are major determinants of Lyme arthritis severity. Two mouse strains, C57BL/6 (B6) and C3H, display extremes of arthritis severity and have been used extensively as experimental models for study of disease. These studies have revealed involvement of numerous components of the inflammatory response to *B. burgdorferi* in the development and resolution of Lyme arthritis, similar to those implicated in human disease (17). Previously, using global gene expression analysis, we identified an IFN signature response in the joint tissue of *B. burgdorferi*–infected C3H mice that preceded the development of severe arthritis and was absent from mildly arthritic B6 mice (18). Blocking the type I IFN receptor (IFNAR1), either with a neutralizing mAb or by gene ablation, reduced the severity of arthritis in C3H mice, formally linking type I IFN to Lyme arthritis (19, 20). Numerous investigators have studied the type I IFN response to *B. burgdorferi* in murine and human myeloid cells, and identified pathogen receptor signaling pathways involved in this response (21–25). Pathological production of type I IFN has also been implicated in a number of inflammatory conditions, suggesting a predisposition to IFN production could be a common contributor to inflammatory disease (26–29).

*Division of Microbiology and Immunology, Department of Pathology, University of Utah, Salt Lake City, UT 84112; †Department of Veterinary Pathobiology, University of Illinois at Urbana-Champaign, Urbana, IL 61802; and ‡Department of Medicine, University of Vermont, Burlington, VT 05405

Received for publication July 10, 2014. Accepted for publication October 15, 2014.

This work was supported by National Institutes of Health/National Institute of Allergy and Infectious Disease Grants T32AI055434 (to R.B.L. and K.K.C.B.) and AI32223 (to J.J.W.), National Institutes of Health/National Institute of Arthritis and Musculoskeletal and Skin Diseases Grant AR43521 (to C.T. and J.J.W.), and Arthritis Foundation Grant 6133 (to K.K.C.B.). The DNA/Peptide Core is supported by Cancer Center Support Grant P30 CA04201.

The content is solely the responsibility of the authors and does not necessarily represent the official views of the National Institutes of Health. This article is subject to the National Institutes of Health Public Access Policy.

Address correspondence and reprint requests to Dr. Janis J. Weis, Department of Pathology, Division of Microbiology and Immunology, University of Utah, 15 North Medical Drive, Salt Lake City, UT 84112. E-mail address: janis.weis@path.utah.edu

Abbreviations used in this article: B6, C57BL/6; *Bbaa*, *Borrelia burgdorferi*–associated locus; BMDM, bone marrow–derived macrophage; BSK, Barbour–Stoenner–Kelly medium; IFNAR1, type I IFN receptor; ISCL, interval-specific congenic line; poly(I:C), polyinosinic-polycytidylic acid; QTL, quantitative trait locus; RA, rheumatoid arthritis.

www.jimmunol.org/cgi/doi/10.4049/jimmunol.1401746

We have also used forward genetic analysis to identify quantitative trait loci (QTLs) controlling the difference in Lyme arthritis severity in B6 and C3H mice. This approach led to the identification of 23 *B. burgdorferi*–associated loci (*Bbaa*) regulating responses to *B. burgdorferi* infection and included six *Bbaa* regulating arthritis severity (30–32). We have recently validated the utility of this rigorous and unbiased approach with the positional cloning of β-glucuronidase, *Gusb*, within *Bbaa2* on Chr5, as a major determinant of Lyme arthritis severity in mice (33). *Gusb* also regulates the severity of rheumatoid arthritis (RA) in mice. In this study, we have extended our analysis of *Bbaa1* on Chr4 and have identified the type I IFN gene cluster (IFN-β and 14 IFN-α genes, 88.5–88.7 Mbp) as positional candidates for *Bbaa1* (34). The development of interval-specific congenic lines (ISCL) on the B6 and C3H backgrounds allowed direct assessment of the contribution of *Bbaa1* to Lyme arthritis and RA, and the dependence on production of type I IFN. The studies reported in this article identify *Bbaa1* as a regulator of type I IFN during both Lyme arthritis and RA development, thus indicating a second example of QTL analysis of Lyme arthritis providing novel insight to other models of inflammatory arthritis. These findings suggest type I IFN as a tractable target for therapeutic intervention in Lyme and RA, and other syndromes associated with IFN dysregulation.

Materials and Methods

Mice

C3H/HeNCrl mice were obtained from Charles River Breeding laboratories. C57BL/6NCr (B6) mice from the National Cancer Institute were maintained as a colony in our Animal Research Center. Reciprocal ISCL for *Bbaa1* on Chr4 were generated on both B6 and C3H backgrounds as described previously (32) and are indicated as B6.C3-*Bbaa1* (9.32–94.97 Mbp) and C3.B6-*Bbaa1* (3.58–150.8 Mbp) with introgressed region of Chr4 indicated in parentheses. B6-IFNAR1$^{-/-}$ mice were provided by Dr. Murali-Krisna Kaja (University of Washington, Seattle, WA) and backcrossed to C3H to generate C3H-IFNAR1$^{-/-}$ mice as described previously (19). All mice were housed in the University of Utah Animal Research Center (Salt Lake City, UT) and followed protocols approved by the institutional review committee for the care and use of mice in biomedical research.

Bacterial cultures and infections, and assessment of arthritis severity

A low-passage clonal derivative of *B. burgdorferi* strain N40 was stored at −80°C and cultured 4–5 d in Barbour–Stoenner–Kelly medium (BSK) before infection experiments. Mice were infected with 2×10^4 spirochetes by intradermal injection into the skin of the back (35). Ankle measurements were obtained using a metric caliper before and at 4 wk of infection. Rear ankle joints were prepared for assessment of histopathology by removal of skin and fixation of the tissue in 10% neutral-buffered formalin as described previously (19). Decalcified joints were embedded in paraffin, sectioned at 3 μm, and stained with H&E. Coded slides were scored from 0 to 5 for various aspects of disease, including severity and extent of the lesion, PMN leukocyte and mononuclear cell (e.g., monocyte, macrophage) infiltration, tendon sheath thickening (e.g., synoviocyte and fibroblast hyperplasia), and reactive/reparative responses (e.g., periosteal hyperplasia and new bone formation and remodeling), with 5 representing the most severe lesion and 0 representing no lesion. Infection was confirmed in mice euthanized before 14 d postinfection by culturing bladder tissue in BSK II media containing 6% rabbit serum, phosphomycin, and rifampicin. ELISA quantification of *B. burgdorferi*–specific IgM and IgG concentrations were used to confirm infection in mice euthanized at and after 14 d postinfection as described previously (36).

In vivo blocking of IFNAR1

The IFNAR1 blocking mAb MAR1-5A3 or isotype control (Bio-XCell) was administered by a single i.p. injection of 2.5 mg mAb the day before infection with *B. burgdorferi* or the administration of K/B×N serum (Figs. 2, 9) (20, 37).

K/B×N serum transfer model of RA

K/B×N serum was collected from KRN×NOD offspring at the peak of spontaneous arthritis (9 wk), as described previously (38). K/B×N serum (100 μl) was administered by i.p. injection on days 0 and 2 (33, 39). Rear ankle measurements were made before serum transfer on day 0, and on days 1, 2, 4, and 7. At day 7, joints were removed for histopathological assessment of arthritis, as described for Lyme arthritis.

Isolation of RNA and quantitative RT-PCR

For all experiments examining gene expression in joint tissue, mice were killed, and the skin was removed from the tibiotarsal joints. Ankle joints were excised, immersed in RNA Later (Qiagen), and stored at −80°C. Total RNA was recovered from homogenized tissue using TRIzol reagent (Invitrogen) (19). RNA recovered from tissue and cells was reverse transcribed, and transcripts were quantified using a Roche LC-480 according to our previously described protocols (32). Primer sequences used in this study for *β-actin*, *Igtp*, *Iigp*, *Stat1*, *Nos2*, *Arg* (18), *Cxcl9*, *Cxcl10*, *Oasl2*, *Tyki* (20), *Gbp2* (25), *Tnfα*, *Ifnβ* (40), *IL-10* (41), and *Mrc1* (42) can be found in the indicated citations. Primers for *Stat2* were: *Stat2* forward (5′-GCTTCCTCTATCCCCGAATC-3′) and reverse (5′-ATCAATGG-CAACTCCTGGTC-3′).

Cell culture

Bone marrow–derived macrophages (BMDMs) were isolated from the femurs and tibias of mice that were cultured for 7 d in L929-cell conditioned media as a source of M-CSF, as previously described (43). Macrophage cultures were plated in 12-well dishes at a density of 7.5×10^5/ml in media containing the serum replacement Nutridoma (Roche) and stimulated with live *B. burgdorferi* cN40 (7.4×10^6/ml), sonicated *B. burgdorferi* (5 μg/ml) (40), or polyinosinic-polycytidylic acid [poly(I:C)] (10 ng/ml; Sigma-Aldrich). Macrophage cultures were stimulated at 37°C, 5% CO_2, and harvested either at 1, 3, or 6 h for RNA extraction, as indicated. IFN-β (PBL Laboratories) was added at the indicated concentrations.

Phagocytosis assay

Peritoneal macrophages were harvested 4 d after i.p. administration of 3 ml 3% sterile thioglycolate. Macrophages were collected with ice-cold PBS, and RBCs were lysed with ACK lysis buffer. Cells in RPMI 1640 10% FBS were plated at 5×10^5/well in 12-well plate and allowed to adhere overnight, when nonadherent cells were removed by washing. *B. burgdorferi* N40-expressing GFP were added to the macrophages in RPMU.B (75% RPMI 1640 + 10% FBS + 24% BSK II) at a 50:1 ratio (44, 45). Plates were centrifuged at 500 × *g* for 5 min and incubated for 1 or 2 h at 37°C, conditions previously shown to capture midway and maximal phagocytosis (46). Wells were washed to remove unassociated bacteria. Cells from one set of replicate wells were collected with a cell scraper and represented total cell-associated bacteria. A second set of replicate cells was incubated with 0.25% trypsin in RPMI 1640 for 7 min at 37°C to release extracellular bacteria from the macrophages before collecting, and are referred to as trypsin resistant (47). Cells collected in both manners were washed three times in cold PBS, suspended in flow buffer, and analyzed using a BD LSRII flow cytometer. Baseline fluorescence was determined for cells not receiving GFP *B. burgdorferi* in each treatment group.

Data and statistical analyses

All graphical data represent the mean ± SEM. Statistical analysis was performed using Prism 5.0c software. Multiple-sample data sets were analyzed by one-way ANOVA with appropriate post hoc test as indicated: Bonferroni (Figs. 3, 4, 7, 9, Table I). Two-sample data sets were analyzed by Student *t* test (Figs. 1, 2, 6, 8). Categorical data for histopathology were assessed by the Mann–Whitney *U* test (Figs. 1, 2, 8, 9) or Kruskal–Wallis test with Dunn's multiple comparison (Fig. 9). Statistical significance ($*p < 0.05$, $**p < 0.01$, $***p < 0.001$, $****p < 0.0001$) is indicated.

Results

C3H allele of Bbaa1 *confers increased arthritis severity when transferred to B6 mice*

Our previous studies revealed a major, differential contribution of type I IFN to the development of Lyme arthritis in C3H mice, which could be overcome by blocking the IFNAR1 signaling with neutralizing mAb or by gene ablation (19, 20). We also noted that *Bbaa1*, a QTL controlling the severity of Lyme arthritis on Chr4, encompassed a cluster of 15 type I IFN genes, prompting a more mechanistic analysis of the role of *Bbaa1* as a regulator of Lyme arthritis severity (30, 32).

To assess the impact of *Bbaa1* on Lyme arthritis severity, we developed reciprocal ISCL in which *Bbaa1* was introgressed onto each background. B6 mice possessing C3H *Bbaa1* (B6.C3-*Bbaa1*) displayed more severe Lyme arthritis than B6 mice at 4 wk of infection with *B. burgdorferi*, as assessed by ankle swelling and histopathology (Fig. 1A, 1B). Importantly, arthritis in B6.C3-*Bbaa1* mice was intermediate between that of the B6 and C3H parental strains, consistent with the presence of multiple other QTLs that were not transferred to the B6 background in the *Bbaa1* congenic. Notably, the reciprocal transfer of the B6 allele of *Bbaa1* onto the C3H background (C3.B6-*Bbaa1*) did not result in a reduction in *B. burgdorferi*–induced arthritis severity when compared with the infected C3H parent. This may reflect the presence of allelic loci outside of *Bbaa1* that mask its impact, and is consistent with the identification of *Bbaa1* with the (B6×C3)F_2 intercross, but not with the (B6×C3)F_1 crossed to either B6 or C3H parent (30).

*Effect of blocking IFNAR1 on Lyme arthritis in B6.C3-*Bbaa1 *mice*

The results from Fig. 1 demonstrated that *Bbaa1* regulates arthritis severity on the B6 background. Although the B6.C3-*Bbaa1* congenic interval is large (9.32–94.97 Mbp) and encodes numerous genes, it nevertheless encompasses the IFN-α/β cluster (88.5–88.7 Mbp) that encodes type I IFNs implicated in Lyme arthritis (19, 20, 34). All IFN-α and IFN-β proteins signal through the IFNAR, composed of IFNAR1 and IFNAR2 chains (48, 49). To determine whether the greater arthritis in B6.C3-*Bbaa1* mice relative to B6 mice was dependent on type I IFN, we treated B6.C3-*Bbaa1* mice with a blocking mAb to IFNAR1 component of the IFNAR1 (MAR1-5A3) 1 d before infection (20). B6.C3-*Bbaa1* mice treated with isotype control mAb developed more severe Lyme arthritis than B6 mice as assessed by ankle measurement and lesion scoring (Fig. 2), similar to the results of Fig. 1. Administration of the receptor-blocking mAb reduced arthritis severity to levels indistinguishable from wild type B6 (Fig. 2). Thus, the increased arthritis severity of B6.C3-*Bbaa1* mice is a function of type I IFN responses dependent on feed-forward amplification through the IFNAR1 and identify the IFN-αβ cluster as a positional candidate for *Bbaa1*.

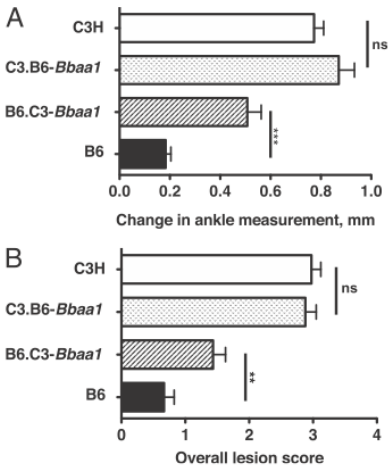

FIGURE 1. Interval-specific congenic mice reveal contribution of C3H allele of *Bbaa1* to Lyme arthritis severity. B6, C3H, B6.C3-*Bbaa1*, and C3.B6-*Bbaa1* mice were infected with 2×10^4 *B. burgdorferi*, and arthritis was assessed at 4 wk of infection, as described in *Materials and Methods* and shown for (**A**) change in ankle measurement and (**B**) overall lesion score. Statistical significance of differences between ISCL and background parental strain were determined by Student *t* test for ankle swelling and Mann–Whitney *U* test for overall lesion. All categories were negative for uninfected mice, injected with BSK media, and are not shown in the figure. Groups consisted of approximately equal numbers of male and female mice, with $n = 22$ B6, 20 C3H, 23 B6.C3-*Bbaa1*, and 30 C3.B6-*Bbaa1*. $^{**}p < 0.01$, $^{***}p < 0.001$.

Magnitude of the type I IFN response in joint tissue is partially regulated by Bbaa1

As previously reported, joint tissue of *B. burgdorferi*–infected C3H mice revealed a strong IFN signature at 1 wk of infection that was absent in B6 mice (18). Tissue from B6.C3-*Bbaa1* also displayed an elevation in several of the transcripts previously characterized as upregulated only in C3H mice (Table I). Interestingly, the magnitude of transcriptional upregulation of the relatively long-lived chemokines *Cxcl9* and *Cxcl10* approached the magnitude seen in C3H joint tissue (Table I). Because these and other chemokines directly participate in recruitment of inflammatory cells to the joint, their upregulation is highly relevant to arthritis (50, 51). These results are consistent with the combined contribution of *Bbaa1* and additional *Bbaa* to the complete IFN transcriptional profile seen C3H mice. Importantly, the biological significance of the portion of the IFN response regulated by *Bbaa1* was demonstrated by the impact of receptor-blocking mAb on arthritis development in infected B6.C3-*Bbaa1* mice (Fig. 2).

Bbaa1-*dependent regulation of type I IFN activation revealed in BMDMs*

Previously, ex vivo analysis of cells from the joint tissue of uninfected C3H mice identified myeloid cells as the likely initiators

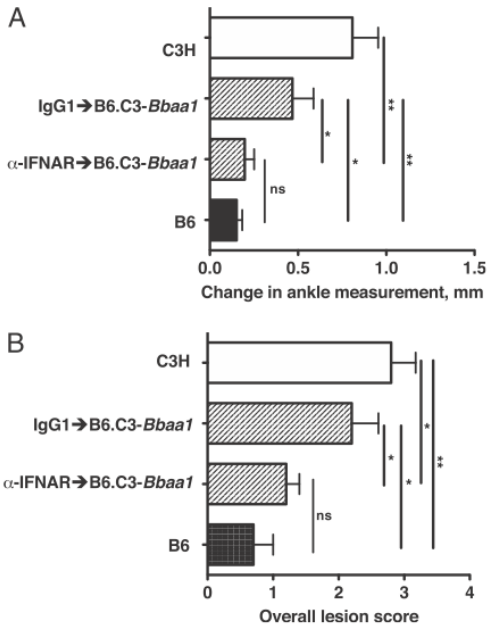

FIGURE 2. mAb blocking of type I IFN signaling prevents the *Bbaa1*-dependent increase in arthritis in *B. burgdorferi*–infected mice. B6.C3-*Bbaa1* mice were treated with 2.5 mg MAR1-5A3 blocking mAb or isotype control the day before infection. Congenic and parental B6 and C3H mice were infected with *B. burgdorferi*, and arthritis severity was analyzed at 4 wk of infection, shown for (**A**) change in ankle measurement and (**B**) overall lesion score. Statistical significance was determined by Student *t* test for ankle swelling, whereas the Mann–Whitney *U* test was used for overall lesion. $n = 5$ per group. $^{*}p < 0.05$, $^{**}p < 0.01$.

Table I. Upregulation of IFN-inducible genes in joint tissue of *B. burgdorferi*–infected B6.C3-*Bbaa1* mice at 1 wk of infection

	Gbp2	*Igtp*	*Cxcl10*	*Iigp*	*Cxcl9*
B6 (mean ± SE)	1.21 ± 0.12[a]	0.92 ± 0.06	1.58 ± 0.30	1.44 ± 0.09	1.27 ± 0.11
B6.C3-*Bbaa1* (mean ± SE)	**2.28 ± 0.29**	**1.44 ± 0.15**	**4.93 ± 0.92**	**3.04 ± 0.36**	**4.33 ± 0.78**
C3H/HeN (mean ± SE)	5.06 ± 0.36	8.48 ± 1.32	9.86 ± 1.71	9.38 ± 0.74	3.8 ± 0.48

Boldface indicates values in B6.C3-*Bbaa1* mice significantly greater than in B6 mice.
[a]Transcript levels were determined in samples collected at 1 wk postinfection, normalized to *β-actin*, and reported as fold-change relative to uninfected controls.

of *B. burgdorferi*–induced IFN production (19). Myeloid cells are present at relatively low levels in the joint tissue and are difficult to recover; therefore, BMDMs were used as a pure population to assess the impact of the *Bbaa1* locus on IFN induction and signature response, further using the *Bbaa1* ISCLs. BMDMs were generated from 6- to 8-wk-old B6, C3H, and the two *Bbaa1* ISCLs by culture of bone marrow cells for 6 d in the presence of M-CSF. Transcriptional responses of BMDMs were analyzed at 6 h after addition of living or sonicated *B. burgdorferi* or media control. As reported previously, macrophages from C3H mice displayed a higher level of transcriptional induction of IFN-β and numerous IFN-inducible transcripts than did macrophages from B6 mice (20, 25, 32). B6.C3-*Bbaa1* macrophages displayed elevated transcriptional responses, similar to those seen in C3H macrophages and consistent with *Bbaa1* regulation of the IFN responses (Fig. 3). The IFN transcriptional response of C3.B6-*Bbaa1* macrophages was greatly reduced relative to C3H macrophages, consistent with a reduced induction of type I IFN when the B6-*Bbaa1* allele was present. Sonicated *B. burgdorferi* elicited responses similar to living *B. burgdorferi*, indicating that ligands only present in viable organisms were not responsible for the differential magnitude.

This finding supports a major regulatory role for C3-*Bbaa1* in regulating type I IFN responses in B6.C3-*Bbaa1* myeloid lineage cells, which translates to the arthritis exacerbating effect also seen in B6.C3-*Bbaa1*. The reciprocal situation is somewhat confounding, in that the suppressive effect of B6-*Bbaa1* on IFN responses was readily demonstrated in highly purified BMDMs from C3.B6-*Bbaa1* mice (Fig. 3) but did not translate to reduced severity of Lyme arthritis (Fig. 1). This suggests that distinct pathways play a major role in arthritis development in C3H mice, and may overwhelm the impact of myeloid-produced type I IFN in the complex context of the joint tissue. Consistent with this is the less stringent control of expression of the NF-κB–dependent cytokine *TNFα*, a component of an important distinct signaling pathway (Fig. 3).

One interpretation of the findings of Fig. 3 was that *Bbaa1* encoded a sensor for *B. burgdorferi* that was responsible for the range in magnitude of the IFN response. Alternatively, the effect of *Bbaa1* could be dependent on a component of phagocytic recognition or internalization necessary for degradation/trafficking of *B. burgdorferi* that has been linked to macrophage initiation of IFN responses to this organism (21, 52, 53). Peritoneal macrophages from B6 and C3H mice were used to assess the impact of *Bbaa1* on the uptake of GFP-expressing *B. burgdorferi* at 1- and 2-h incubation, times previously determined to capture intermediate and maximal phagocytosis (46). Trypsin treatment was used to release adherent extracellular bacteria and allow estimation of those that had been incorporated into an intracellular compartment. Macrophages from C3H mice displayed somewhat greater association and phagocytosis of *B. burgdorferi* than those from B6 mice at 1 h, but by 2 h both cell-associated and trypsin-resistant

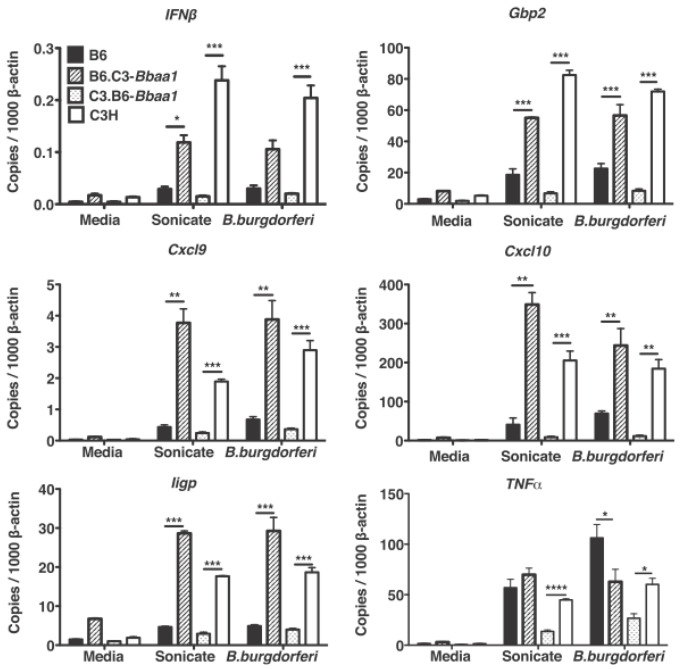

FIGURE 3. BMDMs reveal *Bbaa1* regulates the magnitude of the IFN response to *B. burgdorferi*. RT-PCR analysis of transcripts in BMDMs from B6, C3H, B6.C3-*Bba1*, and C3.B6-*Bbaa1* mice treated with media, sonicated *B. burgdorferi* (sonicate), or living *B. burgdorferi* (*B. burgdorferi*) for 6 h. Transcript levels for *Ifnβ*, *Gbp2*, *Cxcl9*, *Cxcl10*, *Iigp*, and *Tnfα* were normalized to β-actin. Data are averages ± SE, with trends representative of five separate experiments. Significance determined by ANOVA, with Bonferroni post hoc comparison, shown for ISCLs with appropriate background parental strain. Differences between B6 and C3H for *Ifnβ*, *Gbp2*, *Cxcl9*, *Cxcl10*, and *Iigp* were also significant (data not shown). $*p < 0.05$, $**p < 0.01$, $***p < 0.001$, $****p < 0.0001$.

bacteria were equivalent, arguing that the dramatic difference in magnitude of the IFN response at 6 h was not reflective of major differences in phagocytic capacity (Fig. 4).

To test the generality of *Bbaa1* alleles on IFN induction, we assessed the TLR3 ligand poly(I:C), a surrogate for double-stranded viral RNA. In fact, the relative induction of IFN-β and downstream transcripts in B6, C3H, and *Bbaa1* congenic macrophages revealed a pattern for poly(I:C) similar to that observed with *B. burgdorferi* (Fig. 5). This argues that the impact of alleles of *Bbaa1* on IFN dysregulation is not limited to a particular bacterial sensor or to a bacterial-specific trafficking pathway. Rather, the hyperinduction of type I IFN associated with the C3H allele of *Bbaa1* is an inherent property of this locus and is not unique to the responses to *B. burgdorferi* and Lyme arthritis.

Are macrophages from C3H mice "primed" for the type I IFN response?

The heightened IFN signature response of C3H and B6.C3-*Bbaa1* macrophages suggested that the C3H allele of *Bbaa1* promotes transcriptional priming of macrophage responses to *B. burgdorferi* or other stimuli. To interrogate the initial response to *B. burgdorferi*, dissociated from the receptor-dependent feed-forward stage, we treated BMDMs from C3H and B6 mice deficient in the IFNAR1 gene with *B. burgdorferi* or poly(I:C) and assessed for elevation in transcripts. None of the IFN-inducible transcripts was elevated in resting BMDMs from IFNAR1$^{-/-}$ mice on either background, and none of the IFN-inducible transcripts was up-regulated after treatment with *B. burgdorferi* or poly(I:C) (Fig. 6). Thus, responses to *B. burgdorferi* were dependent on autocrine release of type I IFN and amplification through the IFNAR1. This was true even for very early transcriptional responses reported to be independent of feed-forward engagement in the response to

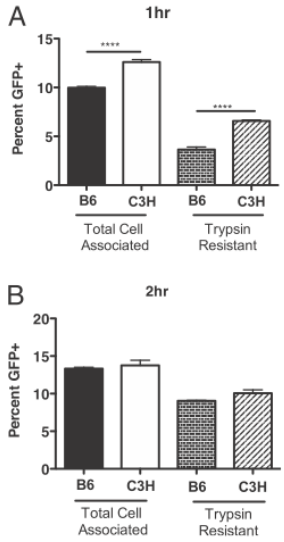

FIGURE 4. Phagocytic capacity of macrophages from B6 and C3H mice. Peritoneal macrophages (5×10^5) were incubated with GFP-*B. burgdorferi* for 1 (**A**) and 2 h (**B**) at 37°C. Cells collected in the absence of trypsin (total cell associated) or after incubation with trypsin (trypsin resistant) to remove extracellular bacteria. The percentage of macrophages with associated bacteria was determined by flow cytometry, as compared with cells not receiving bacteria. Data are averages ± SE and are representative of two separate experiments. Significance was determined by ANOVA, with Bonferroni post hoc comparison, for B6 versus C3H in each treatment group. ****$p < 0.0001$.

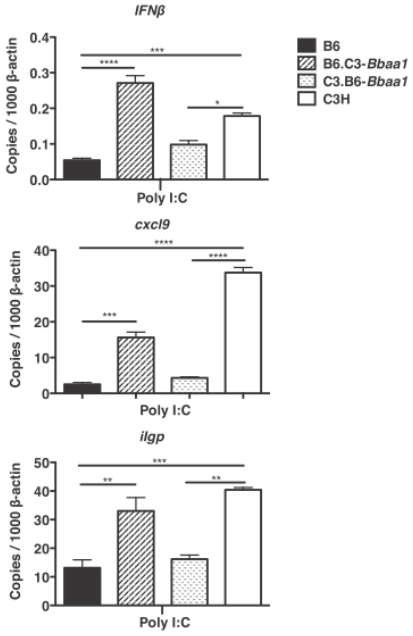

FIGURE 5. *Bbaa1* regulates BMDM responses to poly(I:C). RT-PCR analysis of transcript induction in BMDMs from B6, C3H, B6-C3.*Bba1*, and C3.B6-*Bbaa1* mice treated with poly(I:C) for 6 h. Transcript levels for *Ifnβ*, *Gbp2*, and *Iigp* were normalized to β-actin. Data are averages ± SE, with trends representative of two separate experiments. Significance determined by ANOVA, with Bonferroni post hoc comparison; shown for ISCLs with appropriate background parental strain and for B6 versus C3H. *$p < 0.05$, **$p < 0.01$, ***$p < 0.001$, ****$p < 0.0001$.

certain intracellular bacterial pathogens (*Stat1*, *Stat2*, *Tyki*) (54) (Fig. 6). These transcripts were also not detectable at 1 h of stimulation (data not shown). Thus, the manifestation of hyperactivation of type I IFN is dependent on a functioning IFN receptor. *B. burgdorferi* induction of TNF-α and IL-10 was not influenced by the absence of IFNAR1, consistent with the known dependence of these cytokines on NF-κB–mediated responses to the spirochete and confirming the fidelity of NF-κB pathway in IFNAR1$^{-/-}$ BMDMs. Interestingly, poly(I:C) induction of IL-10 was dependent on IFNAR1 signaling, whereas poly(I:C) induction of TNF-α was too low to determine the impact of receptor deletion (Fig. 6).

We considered the possibility that BMDMs from C3H mice and B6.C3-*Bbaa1* mice were poised to respond to type I IFN by expressing a higher resting level of the IFN receptor–associated signal transducers and activators of transcription family members *Stat1* and *Stat2*, relative to B6 and C3.B6-*Bbaa1* BMDMs (55). In fact, resting levels of *Stat1* and *Stat2* transcripts were similar in all four genotypes of BMDMs, therefore not supporting a C3H-*Bbaa1*–dependent poised state (Fig. 6 and data not shown). The resting levels of the transcription factor IRF3, upstream of IFN initiation, were also similar in all four BMDM genotypes, as were the extremely low levels of the inducible transcription factor IRF7 (data not shown) (56, 57). Additional experiments also failed to reveal increased presence of STAT1 protein or phosphorylated STAT1 in resting C3H or B6.C3-*Bbaa1* BMDMs (data not shown).

The results of Fig. 6 demonstrated that *Bbaa1* regulation of IFN-inducible transcripts by *B. burgdorferi* and poly(I:C) was only observable in the later stage of induction, after autocrine/

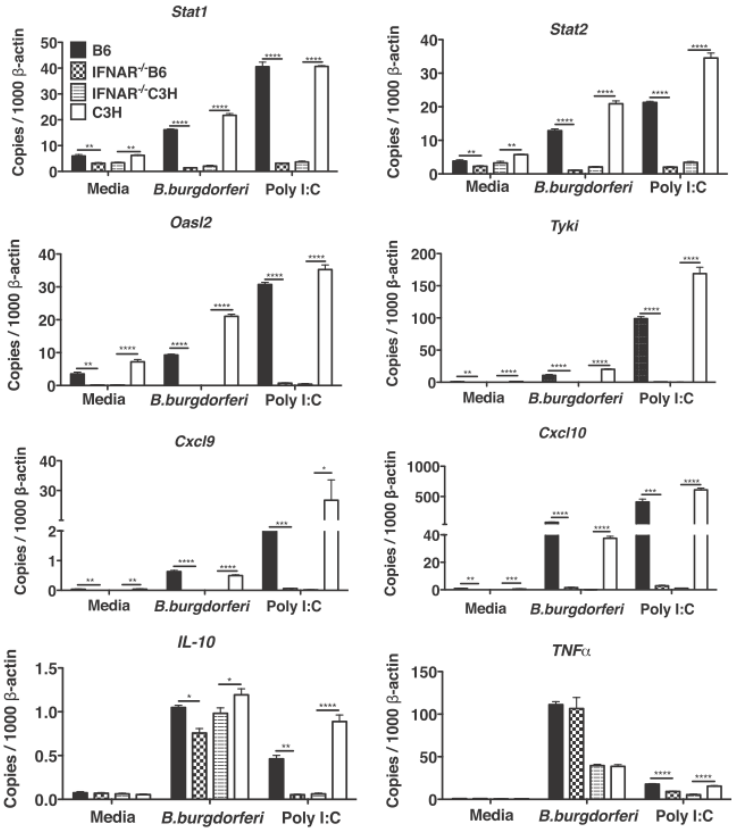

FIGURE 6. *Bbaa1* regulation of IFN profile is dependent on IFNAR feed forward. RT-PCR of transcript induction in BMDMs from B6, C3H, B6-IFNAR1$^{-/-}$, and C3H-IFNAR1$^{-/-}$ mice incubated with media, *B. burgdorferi*, or poly(I:C) for 6 h. Transcript levels for *Stat1*, *Stat2*, *Oasl2*, *Nos2*, *Tyki*, *Cxcl9*, *Cxcl10*, *IL-10*, and *Tnfα* were normalized to *β-actin*. Significance was determined by ANOVA, with Bonferroni post hoc comparison; shown for B6 versus B6-IFNAR1$^{-/-}$ and C3H versus C3H-IFNAR1$^{-/-}$. $*p < 0.05$, $**p < 0.01$, $***p < 0.001$, $****p < 0.0001$.

paracrine activities of type I IFN. To determine the impact of *Bbaa1* allele on this amplification stage of the IFN response, we treated BMDMs from C3H and B6 mice with increasing concentrations of IFN-β, and transcripts were analyzed. By assessing the response to IFN-β, any possible differences in uptake and sensing of *B. burgdorferi* were eliminated. BMDMs from B6 and C3H mice revealed virtually identical magnitude of induction of numerous IFN signature genes at 3 h of treatment (Fig. 7A). Importantly, dose–response curves revealed similar thresholds and maximal responses to IFN-β by both mouse strains. This is consistent with similar ligand affinity and activation state of the IFNAR1 expressed by B6 and C3H macrophages, and independence from *Bbaa1* regulation at this stage of the response.

Transcripts known to be associated with the well-characterized macrophage effector states M1 and M2 were also assessed in B6 and C3H treated with IFN-β (58). Transcripts for the M1-associated enzyme-inducible NO synthase (*Nos2*) were more highly upregulated in response to IFN-β in C3H than B6 macrophages (Fig. 7B). In contrast, transcripts for the alternatively activated M2 macrophage marker, arginase (*Arg1*), were more highly induced in BMDMs from B6 than C3H mice (Fig. 7B) (59). Levels of a second M2 macrophage marker, *Mrc1*, trended higher in B6 than C3H macrophages. These findings suggest the interesting hypothesis that *Bbaa1* impacts the functional phenotype of macrophages by modulating downstream signaling pathways. Because M1 macrophages are considered to be proinflammatory, whereas M2 macrophages are associated with wound repair and modulation of inflammation, this difference could be highly relevant to the inflammatory state of the *B. burgdorferi*–infected joint (60).

Does Bbaa1 *regulate expression of M1 and M2 markers in macrophages?*

BMDMs generated by culturing with M-CSF are considered to possess characteristics associated with M2 phenotype macrophages, functionally associated with wound repair and restriction of inflammation (59). In fact, we previously identified *Arg1* as transcriptionally upregulated in joint tissue of *B. burgdorferi*–infected B6 mice, but not C3H mice, suggesting correlation of *Arg1* expression with the reduced inflammation and arthritis seen in B6 mice (18). To test the intriguing possibility that *Bbaa1* alleles influence the functional phenotype of macrophages, we assessed freshly derived and fully differentiated BMDMs from B6, C3H, B6.C3-*Bbaa1*, and C3.B6-*Bbaa1* mice for *Arg1* and *Mrc1*. Remarkably, resting macrophages from B6 mice expressed higher levels of *Arg1* than did macrophages from C3H mice, and this distinction was dependent on *Bbaa1*, as indicated with macrophages from *Bbaa1* congenic mice (Fig. 8). In contrast, although the level of *Mrc1* was greater in B6 than C3H macrophages, this difference was not regulated by *Bbaa1* (Fig. 8). Transcripts for the M1 marker *Nos2* were not expressed in resting BMDMs (data not shown) but were rapidly upregulated in response to *B. burgdorferi* (Fig. 8). Induction of *Nos2* was regulated by *Bbaa1*, as levels were higher in BMDMs from C3H and B6.C3-*Bbaa1* mice than from B6 and C3.B6-*Bbaa1* mice (Fig 8). This finding is consistent with the hypothesis that inherent patterns of gene expression, regulated by *Bbaa1* alleles, direct the functional phenotype of macrophages as classically (M1) versus alternatively (M2) poised. Importantly, *Nos2* was previously found to be dispensable for arthritis development; therefore, its expression should be considered

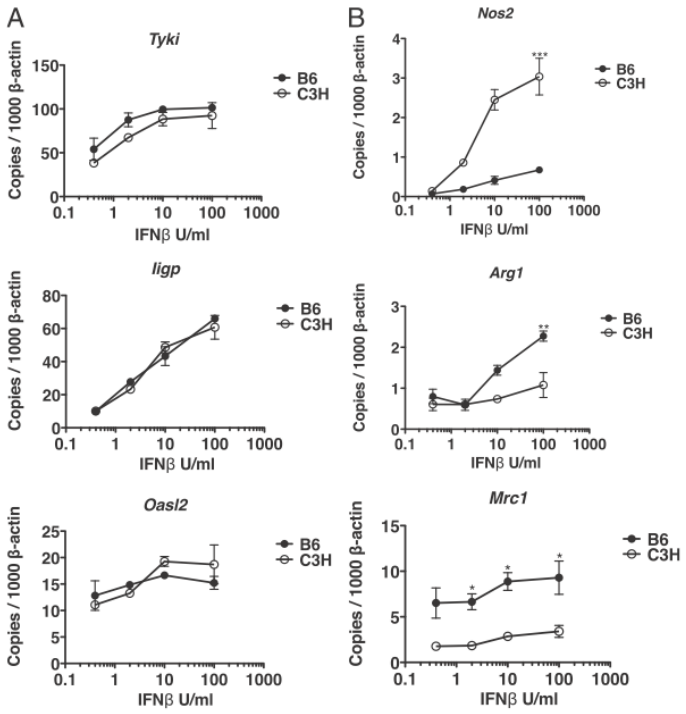

FIGURE 7. Responses of BMDMs to increasing doses of IFN-β. BMDMs from B6 and C3H mice were treated with 0.4–100 U/ml IFN-β, and transcriptional responses were measured at 3 h. (**A**) Levels of IFN-inducible transcripts *Tyki*, *Iigp*, and *Oasl2*. (**B**) Levels of M1/M2 polarization markers *Nos2*, *Arg1*, and *Mrc1*. Transcript levels of *Tyki*, *Nos2*, *Iigp*, *Arg1*, *Oasl2*, and *Mrc1* were normalized to *β-actin*. Data points indicate mean ± SE. Statistical significance between mouse strains was determined by Student *t* test, as are indicated for *Nos2* and *Arg1*. $*p < 0.05$, $**p < 0.01$, $***p < 0.001$.

an indicator of macrophage phenotype rather than a mediator of disease (61).

Impact of Bbaa1 on the K/B×N serum transfer model of RA

QTL analysis for Lyme disease severity that recently allowed identification of *Gusb* as a major regulator of Lyme arthritis also revealed a similar regulatory potential for the K/B×N serum transfer model of RA (33). This prompted us to consider the possibility that *Bbaa1* might also regulate RA. In addition, an IFN signature has recently been described in a subgroup of RA patients who fail to respond to TNF blocking therapies, suggesting an existing patient population with dysregulated type I IFN (62). The K/B×N serum transfer model has been used extensively to assess factors that contribute to the effector stage of arthritis as it bypasses the requirement for permissive MHC alleles (39). K/B×N serum contains an autoantibody to glucose-6-phosphate isomerase, which is widely expressed and particularly accessible on bone within the joints, and the severity of this arthritis can be regulated by limiting quantities of administered K/B×N serum. To test the impact of *Bbaa1*, we gave a submaximal dose (100 μl) of K/B×N serum to B6 and B6.C3-*Bbaa1* mice. C3H mice were included as a control in this experiment as their response to K/B×N serum has not previously been reported. Measurement of the rear ankle joints indicated more severe arthritis in C3H than

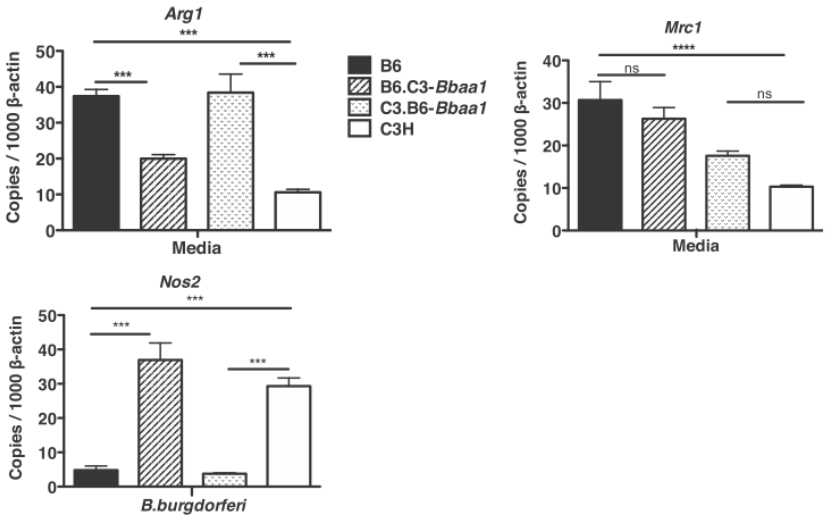

FIGURE 8. *Bbaa1* regulated levels of expression of M1 and M2 markers in resting and activated macrophages. BMDMs from B6, C3H, B6.C3-*Bbaa1*, and C3.B6-*Bbaa1* mice were assessed for M2 markers *Arg1* and *Mrc1* before addition of stimulant. Expression of the M1 marker *Nos2* was assessed at 6 h of stimulation with *B. burgdorferi*. All transcripts were normalized to *β-actin*. Shown are mean ± SE for one experiment, representative of two separate experiments. Significance was determined by ANOVA, with Bonferroni post hoc comparison; shown for ISCLs with appropriate background parental strain and for B6 versus C3H. $***p < 0.001$, $****p < 0.0001$.

B6 mice as early as 1 d after the first dose of K/B×N serum, and much greater severity by day 7 (Fig. 9A). By day 7, ankle swelling in B6.C3-*Bbaa1* mice was much greater than seen in B6 mice and was indistinguishable from C3H (Fig. 9A). Histopathological assessment of the overall lesion score was determined at day 7, and confirmed severe lesions in C3H and B6.C3-*Bbaa1* mice and very mild disease in B6 mice (Fig. 9B). Thus, *Bbaa1* is a robust regulator of RA severity.

To determine whether the effect of *Bbaa1* was mediated through type I IFN production and feed forward, we treated the B6.C3-*Bbaa1* mice with IFNAR1 blocking mAb, as in the Lyme arthritis experiment in Fig. 2. B6.C3-*Bbaa1* ISCLs received a single dose of MAR1-5A3 or isotype control the day before the first administration of K/B×N serum. Blocking the IFNAR1 in B6.C3-*Bbaa1* resulted in a reduction in arthritis severity to the level seen in B6 mice, implicating type I IFN in this model of RA (Fig. 10A). Histopathological analysis also revealed greatly reduced lesion scores in receptor-blocked B6.C3-*Bbaa1* mice (Fig. 10B).

Discussion

In this study, forward genetic analysis of Lyme arthritis severity has implicated the IFN-αβ gene cluster within *Bbaa1* as a candidate regulator of Lyme arthritis: *B. burgdorferi* infection of the B6.C3-*Bbaa1* ISCLs resulted in more severe ankle swelling and arthritic lesions than seen in parental B6 mice (Fig. 1). A second major finding was that *Bbaa1* also regulated RA, as demonstrated in B6.C3-*Bbaa1* mice treated with K/B×N serum (Fig. 9). In both arthritis models, the heightened severity in B6.C3-*Bbaa1* mice was reduced by treatment with an IFN receptor-blocking mAb (Figs. 2, 10). Thus, the exacerbated Lyme and RA in B6.C3-*Bbaa1* mice is dependent on type I IFN production and feed-forward amplification, directly establishing a shared pathological process dependent on localized production of type I IFN.

This is the second example of forward genetics identification of a Lyme arthritis QTL that also influences RA. *Gusb* was positionally cloned as a major regulator of Lyme arthritis severity

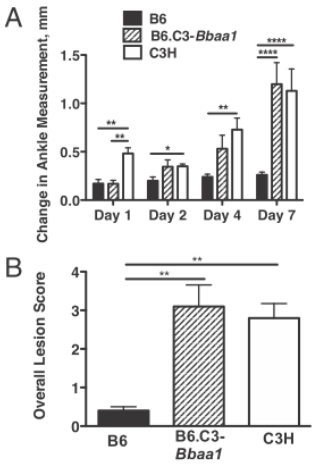

FIGURE 9. Impact of *Bbaa1* on severity of K/B×N serum transfer arthritis. B6, B6.C3-*Bbaa1*, and C3H mice were treated with 100 μl K/B×N serum on days 0 and 2, and arthritis was assessed by change in ankle measurement on days 1–7 (**A**) and by histopathological scoring for overall lesion score on day 7 (**B**), as described in *Materials and Methods*. Statistical significance was determined by Student *t* test for ankle swelling and Mann–Whitney *U* test overall lesion. $n = 5$. $*p < 0.05$, $**p < 0.01$, $****p < 0.0001$.

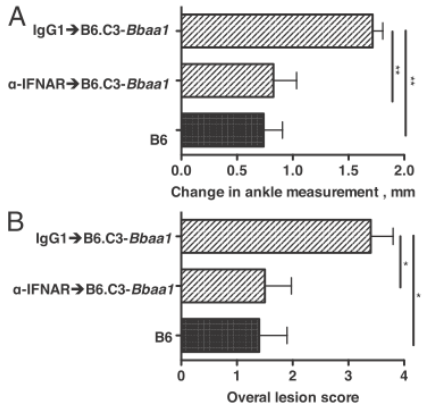

FIGURE 10. Enhanced RA in B6.C3-*Bbaa1* mice is dependent on type I IFN. B6.C3-*Bbaa1* mice were treated with 2.5 mg MAR1-5A3 blocking mAb or isotype control the day before administration of K/B×N serum. B6.C3-*Bbaa1* and B6 mice received 100 μl K/B×N serum on days 0 and 2. Arthritis was assessed by change in ankle measurement on day 17 (**A**) and by histopathological scoring for overall lesion score on day 7 (**B**), as described in *Materials and Methods*. Statistical significance was determined by ANOVA, with Bonferroni post hoc comparison for ankle measurements, and Kruskal–Wallis test with Dunn's multiple comparison for overall lesion. $n = 5$. $*p < 0.05$, $**p < 0.01$.

within *Bbaa2* on Chr5, and the disease-exacerbating *Gusb* allele was also found to increase the severity of the K/B×N model of RA (33). The identification of *Gusb* provided an unexpected correlation of disease severity with reduced lysosomal enzyme activity and the subsequent accumulation of undigested glycosaminoglycans in joint tissue of both *B. burgdorferi*–infected and autoantibody-treated arthritis. Thus, both infection-triggered and Ab-induced arthritis share a second pathway for exacerbated disease.

In the case of *Bbaa1*, the involvement of type I IFN in Lyme arthritis in C3H mice had previously been established through ablation of the IFNAR1 gene and by blocking IFNAR function with mAb (19, 20). Type I IFNs have also been identified in patients with various manifestations of Lyme disease, including skin lesions and cognitive deficits (63, 64), and have been implicated in B lymphocyte accumulation in the lymph nodes of infected mice (65). Taken in context with these previous findings, the current genetic identification of *Bbaa1* implicates the cluster encoding the IFN-αβ genes as a candidate regulator of Lyme arthritis. Importantly, disruption of IFNAR signaling had no effect on control of *B. burgdorferi* in joint or other tissue, indicating type I IFN is selectively involved in pathological arthritis development and, therefore, could serve as a target for therapeutic intervention in patients (19, 20). The linkage of *Bbaa1* to RA was somewhat surprising as others have reported that exogenous administration of human IFN-α reduces the severity of RA in a murine model of collagen Ab-induced arthritis (66). However, our findings are consistent with several published patient studies that have characterized a type I IFN signature in synovial and blood cells from a cohort of patients who fail to respond to TNF targeting biologicals (62, 67). Therefore, the B6.C3-*Bbaa1* mouse could provide an important new animal model for this RA patient group. Dysregulation of type I IFN has also been associated with the pathological development of systemic lupus erythematosus, Sjögren's syndrome, scleroderma, type I diabetes (29, 68–72), and in serious side effects from therapeutic use of IFN-α/β in patients with hepatitis C virus and multiple sclerosis (26, 28). Thus, the

identification of a genetic predisposition to exaggerated IFN responses could ultimately impact additional pathological conditions.

The identification of a genetic predisposition to type I IFN hyperactivation in Lyme and RA emphasizes that entirely distinct initiators can trigger common pathways of arthritis exacerbation. It further validates the unbiased approach of forward genetics in identification of biologically relevant pathological pathways. Interestingly, neither *Gusb* nor type I IFN have been identified as candidates for RA in numerous other murine QTL analyses, possibly reflecting the exclusion of C3H mice in collagen-induced arthritis studies because of lack of required MHC susceptibility allele (73). Genome-wide association studies studies of patients with RA and juvenile idiopathic arthritis have identified polymorphisms in genes involved in the IFN signaling cascade such as *Irf5*, *Irf8*, *Tyk2*, and *IL-21*, although the type I IFN gene cluster itself has not been identified (74, 75). Thus, the B6.C3-*Bbaa1* mouse provides a new experimental model to assess genetic predisposition to both microbial and autoimmune-induced type I IFN.

In considering the type I IFN cluster as a candidate for Lyme arthritis and RA, IFN-β is the most obvious candidate gene because it is expressed at higher levels than any of the IFN-α genes in response to *B. burgdorferi* in joint tissue and macrophages (20, 76). In addition, the affinity of the IFNAR for IFN-β protein is much higher than for any of the IFN-α proteins, making it a dominant contributor to the receptor-dependent induction of downstream effectors (77, 78). However, support for IFN-β as a candidate gene is undermined by the complete absence of SNPs distinguishing C3H and B6 IFN-β genes, including the coding sequences and 3000 bp of flanking sequence that encompasses the well-characterized promoter/enhancer region (34, 79). Interestingly, there are numerous SNPs within and immediately adjacent to the IFN-α genes. SNPs in IFN-α1, IFN-α2, IFN-α4, IFN-α6, IFN-α11, and IFN-αb result in altered protein sequences that potentially influence function, whereas other SNPs are positioned within putative regulatory regions and could influence promoter strength or RNA stability. There are also transcribed pseudogenes within this 200,000-bp region whose regulatory functions have not been investigated. In addition, there are a large number of non-IFN genes within *Bbaa1* that could act to influence the level of IFN-αβ transcription, possibly through assembly of transcriptional complexes or through altered chromatin accessibility. Future studies will require development of advanced recombinant ISCLs to identify and critically test candidate genes.

The development of *Bbaa1* ISCL provides a powerful tool to assess the regulation of type I IFN induction. Several laboratories have characterized a type I IFN response to *B. burgdorferi* RNA in human mononuclear cells that is dependent on TLR7 or TLR8 and MyD88, whereas others have characterized MyD88-independent responses to *B. burgdorferi* RNA and other components in murine BMDMs (21–25, 52). Together, these findings present a complex picture of the type I IFN response in human and murine cells, involving multiple ligands that vary with particular cell types. Our findings with macrophages from *Bbaa1* ISCLs indicate a dominant effect of this locus on the magnitude of IFN response to *B. burgdorferi* ligands and to the viral mimic poly(I:C) (Figs. 3–6). Thus, *Bbaa1* appears to function as a global rheostat of type I IFN responses, regulating the initial production of type I IFN and the ultimate magnitude of the autocrine/paracrine-amplified response (Fig. 7). These findings clearly translate to the increased arthritis seen in *B. burgdorferi*–infected B6.C3-*Bbaa1* mice, indicating relevance to disease pathogenesis in the context of the B6 background (Fig. 1).

Unexpectedly, BMDMs from *Bbaa1* congenic mice also revealed differential expression of classic markers of the M1/M2 phenotype in BMDMs (Figs. 7, 8). It has recently been suggested that low or "tonic" levels of type I IFN actually prime macrophages for an M1 response, consistent with the hyperactivation of type I IFN in BMDMs from C3H and B6.C3-*Bbaa1* mice (80, 81). In fact, our previous global gene expression analysis identified *Arg1* as strongly upregulated in joint tissue of *B. burgdorferi*–infected B6, but not C3H, mice, which is also consistent with a modulatory role of *Arg1* in B6 responses and possible suppression of the type I IFN response (18). Taken together, these findings lead to the hypothesis that type I IFN exacerbates arthritis development in C3H mice by promoting a proarthritic M1 macrophage response in the joint tissue, whereas the M2 response inherent to B6 mice modulates localized inflammation and prevents severe arthritis. This is an unexpected finding with clear implications for understanding and counteracting inflammatory responses involved in arthritic lesion formation, but distinct from host defense. It also poses the intriguing possibility that type I IFN promotes M1 macrophage development in vivo, impacting the severity of Lyme arthritis and RA. Thus, the continued development of advanced *Bbaa1* congenic lines will provide an opportunity for identification of genetic elements linked to type I IFN expression and their involvement in pathological conditions extending beyond Lyme arthritis.

Acknowledgments

We thank members of the Weis laboratories for helpful discussions during the course of these studies and acknowledge the technical assistance of James E. Brewster.

Disclosures

The authors have no financial conflicts of interest.

References

1. Steere, A. C., R. T. Schoen, and E. Taylor. 1987. The clinical evolution of Lyme arthritis. *Ann. Intern. Med.* 107: 725–731.
2. Steere, A. C., and L. Glickstein. 2004. Elucidation of Lyme arthritis. *Nat. Rev. Immunol.* 4: 143–152.
3. Wormser, G. P., R. J. Dattwyler, E. D. Shapiro, J. J. Halperin, A. C. Steere, M. S. Klempner, P. J. Krause, J. S. Bakken, F. Strle, G. Stanek, et al. 2006. The clinical assessment, treatment, and prevention of lyme disease, human granulocytic anaplasmosis, and babesiosis: clinical practice guidelines by the Infectious Diseases Society of America. *Clin. Infect. Dis.* 43: 1089–1134.
4. Centers for Disease Control and Prevention. 2010. Lyme Disease Data US, 1996-2010. Available at: http://www.cdc.gov/lyme/stats/index.html. Accessed: June 15, 2014.
5. Dykhuizen, D. E., D. Brisson, S. Sandigursky, G. P. Wormser, J. Nowakowski, R. B. Nadelman, and I. Schwartz. 2008. The propensity of different *Borrelia burgdorferi* sensu stricto genotypes to cause disseminated infections in humans. *Am. J. Trop. Med. Hyg.* 78: 806–810.
6. Barthold, S. W., D. S. Beck, G. M. Hansen, G. A. Terwilliger, and K. D. Moody. 1990. Lyme borreliosis in selected strains and ages of laboratory mice. *J. Infect. Dis.* 162: 133–138.
7. Steere, A. C., E. Dwyer, and R. Winchester. 1990. Association of chronic Lyme arthritis with HLA-DR4 and HLA-DR2 alleles. *N. Engl. J. Med.* 323: 219–223.
8. Drouin, E. E., R. J. Seward, K. Strle, G. McHugh, K. Katchar, D. Londoño, C. Yao, C. E. Costello, and A. C. Steere. 2013. A novel human autoantigen, endothelial cell growth factor, is a target of T and B cell responses in patients with Lyme disease. *Arthritis Rheum.* 65: 186–196.
9. Schröder, N. W., I. Diterich, A. Zinke, J. Eckert, C. Draing, V. von Baehr, D. Hassler, S. Priem, K. Hahn, K. S. Michelsen, et al. 2005. Heterozygous Arg753Gln polymorphism of human TLR-2 impairs immune activation by *Borrelia burgdorferi* and protects from late stage Lyme disease. *J. Immunol.* 175: 2534–2540.
10. Oosting, M., H. Ter Hofstede, P. Sturm, G. J. Adema, B. J. Kullberg, J. W. van der Meer, M. G. Netea, and L. A. Joosten. 2011. TLR1/TLR2 heterodimers play an important role in the recognition of *Borrelia* spirochetes. *PLoS ONE* 6: e25998.
11. Oosting, M., H. ter Hofstede, F. L. van de Veerdonk, P. Sturm, B. J. Kullberg, J. W. van der Meer, M. G. Netea, and L. A. Joosten. 2011. Role of interleukin-23 (IL-23) receptor signaling for IL-17 responses in human Lyme disease. *Infect. Immun.* 79: 4681–4687.

12. Strle, K., J. J. Shin, L. J. Glickstein, and A. C. Steere. 2012. Association of a Toll-like receptor 1 polymorphism with heightened Th1 inflammatory responses and antibiotic-refractory Lyme arthritis. *Arthritis Rheum.* 64: 1497–1507.
13. Alexopoulou, L., V. Thomas, M. Schnare, Y. Lobet, J. Anguita, R. T. Schoen, R. Medzhitov, E. Fikrig, and R. A. Flavell. 2002. Hyporesponsiveness to vaccination with *Borrelia burgdorferi* OspA in humans and in TLR1- and TLR2-deficient mice. *Nat. Med.* 8: 878–884.
14. Kang, I., S. W. Barthold, D. H. Persing, and L. K. Bockenstedt. 1997. T-helper-cell cytokines in the early evolution of murine Lyme arthritis. *Infect. Immun.* 65: 3107–3111.
15. Steere, A. C., W. Klitz, E. E. Drouin, B. A. Falk, W. W. Kwok, G. T. Nepom, and L. A. Baxter-Lowe. 2006. Antibiotic-refractory Lyme arthritis is associated with HLA-DR molecules that bind a *Borrelia burgdorferi* peptide. *J. Exp. Med.* 203: 961–971.
16. Steere, A. C., and S. M. Angelis. 2006. Therapy for Lyme arthritis: strategies for the treatment of antibiotic-refractory arthritis. *Arthritis Rheum.* 54: 3079–3086.
17. Steere, A. C., J. Coburn, and L. Glickstein. 2004. The emergence of Lyme disease. *J. Clin. Invest.* 113: 1093–1101.
18. Crandall, H., D. M. Dunn, Y. Ma, R. M. Wooten, J. F. Zachary, J. H. Weis, R. B. Weiss, and J. J. Weis. 2006. Gene expression profiling reveals unique pathways associated with differential severity of lyme arthritis. *J. Immunol.* 177: 7930–7942.
19. Lochhead, R. B., F. L. Sonderegger, Y. Ma, J. E. Brewster, D. Cornwall, H. Maylor-Hagen, J. C. Miller, J. F. Zachary, J. H. Weis, and J. J. Weis. 2012. Endothelial cells and fibroblasts amplify the arthritogenic type I IFN response in murine Lyme disease and are major sources of chemokines in *Borrelia burgdorferi*-infected joint tissue. *J. Immunol.* 189: 2488–2501.
20. Miller, J. C., Y. Ma, J. Bian, K. C. Sheehan, J. F. Zachary, J. H. Weis, R. D. Schreiber, and J. J. Weis. 2008. A critical role for type I IFN in arthritis development following *Borrelia burgdorferi* infection of mice. *J. Immunol.* 181: 8492–8503.
21. Cervantes, J. L., S. M. Dunham-Ems, C. J. La Vake, M. M. Petzke, B. Sahay, T. J. Sellati, J. D. Radolf, and J. C. Salazar. 2011. Phagosomal signaling by *Borrelia burgdorferi* in human monocytes involves Toll-like receptor (TLR) 2 and TLR8 cooperativity and TLR8-mediated induction of IFN-beta. *Proc. Natl. Acad. Sci. USA* 108: 3683–3688.
22. Petzke, M. M., A. Brooks, M. A. Krupna, D. Mordue, and I. Schwartz. 2009. Recognition of *Borrelia burgdorferi*, the Lyme disease spirochete, by TLR7 and TLR9 induces a type I IFN response by human immune cells. *J. Immunol.* 183: 5279–5292.
23. Cervantes, J. L., C. J. La Vake, B. Weinerman, S. Luu, C. O'Connell, P. H. Verardi, and J. C. Salazar. 2013. Human TLR8 is activated upon recognition of *Borrelia burgdorferi* RNA in the phagosome of human monocytes. *J. Leukoc. Biol.* 94: 1231–1241.
24. Love, A. C., I. Schwartz, and M. M. Petzke. 2014. Borrelia burgdorferi RNA induces type I and III interferons via Toll-like receptor 7 and contributes to production of NF-κB-dependent cytokines. *Infect. Immun.* 82: 2405–2416.
25. Miller, J. C., H. Maylor-Hagen, Y. Ma, J. H. Weis, and J. J. Weis. 2010. The Lyme disease spirochete *Borrelia burgdorferi* utilizes multiple ligands, including RNA, for interferon regulatory factor 3-dependent induction of type I interferon-responsive genes. *Infect. Immun.* 78: 3144–3153.
26. Baccala, R., K. Hoebe, D. H. Kono, B. Beutler, and A. N. Theofilopoulos. 2007. TLR-dependent and TLR-independent pathways of type I interferon induction in systemic autoimmunity. *Nat. Med.* 13: 543–551.
27. Chaussabel, D., W. Allman, A. Mejias, W. Chung, L. Bennett, O. Ramilo, V. Pascual, A. K. Palucka, and J. Banchereau. 2005. Analysis of significance patterns identifies ubiquitous and disease-specific gene-expression signatures in patient peripheral blood leukocytes. *Ann. N. Y. Acad. Sci.* 1062: 146–154.
28. Wilson, L. E., D. Widman, S. H. Dikman, and P. D. Gorevic. 2002. Autoimmune disease complicating antiviral therapy for hepatitis C virus infection. *Semin. Arthritis Rheum.* 32: 163–173.
29. Higgs, B. W., Z. Liu, B. White, W. Zhu, W. I. White, C. Morehouse, P. Brohawn, P. A. Kiener, L. Richman, D. Fiorentino, et al. 2011. Patients with systemic lupus erythematosus, myositis, rheumatoid arthritis and scleroderma share activation of a common type I interferon pathway. *Ann. Rheum. Dis.* 70: 2029–2036.
30. Weis, J. J., B. A. McCracken, Y. Ma, D. Fairbairn, R. J. Roper, T. B. Morrison, J. H. Weis, J. F. Zachary, R. W. Doerge, and C. Teuscher. 1999. Identification of quantitative trait loci governing arthritis severity and humoral responses in the murine model of Lyme disease. *J. Immunol.* 162: 948–956.
31. Roper, R. J., J. J. Weis, B. A. McCracken, C. B. Green, Y. Ma, K. S. Weber, D. Fairbairn, R. J. Butterfield, M. R. Potter, J. F. Zachary, et al. 2001. Genetic control of susceptibility to experimental Lyme arthritis is polygenic and exhibits consistent linkage to multiple loci on chromosome 5 in four independent mouse crosses. *Genes Immun.* 2: 388–397.
32. Ma, Y., J. C. Miller, H. Crandall, E. T. Larsen, D. M. Dunn, R. B. Weiss, M. Subramanian, J. H. Weis, J. F. Zachary, C. Teuscher, and J. J. Weis. 2009. Interval-specific congenic lines reveal quantitative trait Loci with penetrant lyme arthritis phenotypes on chromosomes 5, 11, and 12. *Infect. Immun.* 77: 3302–3311.
33. Bramwell, K. K., Y. Ma, J. H. Weis, X. Chen, J. F. Zachary, C. Teuscher, and J. J. Weis. 2014. Lysosomal β-glucuronidase regulates Lyme and rheumatoid arthritis severity. *J. Clin. Invest.* 124: 311–320.
34. Hardy, M. P., C. M. Owczarek, L. S. Jermiin, M. Ejdebäck, and P. J. Hertzog. 2004. Characterization of the type I interferon locus and identification of novel genes. *Genomics* 84: 331–345.
35. Barthold, S. W., D. H. Persing, A. L. Armstrong, and R. A. Peeples. 1991. Kinetics of *Borrelia burgdorferi* dissemination and evolution of disease after intradermal inoculation of mice. *Am. J. Pathol.* 139: 263–273.
36. Wooten, R. M., Y. Ma, R. A. Yoder, J. P. Brown, J. H. Weis, J. F. Zachary, C. J. Kirschning, and J. J. Weis. 2002. Toll-like receptor 2 is required for innate, but not acquired, host defense to *Borrelia burgdorferi*. *J. Immunol.* 168: 348–355.
37. Sheehan, K. C., K. S. Lai, G. P. Dunn, A. T. Bruce, M. S. Diamond, J. D. Heutel, C. Dungo-Arthur, J. A. Carrero, J. M. White, P. J. Hertzog, and R. D. Schreiber. 2006. Blocking monoclonal antibodies specific for mouse IFN-alpha/beta receptor subunit 1 (IFNAR-1) from mice immunized by in vivo hydrodynamic transfection. *J. Interferon Cytokine Res.* 26: 804–819.
38. Monach, P. A., D. Mathis, and C. Benoist. 2008. The K/BxN arthritis model. *Curr. Protoc. Immunol.* Chapter 15: Unit 15.22.
39. Korganow, A. S., H. Ji, S. Mangialaio, V. Duchatelle, R. Pelanda, T. Martin, C. Degott, H. Kikutani, K. Rajewsky, J. L. Pasquali, et al. 1999. From systemic T cell self-reactivity to organ-specific autoimmune disease via immunoglobulins. *Immunity* 10: 451–461.
40. Ma, Y., K. P. Seiler, K. F. Tai, L. Yang, M. Woods, and J. J. Weis. 1994. Outer surface lipoproteins of *Borrelia burgdorferi* stimulate nitric oxide production by the cytokine-inducible pathway. *Infect. Immun.* 62: 3663–3671.
41. Brown, J. P., J. F. Zachary, C. Teuscher, J. J. Weis, and R. M. Wooten. 1999. Dual role of interleukin-10 in murine Lyme disease: regulation of arthritis severity and host defense. *Infect. Immun.* 67: 5142–5150.
42. Menzies, F. M., F. L. Henriquez, J. Alexander, and C. W. Roberts. 2010. Sequential expression of macrophage anti-microbial/inflammatory and wound healing markers following innate, alternative and classical activation. *Clin. Exp. Immunol.* 160: 369–379.
43. Meerpohl, H. G., M. L. Lohmann-Matthes, and H. Fischer. 1976. Studies on the activation of mouse bone marrow-derived macrophages by the macrophage cytotoxicity factor (MCF). *Eur. J. Immunol.* 6: 213–217.
44. Lazarus, J. J., M. A. Kay, A. L. McCarter, and R. M. Wooten. 2008. Viable *Borrelia burgdorferi* enhances interleukin-10 production and suppresses activation of murine macrophages. *Infect. Immun.* 76: 1153–1162.
45. Carroll, J. A., P. E. Stewart, P. Rosa, A. F. Elias, and C. F. Garon. 2003. An enhanced GFP reporter system to monitor gene expression in *Borrelia burgdorferi*. *Microbiology* 149: 1819–1828.
46. Lochhead, R. B., Y. Ma, J. F. Zachary, D. Baltimore, J. L. Zhao, J. H. Weis, R. M. O'Connell, and J. J. Weis. 2014. MicroRNA-146a provides feedback regulation of lyme arthritis but not carditis during infection with *Borrelia burgdorferi*. *PLoS Pathog.* 10: e1004212.
47. Ma, Y., A. Sturrock, and J. J. Weis. 1991. Intracellular localization of *Borrelia burgdorferi* within human endothelial cells. *Infect. Immun.* 59: 671–678.
48. Pestka, S. 2007. The interferons: 50 years after their discovery, there is much more to learn. *J. Biol. Chem.* 282: 20047–20051.
49. Platanias, L. C. 2005. Mechanisms of type-I- and type-II-interferon-mediated signalling. *Nat. Rev. Immunol.* 5: 375–386.
50. Brown, C. R., V. A. Blaho, and C. M. Loiacono. 2003. Susceptibility to experimental Lyme arthritis correlates with KC and monocyte chemoattractant protein-1 production in joints and requires neutrophil recruitment via CXCR2. *J. Immunol.* 171: 893–901.
51. Trinchieri, G. 2010. Type I interferon: friend or foe? *J. Exp. Med.* 207: 2053–2063.
52. Petnicki-Ocwieja, T., E. Chung, D. I. Acosta, L. T. Ramos, O. S. Shin, S. Ghosh, L. Kobzik, X. Li, and L. T. Hu. 2013. TRIF mediates Toll-like receptor 2-dependent inflammatory responses to *Borrelia burgdorferi*. *Infect. Immun.* 81: 402–410.
53. Shin, O. S., R. R. Isberg, S. Akira, S. Uematsu, A. K. Behera, and L. T. Hu. 2008. Distinct roles for MyD88 and Toll-like receptors 2, 5, and 9 in phagocytosis of *Borrelia burgdorferi* and cytokine induction. *Infect. Immun.* 76: 2341–2351.
54. Herskovits, A. A., V. Auerbuch, and D. A. Portnoy. 2007. Bacterial ligands generated in a phagosome are targets of the cytosolic innate immune system. *PLoS Pathog.* 3: e51.
55. Takaoka, A., and H. Yanai. 2006. Interferon signalling network in innate defence. *Cell. Microbiol.* 8: 907–922.
56. Stockinger, S., B. Reutterer, B. Schaljo, C. Schellack, S. Brunner, T. Materna, M. Yamamoto, S. Akira, T. Taniguchi, P. J. Murray, et al. 2004. IFN regulatory factor 3-dependent induction of type I IFNs by intracellular bacteria is mediated by a TLR- and Nod2-independent mechanism. *J. Immunol.* 173: 7416–7425.
57. Honda, K., H. Yanai, H. Negishi, M. Asagiri, M. Sato, T. Mizutani, N. Shimada, Y. Ohba, A. Takaoka, N. Yoshida, and T. Taniguchi. 2005. IRF-7 is the master regulator of type-I interferon-dependent immune responses. *Nature* 434: 772–777.
58. Mosser, D. M., and J. P. Edwards. 2008. Exploring the full spectrum of macrophage activation. *Nat. Rev. Immunol.* 8: 958–969.
59. Raes, G., R. Van den Bergh, P. De Baetselier, G. H. Ghassabeh, C. Scotton, M. Locati, A. Mantovani, and S. Sozzani. 2005. Arginase-1 and Ym1 are markers for murine, but not human, alternatively activated myeloid cells. *J. Immunol.* 174: 6561, author reply 6561–6562.
60. Mantovani, A., A. Sica, and M. Locati. 2005. Macrophage polarization comes of age. *Immunity* 23: 344–346.
61. Brown, C. R., and S. L. Reiner. 1999. Development of lyme arthritis in mice deficient in inducible nitric oxide synthase. *J. Infect. Dis.* 179: 1573–1576.
62. van der Pouw Kraan, T. C., C. A. Wijbrandts, L. G. van Baarsen, A. E. Voskuyl, F. Rustenburg, J. M. Baggen, S. M. Ibrahim, M. Fero, B. A. Dijkmans, P. P. Tak, and C. L. Verweij. 2007. Rheumatoid arthritis subtypes identified by genomic

profiling of peripheral blood cells: assignment of a type I interferon signature in a subpopulation of patients. *Ann. Rheum. Dis.* 66: 1008–1014.

63. Salazar, J. C., C. D. Pope, T. J. Sellati, H. M. Feder, Jr., T. G. Kiely, K. R. Dardick, R. L. Buckman, M. W. Moore, M. J. Caimano, J. G. Pope, et al; Lyme Disease Network. 2003. Coevolution of markers of innate and adaptive immunity in skin and peripheral blood of patients with erythema migrans. *J. Immunol.* 171: 2660–2670.
64. Jacek, E., B. A. Fallon, A. Chandra, M. K. Crow, G. P. Wormser, and A. Alaedini. 2013. Increased IFNα activity and differential antibody response in patients with a history of Lyme disease and persistent cognitive deficits. *J. Neuroimmunol.* 255: 85–91.
65. Hastey, C. J., J. Ochoa, K. J. Olsen, S. W. Barthold, and N. Baumgarth. 2014. MyD88- and TRIF-independent induction of type I interferon drives naive B cell accumulation but not loss of lymph node architecture in Lyme disease. *Infect. Immun.* 82: 1548–1558.
66. Yarilina, A., E. DiCarlo, and L. B. Ivashkiv. 2007. Suppression of the effector phase of inflammatory arthritis by double-stranded RNA is mediated by type I IFNs. *J. Immunol.* 178: 2204–2211.
67. van Baarsen, L. G., C. A. Wijbrandts, F. Rustenburg, T. Cantaert, T. C. van der Pouw Kraan, D. L. Baeten, B. A. Dijkmans, P. P. Tak, and C. L. Verweij. 2010. Regulation of IFN response gene activity during infliximab treatment in rheumatoid arthritis is associated with clinical response to treatment. *Arthritis Res. Ther.* 12: R11.
68. Crow, M. K., K. A. Kirou, and J. Wohlgemuth. 2003. Microarray analysis of interferon-regulated genes in SLE. *Autoimmunity* 36: 481–490.
69. Gill, M. A., P. Blanco, E. Arce, V. Pascual, J. Banchereau, and A. K. Palucka. 2002. Blood dendritic cells and DC-poietins in systemic lupus erythematosus. *Hum. Immunol.* 63: 1172–1180.
70. Mathian, A., A. Weinberg, M. Gallegos, J. Banchereau, and S. Koutouzov. 2005. IFN-alpha induces early lethal lupus in preautoimmune (New Zealand Black x New Zealand White) F1 but not in BALB/c mice. *J. Immunol.* 174: 2499–2506.
71. Emamian, E. S., J. M. Leon, C. J. Lessard, M. Grandits, E. C. Baechler, P. M. Gaffney, B. Segal, N. L. Rhodus, and K. L. Moser. 2009. Peripheral blood gene expression profiling in Sjögren's syndrome. *Genes Immun.* 10: 285–296.
72. Ferreira, R. C., H. Guo, R. M. Coulson, D. J. Smyth, M. L. Pekalski, O. S. Burren, A. J. Cutler, J. D. Doecke, S. Flint, E. F. McKinney, et al. 2014. A type I interferon transcriptional signature precedes autoimmunity in children genetically at risk for type 1 diabetes. *Diabetes* 63: 2538–2550.
73. Holmdahl, R. 2006. Dissection of the genetic complexity of arthritis using animal models. *Immunol. Lett.* 103: 86–91.
74. Eyre, S., J. Bowes, D. Diogo, A. Lee, A. Barton, P. Martin, A. Zhernakova, E. Stahl, S. Viatte, K. McAllister, et al. 2012. High-density genetic mapping identifies new susceptibility loci for rheumatoid arthritis. *Nat. Genet.* 44: 1336–1340.
75. Hinks, A., J. Cobb, M. C. Marion, S. Prahalad, M. Sudman, J. Bowes, P. Martin, M. E. Comeau, S. Sajuthi, R. Andrews, et al. 2013. Dense genotyping of immune-related disease regions identifies 14 new susceptibility loci for juvenile idiopathic arthritis. *Nat. Genet.* 45: 664–669.
76. Miller, J. C., Y. Ma, H. Crandall, X. Wang, and J. J. Weis. 2008. Gene expression profiling provides insights into the pathways involved in inflammatory arthritis development: murine model of Lyme disease. *Exp. Mol. Pathol.* 85: 20–27.
77. Piehler, J., C. Thomas, K. C. Garcia, and G. Schreiber. 2012. Structural and dynamic determinants of type I interferon receptor assembly and their functional interpretation. *Immunol. Rev.* 250: 317–334.
78. Jaks, E., M. Gavutis, G. Uzé, J. Martal, and J. Piehler. 2007. Differential receptor subunit affinities of type I interferons govern differential signal activation. *J. Mol. Biol.* 366: 525–539.
79. Keane, T. M., L. Goodstadt, P. Danecek, M. A. White, K. Wong, B. Yalcin, A. Heger, A. Agam, G. Slater, M. Goodson, et al. 2011. Mouse genomic variation and its effect on phenotypes and gene regulation. *Nature* 477: 289–294.
80. Fleetwood, A. J., H. Dinh, A. D. Cook, P. J. Hertzog, and J. A. Hamilton. 2009. GM-CSF- and M-CSF-dependent macrophage phenotypes display differential dependence on type I interferon signaling. *J. Leukoc. Biol.* 86: 411–421.
81. Gough, D. J., N. L. Messina, C. J. Clarke, R. W. Johnstone, and D. E. Levy. 2012. Constitutive type I interferon modulates homeostatic balance through tonic signaling. *Immunity* 36: 166–174.

CHAPTER 3

DYSREGULATED PRODUCTION OF IFN-β BY *BORRELIA BURGDORFERI* ARTHRITIS-ASSOCIATED LOCUS 1 (*BBAA1*) DRIVES LYME ARTHRITIS THROUGH MYOSTATIN UPREGULATION

Abstract

Forward genetics previously identified a genetic locus, denoted *B. burgdorferi* arthritis-associated locus 1 (*Bbaa1*), which regulates Lyme arthritis through heightened production of type I IFN and which physically encompasses the type I IFN gene cluster. In this study, mAb blockade of IFN-β, but not IFN-α, suppressed Lyme arthritis development in B6.C3-*Bbaa1* mice. *Bbaa1* regulation of IFN-β was also identified in bone marrow-derived macrophages stimulated with *B. burgdorferi,* and was responsible for feed-forward amplification of interferon-stimulated genes. Reciprocal radiation chimeras between B6.C3-*Bbaa1* and B6 mice revealed that arthritis is initiated by radiation-sensitive cells, but orchestrated by radiation-resistant components of the joint tissue. Advanced congenic lines were developed in order to reduce the physical size of the *Bbaa1* interval, and confirmed the contribution of type I IFN genes to Lyme arthritis. RNA-seq of the resident $CD45^-$ joint cellular fraction from advanced interval specific recombinant congenic lines (ISRCL4 and ISRCL3) identified myostatin as uniquely upregulated in association with *Bbaa1* arthritis development, and demonstrated myostatin expression to be linked to IFN-β production. Furthermore, *in vivo* inhibition of myostatin suppressed Lyme arthritis in *Bbaa1* (ISRCL4) congenic mice, formally implicating myostatin as a downstream mediator of joint-specific inflammatory response to *B. burgdorferi*. These findings suggest a previously unappreciated role for myostatin in Lyme arthritis development.

Introduction

Lyme disease, caused by infection with the bacteria *Borrelia burgdorferi*, affects 300,000 Americans each year (1). Disease outcomes range from acute to chronic, sometimes resulting in irreversible damage to the nervous (2) and cardiovascular (3, 4) systems. Arthritis is the most common late disease manifestation (5), affecting up to 60% of patients and persisting in 10% of patients despite antibiotic therapy (6). Lyme arthritis is frequently characterized by synovitis at one or both knee joints and may persist for years after infection (6, 7). While both bacterial and host factors contribute to the spectrum of Lyme disease severity (8), many studies have shown that Lyme arthritis results from a genetically determined dysregulated immune response (9–17).

The spectrum of disease severity in humans can be modeled in inbred strains of mice, which display different disease outcomes upon infection with *B. burgdorferi* (13). Specifically, C57BL/6 (B6) mice develop mild arthritis and C3H mice develop severe arthritis in response to the same *B. burgdorferi* inoculum. We have successfully employed these mice during empirical (18, 19) and forward genetic (20–22) approaches to identify genetic determinants of Lyme arthritis severity. Empirical approaches comparing the global gene expression profiles of B6 and C3H joint tissue revealed a type I IFN signature in C3H mice that is absent from B6 mice (18), and a receptor-blocking antibody and receptor ablation formally linked type I IFN expression to Lyme arthritis severity. Independently, forward genetic approaches identified a quantitative trait locus (named *Bbaa1*) that contains the type I IFN gene cluster and controls Lyme arthritis severity (20). An interval specific congenic line in which the C3H *Bbaa1* allele was introgressed onto the B6 background (B6.C3-*Bbaa1*) displays increased Lyme arthritis

relative to B6 mice (20) unless pretreated with the type I IFN receptor-blocking antibody (21), formally linking the expression of type I IFN within *Bbaa1* to increased Lyme arthritis. Interestingly, *Bbaa1* was also found to regulate rheumatoid arthritis (RA) severity through type I IFN production (21), indicating that insight gleaned from our model extends to a distinct inflammatory arthritis.

Our finding of a pathologic type I IFN profile is consistent with several publications that have shown a type I IFN signature in the serum of human Lyme patients at stages of active disease (2, 23) and in the synovial fluid of treatment-refractory RA patients (24). Arthritis is also a transient side effect in hepatitis C and multiple sclerosis patients treated with IFN-α/β (25, 26), further supporting the linkage between elevated levels of type I IFN and arthritis. However, type I IFN is a key element in the innate and adaptive response against a variety of microbial infections, posing an inherent problem to treatment blockade. Because type I IFN regulation requires a sensitive balance, and because IFN-α and IFN-β members play unique roles in various infections, we sought to identify the specific type I IFN driving Lyme arthritis pathogenesis. Our unique genetic tools have allowed us to separate type I IFN production from the IFN response (which is triggered immediately upon cytokine sensing), and to look at type I IFN production in isolation from other QTL contributing to Lyme arthritis severity (20). Herein, we used the B6.C3-*Bbaa1* mouse to identify the specific type I IFN member that causes *Bbaa1* Lyme arthritis, segregated cells that initiate type I IFN in response to *B. burgdorferi* from those that respond to it, and identified myostatin as an IFN-regulated mediator of Lyme arthritis development.

Materials and Methods

Mice

B6 and C3H mice were obtained from Jackson Laboratories. B6.C3-*Bbaa1* mice (Chr4: 9.32-94.97 Mbp) were previously generated (20) and maintained as a colony in our Animal Research Center. Interval specific recombinant congenic lines (ISRCL1-4) with Chr4 *Bbaa1* intervals 11.6 – 77.8 Mbp, 76.48 – 93.46 Mbp, 83.7 – 93.46 Mbp, and 88.3 – 93.46 Mbp were generated through repeated backcrosses of B6.C3-*Bbaa1* to the parental B6 line. Filial offspring were selected based on SNP identification by high-resolution melting analysis as described (27), and homozygous lines were fixed by mating littermates. All mice used in this study were housed in the University of Utah Animal Research Center (Salt Lake City, UT) and handled in accordance with protocols approved by the institutional review committee.

B. burgdorferi cultures, infections, and arthritis assessments

B. burgdorferi strain N40 was cultured for 4 days in Barbour-Stoenner-Kelly II medium containing 6% rabbit serum (Sigma-Aldrich). Mice were infected with 2×10^4 live spirochetes intradermally into the skin of the back (28). Arthritis was assessed by rear ankle joint measurements obtained with a metric caliper at days 0 and 28 post infection, and by histopathological analysis of the most severely swollen rear ankle joint following fixation, decalcification, and H&E staining as described previously (29). Histopathological scores were determined blindly and ranged from 0 to 5 for various aspects of disease, including severity and extent of the lesion, PMN leukocyte and mononuclear cell (e.g. monocyte, macrophage) infiltration, tendon sheath thickening (e.g.

synoviocyte and fibroblast hyperplasia), and reactive/reparative responses (e.g. periosteal hyperplasia and new bone formation and remodeling), with 5 representing the most severe lesion and 0 representing no lesion. Infection was confirmed in mice euthanized 28 days post infection by ELISA quantification of *B. burgdorferi* specific IgG concentrations in serum (30) and *16S rRNA B. burgdorferi* transcripts in joints (31).

Inhibitory reagents and treatments

Monoclonal Abs were used to neutralize murine IFNAR1 (MAR1-5A3), IFN-α (TIF-3C5), or IFN-β (HDβ-4A7) (Leinco Technologies, Inc.). TIF-3C5 is considered a "pan-IFN-α" mAb because it neutralized all IFN-α subtypes available for testing: αA, α1, α4, α5, α11, and α13 (32). Mice received mAbs or isotype controls by intraperitoneal injection following a dosage regimen described previously (32, 33). Briefly, anti-IFNAR1 was administered in a single 2.5mg dose the day before infection with *B. burgdorferi* (19, 21, 33), anti-IFN-β was administered in two doses (300μg each, 600μg total) the day before and 2 days following infection, and anti-IFN-α was administered in three doses (333μg each, 1mg total) the day before and days 1 and 3 post infection. Boosts were determined based on pharmacokinetics previously reported (32) and in consideration with the IFN profile peak 7 days post infection with *B. burgdorferi* (18). For BMDM experiments, 10μg/ml of each mAb was administered in combination with the stimulation. The myostatin inhibitor (MBP-fMSTNpro45-100-Fc) is a recombinant peptide derived from the prodomain of full-length myostatin protein, as described (34). Mice received four intraperitoneal injections of vehicle (PBS) or myostatin inhibitor (400μg each, 1.6mg total) once weekly beginning the day after infection.

Generation of reciprocal radiation chimeras

Chimeras were generated in all pairwise combinations between B6 (CD45.1), B6 (CD45.2), and B6.C3-*Bbaa1* (CD45.2) using a rapid reconstitution protocol as described (35, 36). Rapid reconstitution involves transplanting donor splenocytes into irradiated recipient mice and allows for the infection of young mice <8 wk old, necessary for a reliable arthritis phenotype. Chimerism was evaluated by flow cytometric analysis of peripheral blood leukocytes 25 days post transplant (Figure 3.S3A).

Isolation of CD45$^-$ cells from joint tissue

Mouse rear ankle joints were gently digested into single-cell suspensions as described (36). Briefly, skin was removed and tibiotarsel tissue was teased away from bone using 20-gauge syringe needles followed by 1 hr incubation at 37^{o}C in RPMI 1640 containing 0.2mg/ml endotoxin-free Liberase TM (Roche) and 100µg/ml DNase I (Sigma-Aldrich). Single-cell suspensions were filtered through a 100µm cell strainer, RBCs were lysed in ammonium-chloride-potassium buffer, and cells were labeled with biotinylated anti-CD45.2 (BioLegend) followed by streptavidin magnetic bead labeling (Miltenyi Biotec). Magnetic bead separation was performed on MS columns (Miltenyi Biotec) according to the manufacturer's instructions. Flow cytometric analysis revealed >85% purity in the CD45$^-$ fraction, as previously reported (36). CD45$^-$ cells from both rear ankle joints of two mice were pooled for each *n* sample in order to increase RNA concentration for transcript analysis (Figures 3.6 and 3.7A). For *ex vivo* stimulation, CD45$^-$ cells from both rear ankle joints of >8 mice were pooled, plated in RPMI 1640 containing 2% FBS (36), and stimulated with live *B. burgdorferi* (6×10^6/ml) or 100U/ml

IFN-β (PBL Laboratories) for 3 hr (Figure 3.7B).

Cell culture

Bone marrow-derived macrophages (BMDMs) were prepared by culturing bone marrow isolated from the femurs and tibias of mice for 7 days in L929 cell-conditioned media as a source of M-CSF, as previously described (37). Harvested macrophages were then replated in 24-well dishes at a density of 6×10^5/ml in media containing 1% of the serum replacement Nutridoma (Roche). Cultures were stimulated with live *B. burgdorferi* (6×10^6/ml) for 6hr at 37°C with 5% CO_2.

Flow cytometric analysis of P-Stat 1

Phosphorylated Stat1 was stained as described (32, 38) following 15hr incubation with *B. burgdorferi* and type I IFN blocking mAbs. Briefly, cells were incubated in 0.05% trypsin (Fisher Scientific) and scraped to detach from plate. Cells were fixed using 1.5% paraformaldehyde and permeabilized with 100% methanol. P-Stat1 was stained using an unconjugated Phospho-Stat1 mAb (pY701, Cell Signaling) at a 1:200 dilution and incubated for 1 hr at RT, followed by a secondary stain with Goat anti-Rabbit IgG conjugated to Alexa Fluor 647 (Fisher Scientific) at a 1:500 dilution and incubated for 30 min at RT. Data were collected on a FACSCanto II (BD Biosciences) flow cytometer and analyzed using FlowJo v.10.0.8 software.

Gene expression analysis

Total RNA was recovered using TRIzol reagent (Invitrogen) and purified using the Direct-zol RNA MiniPrep kit (Zymo Research). For RNA-sequencing, libraries were prepared using PolyA enrichment and sequenced with Illumina HiSeq 50 Cycle Single-Read Sequencing version 4 at the University of Utah High Throughput Genomics Core Facility (Salt Lake City, UT). Sequences were aligned and annotated with help from the University of Utah Bioinformatics Core Facility (Salt Lake City, UT). For qRT-PCR analyses, RNA was reverse transcribed, and transcripts were quantified using a Roche LC-480 according to our previously described protocols (20). Primer sequences used in this study for *β-actin, Iigp* (18), *Oasl2, Cxcl10, Tyki* (19)*, Gbp2* (39)*, Tnfa,* and *Ifnb* (40) can be found at the indicated citations. *Mstn* primer sequences designed in this study were as follows: forward (5'-GATCTTGCTGTAACCTTCCC-3') and reverse (5'-CTCCTGAGCAGTAATTGGC-3').

Data and statistical analyses

All graphical data depict the mean ± SEM. Statistical analyses were performed using GraphPad Prism 7.0b software. Multiple-sample data sets were analyzed by one-way ANOVA with Dunnet's post hoc test for pairwise comparisons. Two-sample data sets were analyzed by Student *t* test (2-tailed). Categorical histopathology scores were assessed by the Mann-Whitney *U* test. Statistical significance (*$p < 0.05$, **$p < 0.01$, ***$p < 0.001$, ****$p < 0.0001$) is indicated.

Results

*Determination of the proarthritogenic type I IFN cytokine in B6.C3-*Bbaa1 *mice*

Both empirical and forward genetic studies from our lab have converged on the finding that a pathologic type I IFN profile drives Lyme arthritis in C3H mice (18–21, 36). We identified the type I IFN gene cluster in *Bbaa1,* a QTL regulating Lyme arthritis severity, and generated a congenic line, denoted B6.C3-*Bbaa1* (Chr4: 9.32-94.97 Mbp), wherein we established that dysregulated production of type I IFN within *Bbaa1* drives Lyme arthritis (21). Nevertheless, there are multiple members of the type I IFN family, with the IFN-α subtypes and IFN-β playing the largest roles in pathogenesis to date, and although each signals through a shared receptor heterodimer, their unique roles in host protection and pathogenesis are becoming increasingly appreciated (32, 41).

To assess the specific contribution of IFN-α and IFN-β to Lyme arthritis development, B6.C3-*Bbaa1* mice were treated with a pan-acting mAb that blocks multiple IFN-α subtypes (TIF-3C5) or a mAb that targets IFN-β specifically (HDβ-4A7). We previously showed that the anti-IFNAR1 mAb (MAR1-5A3) suppresses arthritis development to the baseline of B6 (21). Because blocking IFN-β resulted in the same reduction in Lyme arthritis as blocking IFNAR1 (Figure 3.1A), we conclude that IFN-β and not IFN-α is the proarthritic cytokine generated in B6.C3-*Bbaa1* mice. Analysis of anti- *B. burgdorferi* IgG in the serum and *B. burgdorferi 16S rRNA* transcripts in the joint confirm that blocking type I IFN does not impact the ability of the host to generate a B-cell response or to control infection (Figure 3.1B). These findings underscore the fact that *Bbaa1* intrinsically regulates pathologic production of IFN-β *in vivo*, and IFN-β does not

protect the host from *B. burgdorferi* expansion.

Effect of blocking IFN-α or IFN-β on type I IFN activation in BMDMs

We previously showed that BMDMs from B6.C3-*Bbaa1* mice express higher levels of IFN-inducible transcripts in response to *B. burgdorferi* than do BMDMs from B6 mice (21). Thus, B6.C3-*Bbaa1* BMDMs were used as a surrogate for myeloid cells in joint tissue to assess the specific contribution IFN-α or IFN-β to the *Bbaa1*-directed induction of type I IFN. BMDMs were stimulated with *B. burgdorferi* and treated with each mAb for 6 hr. Treatment with anti-IFN-β resulted in complete suppression of IFN inducible genes, indistinguishable from levels of macrophages treated with IFN receptor blockade (Figure 3.2A). In contrast, treatment with anti-IFN-α had no effect on IFN-induction, indicating that IFN-β, and not IFN-α, is regulated by *Bbaa1* in response to *B. burgdorferi*. Isotype control mAbs had no effect (Figure 3.S1). Importantly, none of these treatments impacted the expression of *Tnfa* (Figure 3.2A), which is downstream of the critical MyD88-dependent host defense pathway (42, 43). This highlights the *in vivo* observation that type I IFN is not required for host defense in Lyme arthritis (Figure 3.1B) and its suppression does not influence the expression of initial MyD88-dependent cytokines (21, 36)

Flow cytometric analysis of phosphorylated Stat1 protein was used as a complementary approach to determine the impact of IFN-α and IFN-β protein on the feed-forward IFN amplification. Stat1 is rapidly phosphorylated when IFN-α and IFN-β proteins bind the receptor (32, 44), but stimulation with *B. burgdorferi* requires time for transcription and translation of type I IFNs. Therefore, Stat1 phosphorylation was

assessed in BMDMs 15 hr post stimulation with *B. burgdorferi* and mAb treatment. Strikingly, IFN-β neutralization completely inhibited Stat1 phosphorylation, similar to levels in macrophages treated with receptor blocking mAb, while blocking IFN-α had no effect (Figure 3.2B). Because anti-IFN-α did not impact arthritis severity or macrophage responses to *B. burgdorferi,* mAb functionality was assessed (Figure 3.S2). Confirmation of anti-IFN-α activity supports the conclusion that IFN-β (but not IFN-α) is the type I IFN made in response to *B. burgdorferi* both *in vivo* and *in vitro,* and that low levels of IFN-α do not contribute to response during the feed-forward amplification.

Does Bbaa1 initiate arthritis through hematopoietic or resident cells?

Multiple lines of evidence point to the fact that IFN-β is pathologic in *Bbaa1* congenic mice, leading to the question of whether *Bbaa1* exerts its proarthritic effect through hematopoietic or resident cells. The *Bbaa1* congenic mouse is a unique tool that allows the interrogation of IFN signaling independent of feed-forward IFN amplification because *Bbaa1* initiates IFN-β production. MHC compatibility between mildly arthritic B6 mice and more severely arthritic B6.C3-*Bbaa1* mice allowed reciprocal radiation chimeras to be generated to specifically determine if *Bbaa1* exerts its proarthritic effect through radiosensitive-hematopoietic cells or radioresistant-resident cells in the joint (Figure 3.3A). Chimeras were generated using a rapid reconstitution protocol (35, 36), and reconstitution was determined to be adequate for host defense based on the similar abilities of irradiated mice to generate a B-cell dependent antibody response and sufficient myeloid cells to control infection (Figure 3.S3).

As expected, B6 mice reconstituted with autologous splenocytes (B6→B6)

developed mild arthritis and B6.C3-*Bbaa1* mice reconstituted with autologous splenocytes (*Bbaa1*→*Bbaa1*) developed more severe arthritis 4 wk post infection with *B. burgdorferi* (Figure 3.3B). Notably, B6.C3-*Bbaa1* mice reconstituted with B6 cells (B6→*Bbaa1*) developed mild arthritis similar to B6→B6 chimeras, whereas B6 mice reconstituted with B6.C3-*Bbaa1* cells (*Bbaa1*→B6) developed severe arthritis indistinguishable from *Bbaa1*→*Bbaa1* chimeras (Figure 3.3B). Thus, *Bbaa1* regulates Lyme arthritis severity through the radiosensitive, hematopoietic cellular constituents of the joint. Considering that *Bbaa1* controls the magnitude of *B. burgdorferi*-triggered IFN-β production, we can further deduce that radiosensitive cells in the joint, which are likely myeloid (36), initiate the production of proarthritic IFN-β (Figure 3.3C). This is consistent with our previous findings that $CD45^+$ cells harvested from a naïve mouse joint possess the unique ability to generate an IFN profile upon *ex vivo* stimulation with *B. burgdorferi,* whereas $CD45^-$ cells are capable of responding to but not initiating type I IFN in response to *B. burgdorferi* (Figure 3.S4 and Lochhead *et al.* (36)). Another striking finding is that *Bbaa1*→B6 chimeras develop the full arthritis phenotype, strongly implicating that regardless of genotype, radioresistant-resident cells are fully competent to choreograph arthritis manifestation in the joint (Figure 3.3, B and C). This is consistent with the previous finding that endothelial cells and fibroblasts, both of which are radioresistant cell types in the joint, are major responders to and amplifiers of type I IFN resulting in production of chemokines in infected C3H mice (36). This provides the first *in vivo* evidence for the "pass off" that occurs between cells that initiate IFN-β in response to *B. burgdorferi* and cells that respond to IFN-β to direct arthritis development (Figure 3.3C).

C3H-derived Bbaa1 *genes spanning the type I IFN locus confer increased arthritis on B6 background*

Because the original B6.C3-*Bbaa1* congenic interval was very large (Chr4: 9.32 – 94.97 Mbp) with >450 genes in addition to *Ifnb*, it was necessary to reduce the physical interval by backcrossing B6.C3-*Bbaa1* to the parental B6 line. This led to the generation of four new *Bbaa1* interval specific recombinant congenic lines (denoted ISRCL1-4) harboring various subintervals of *Bbaa1* (Figure 3.3). ISRCL1 contains the largest portion of C3H Chr4 but excludes the C3H type I IFN locus, while ISRCL2-4 retains the C3H type I IFN gene cluster with further reduction in the amount of C3H donor sequence (Figure 3.4). After infection with *B. burgdorferi,* congenic lines retaining C3H-derived *Bbaa1* genes spanning the type I IFN locus displayed more severe arthritis compared to B6 mice (Figure 3.4). Importantly, ISRCL3 mice exhibit the same arthritis phenotype as B6.C3-*Bbaa1* mice*,* indicating that all of the genes required for maximal *Bbaa1* arthritis are contained within Chr4: 83.7 – 93.46 Mbp. Interestingly, ISRCL4 mice displayed a submaximal phenotype that was still significantly increased compared to B6 mice. This indicates that there are 2 loci regulating maximal *Bbaa1* arthritis: the first locus is shared by ISRCL3 and ISRCL4 mice and spans the type I IFN gene cluster, while the second locus is only contained in ISRCL3 mice and is outside of type I IFN genes. Nevertheless, because blocking IFN-β in the full-length B6.C3-*Bbaa1* congenic line completely suppresses Lyme arthritis (Figure 3.1A and Ma *et al*. (21)), we can infer that the phenotype of both of these loci is dependent on IFN-β production.

Next we assessed the magnitude of the IFN response to *B. burgdorferi* in BMDMs from ISRCL3 and ISRCL4 mice, which both possess the C3H allele for the type I IFN

locus. Importantly, BMDMs from ISRCL3 and ISRCL4 mice displayed greater IFN transcriptional responses than BMDMs from B6 mice, with magnitudes similar to full length B6.C3-*Bbaa1* BMDMs (Figure 3.5). This indicates that genes responsible for IFN-β dysregulation are retained in the ISRCL4 *Bbaa1* locus (Chr4: 88.3 – 93.46 Mbp). As shown, *Ifnb* expression is low, but none of the 14 IFN-α transcripts were detectable, further supporting the role of IFN-β in driving Lyme arthritis pathogenesis. The fact that ISRCL3 & ISRCL4 mice display greater arthritis severity and their macrophages express more *Ifnb* compared to B6 macrophages provides a refined tool to study *Bbaa1* Lyme arthritis.

How does Bbaa1 change the transcriptome of the radioresistant-resident responders?

Now that we have established the role of radioresistant-resident cells in directing *Bbaa1* Lyme arthritis downstream of IFN-β, we pursued a better understanding of the mechanism of arthritis development through transcriptome analysis of $CD45^-$ (resident) joint cells. Newly developed ISRCL3 and ISRCL4 lines were compared to B6 mice in order to capture all genes related to IFN-β production and arthritis development with a minimal physical interval. To capture the stage of active arthritis development (as opposed to full-blown arthritis with confounding wound repair pathways), joint cells were harvested from mice 22 days post infection with *B. burgdorferi.* Following recovery of single-cell suspensions, the $CD45^-$ population was isolated by magnetic bead separation and RNA-seq was performed.

Not surprisingly, comparing the transcriptomes of these highly similar genotypes

at a time point submaximal to arthritis development revealed very few differences in gene expression profiles (Figure 3.6A). Of those differences, only five genes were independently identified in both ISRCL4 vs. B6 and ISRCL3 vs. B6 comparisons with ≥1.5-fold change and *p*-adj <0.05 (Figure 3.6A & Figure 3.S5), supporting their involvement in *Bbaa1*-directed arthritis. Importantly, myostatin (*Mstn*) had the greatest induction and achieved the highest level of significance in both analyses (Figure 3.6A & Figure 3.S5), illuminating it as a strong candidate for *Bbaa1* Lyme arthritis development. Quantitative RT-PCR analysis of *Mstn* expression in $CD45^-$ cells from uninfected animals revealed similar expression among uninfected mice of all three genotypes (data not shown), and revealed that *Bbaa1* specifically regulates the induction of myostatin following infection with *B. burgdorferi* (Figure 3.6B). This was a striking finding for *Bbaa1* Lyme arthritis development in light of recent evidence that myostatin is involved in RA development in humans and mice (45).

Impact of IFN-β on myostatin expression in $CD45^-$ cells isolated from joint tissue

To assess the connection between IFN-β production and myostatin expression in *Bbaa1* Lyme arthritis, IFN-β was blocked in ISRCL4 and ISRCL3 mice infected with *B. burgdorferi* (as described in Figure 3.1). $CD45^-$ cells were isolated from joint tissue 22 days post infection, and myostatin expression was assessed by qRT-PCR. Importantly, $CD45^-$ cells from ISRCL4 and ISRCL3 mice infected with *B. burgdorferi* and treated with anti-IFN-β mAb expressed nearly 2-fold fewer *Mstn* transcripts compared to mice treated with isotype control (Figure 3.7A). The fold suppression by blocking IFN-β is

internally consistent with the level of induction found in our RNA-seq (Figure 3.6). This directly connects the *Bbaa1*-dependent production of IFN-β to *Mstn* upregulation *in vivo*.

Several proinflammatory cytokines, TNF-α, IL-1α, and IL-17, were previously shown to directly induce expression of myostatin in the context of RA, but the impact of IFN-β was not addressed (45). To test whether IFN-β directly induces expression of myostatin, $CD45^-$ cells were isolated from the joints of naïve B6 mice and stimulated *ex vivo* with IFN-β, *B. burgdorferi,* or IFN-β and *B. burgdorferi* in combination. *Mstn* expression assessed by qRT-PCR revealed that IFN-β works synergistically with *B. burgdorferi* to directly induce *Mstn* expression (Figure 3.7B). To our knowledge, this is the first report of IFN-β induction of myostatin.

Inhibition of myostatin suppresses Lyme arthritis in Bbaa1 congenic mice

In order to determine whether myostatin is a marker or a mediator of *Bbaa1* Lyme arthritis, infected ISRCL4 mice were treated with a highly effective myostatin propeptide (34) to inhibit myostatin protein activity during arthritis development. Consistent with the dual requirement of *B. burgdorferi* and IFN-β for myostatin upregulation (Figure 3.7, A and B), myostatin inhibition did not impact ankle swelling in uninfected animals (Figure 3.8). However, myostatin inhibition in infected ISRCL4 congenic mice led to a remarkable suppression in arthritis 4 wk post infection with *B. burgdorferi* (Figure 3.8), similar to the low level normally seen in infected B6 mice (Figure 3.4). These findings demonstrate a direct effect of myostatin on joint-specific inflammatory responses.

Discussion

In this study, we established IFN-β as the Lyme arthritis-driving type I IFN that is regulated by a locus, *Bbaa1,* previously identified by forward genetics. This culminates a decade of our work wherein two parallel pathways of investigation revealed a pathologic type I IFN profile in C3H mice infected with *B. burgdorferi* that is suppressed by IFNAR1 blockade (14, 18–21, 36). Others have corroborated the association between pathologic production of type I IFN and Lyme disease pathogenesis in murine studies (46, 47) as well as in human patients at various stages of disease (2, 23), and many investigators have examined the type I IFN response to *B. burgdorferi* in murine and human cells (19, 36, 39, 47–56). But the specific culprit of *B. burgdorferi*-induced type I IFN pathogenicity has remained elusive due to the transient expression of IFN-α/β (57, 58), overlapping interferon-stimulated gene pathways induced by IFN-α/β (59), and differing contexts of *B. burgdorferi* infection in which IFN-α/β transcripts have been detected. The strength of this study centers on the employment of B6.C3-*Bbaa1* mice, which allowed the impact of type I IFN dysregulation to be assessed in isolation from the five other *B. burgdorferi* arthritis-associated QTL contained within the C3H genome (20), coupled with the use of newly available mAbs to assess IFN-α and IFN-β individually.

Multiple mAb experiments along with the transcriptional detection of *Ifnb* in BMDMs from refined congenic lines (and lack of evidence for *Ifna* transcripts) revealed that IFN-β is the sole contributor to the type I IFN profile and arthritogenesis in *Bbaa1*-directed Lyme arthritis. Another major finding was that IFN-β is intrinsically controlled within the *Bbaa1* locus. The intrinsic regulation of IFN-β within *Bbaa1* was surprising

due to the lack of coding or regulatory SNPs within 10,000 flanking base pairs of the *Ifnb* genetic sequence (60, 61) and suggests a novel mechanism for IFN-β regulation, which is a topic of future investigation. Here, the congenic mice provided a unique tool to segregate IFN-β initiation from feed-forward amplification, and radiation chimeras demonstrated that the *Bbaa1* arthritis-initiating lineage is radiation-sensitive in the joint. This finding is in contrast to our previous publication on the *Bbaa2* QTL, in which the hypomorphic allele of *Gusb* drives arthritis through the radiation-resistant resident joint population (22). Thus, our forward genetic approach has identified two distinct QTLs that regulate Lyme arthritis through independent mechanisms and responsible initiating tissues.

In the case of *Bbaa1,* the discrimination among cell types along with refined congenic lines was critical to understanding the mechanism of arthritis development. An unbiased RNA-seq on resident ($CD45^-$) joint cells led to the third major finding that *Bbaa1*-directed production of IFN-β causes myostatin upregulation. This was surprising given that myostatin is widely appreciated for its role as a negative regulator of skeletal muscle growth and regeneration (62), and intensely investigated for its positive impact on food production in the animal agriculture industry. Nevertheless, we were able to utilize newly developed reagents in the field of muscle development to inhibit myostatin protein activity *in vivo* and discovered that myostatin is a direct mediator of *Bbaa1* Lyme arthritis development. Strikingly, myostatin was recently found to be a mediator of a distinct inflammatory arthritis using the TNF-α overexpression model of RA in mice, and found to be expressed by synovial fibroblasts from patients with RA (45).

Although we do not completely understand the mechanism of myostatin-mediated

inflammation in Lyme arthritis development, myostatin promotes RA in TNF-α overexpressing mice by activating osteoclast differentiation (45). Although bone pathologies have not been widely investigated in Lyme arthritis patients or mice, Tang *et al.* recently identified *B. burgdorferi* infection in mice bone, but implicated osteoblast inhibition in bone destruction (63). Interestingly, Hodzic *et al.* have also identified *B. burgdorferi* in quadriceps muscle (64, 65), suggesting that a more global dysregulation of bone and muscle homeostasis could be involved in Lyme arthritis development than previously appreciated. Future studies are needed to investigate the role of myostatin in osteoclasts and other tissues of the joint.

Herein, we modeled the power of forward genetics in allowing the impact of genetics on pathogenic responses to be directly assessed, and this is the second report of forward genetic identification of novel genes associated with Lyme arthritis development (22). Identifying IFN-β as the pathologic type I IFN in *Bbaa1* Lyme arthritis parallels the finding that IFN-β is more pathologic than IFN-α in RA patients (66), and underscores the need to assess IFN-α/β ratios in serum from Lyme patients as an indicator of disease severity. The more selective blockade of a single IFN may also be more amendable to clinical outcomes where the entire type I IFN response has not been ablated, and myostatin may be a tantalizing target for therapeutic intervention that is outside of the conventional inflammatory host defense (67). Together, these findings provide an exciting new platform to help patients with Lyme disease.

References

1. Kuehn, B. M. 2013. CDC estimates 300,000 US cases of Lyme disease annually. *JAMA* 310: 1110.

2. Jacek, E., B. A. Fallon, A. Chandra, M. K. Crow, G. P. Wormser, and A. Alaedini. 2013. Increased IFNα activity and differential antibody response in patients with a history of Lyme disease and persistent cognitive deficits. *J Neuroimmunol* 255: 85–91.

3. Yoon, E. C., E. Vail, G. Kleinman, P. a. Lento, S. Li, G. Wang, R. Limberger, and J. T. Fallon. 2015. Lyme disease: a case report of a 17-year-old male with fatal Lyme carditis. *Cardiovasc Pathol* 2–6.

4. Centers for Disease Control and Prevention. 2013. Three sudden cardiac deaths associated with Lyme carditis — United States, November 2012 – July 2013. *Morb Mortal Wkly Rep* 62: 993–1018.

5. Borchers, A., C. Keen, A. Huntley, and M. E. Gershwin. 2015. Lyme disease: a rigorous review of diagnostic criteria and treatment. *J Autoimmun* 57: 82–115.

6. Steere, A. C., and L. Glickstein. 2004. Elucidation of Lyme arthritis. *Nat Rev Immunol* 4: 143–152.

7. Steere, A. C., R. T. Schoen, and E. Taylor. 1987. The clinical evolution of Lyme arthritis. *Ann Intern Med* 107: 725–731.

8. Petzke, M., and I. Schwartz. 2015. *Borrelia burgdorferi* pathogenesis and the immune response. *Clin Lab Med* 35: 745–764.

9. Steere, A. C., E. Dwyer, and R. Winchester. 1990. Association of chronic Lyme arthritis with HLA-DR4 and HLA-DR2 alleles. *N Engl J Med* 323: 219–223.

10. Schröder, N. W. J., I. Diterich, A. Zinke, J. Eckert, C. Draing, V. Baehr, D. Hassler, S. Priem, K. Hahn, K. S. Michelsen, T. Hartung, G. R. Burmester, U. B. Göbel, C. Hermann, and R. R. Schumann. 2005. Heterozygous Arg753Gln polymorphism of human TLR-2 impairs immune activation by *Borrelia burgdorferi* and protects from late stage Lyme disease. *J Immunol* 175: 2534–2540.

11. Steere, A. C., W. Klitz, E. E. Drouin, B. A. Falk, W. W. Kwok, G. T. Nepom, and L. A. Baxter-Lowe. 2006. Antibiotic-refractory Lyme arthritis is associated with HLA-DR molecules that bind a *Borrelia burgdorferi* peptide. *J Exp Med* 203: 961–971.

12. Strle, K., J. J. Shin, L. J. Glickstein, and A. C. Steere. 2012. Association of a toll-like receptor 1 polymorphism with heightened Th1 inflammatory responses and antibiotic-refractory Lyme arthritis. *Arthritis Rheum* 64: 1497–1507.

13. Barthold, S. W., D. S. Beck, G. M. Hansen, G. A. Terwilliger, S. The, I. Diseases, N. Jul, S. W. Barthold, D. S. Beck, G. M. Hansen, G. A. Terwilliger, and K. D. Moody. 1990. Lyme borreliosis in selected strains and ages of laboratory mice. *J Infect Dis* 162: 133–138.

14. Weis, J. J., B. A. McCracken, Y. Ma, D. Fairbairn, R. J. Roper, T. B. Morrison, J. H. Weis, J. F. Zachary, R. W. Doerge, and C. Teuscher. 1999. Identification of quantitative trait loci governing arthritis severity and humoral responses in the murine model of Lyme disease. *J Immunol* 162: 948–956.

15. Roper, R. J., J. J. Weis, B. A. McCracken, C. B. Green, Y. Ma, K. S. Weber, D. Fairbairn, R. J. Butterfield, M. R. Potter, J. F. Zachary, R. W. Doerge, and C. Teuscher. 2001. Genetic control of susceptibility to experimental Lyme arthritis is polygenic and exhibits consistent linkage to multiple loci on chromosome 5 in four independent mouse crosses. *Genes Immun* 2: 388–397.

16. Ray, A., D. Kumar, A. Shakya, C. R. Brown, J. L. Cook, and B. K. Ray. 2004. Serum amyloid A-activating factor-1 (SAF-1) transgenic mice are prone to develop a severe form of inflammation-induced arthritis. *J Immunol* 173: 4684–4691.

17. Blaho, V. a., W. J. Mitchell, and C. R. Brown. 2008. Arthritis develops but fails to resolve during inhibition of cyclooxygenase 2 in a murine model of lyme disease. *Arthritis Rheum* 58: 1485–1495.

18. Crandall, H., D. M. Dunn, Y. Ma, R. M. Wooten, J. F. Zachary, J. H. Weis, R. B. Weiss, and J. J. Weis. 2006. Gene expression profiling reveals unique pathways associated with differential severity of Lyme arthritis. *J Immunol* 177: 7930–7942.

19. Miller, J. C., Y. Ma, J. Bian, K. C. F. Sheehan, J. F. Zachary, J. H. Weis, R. D. Schreiber, and J. J. Weis. 2008. A critical role for type I IFN in arthritis development following *Borrelia burgdorferi* infection of mice. *J Immunol* 181: 8492–8503.

20. Ma, Y., J. C. Miller, H. Crandall, E. T. Larsen, D. M. Dunn, R. B. Weiss, M. Subramanian, J. H. Weis, J. F. Zachary, C. Teuscher, and J. J. Weis. 2009. Interval-specific congenic lines reveal quantitative trait loci with penetrant Lyme arthritis phenotypes on chromosomes 5, 11, and 12. *Infect Immun* 77: 3302–3311.

21. Ma, Y., K. K. C. Bramwell, R. B. Lochhead, J. K. Paquette, J. F. Zachary, J. H. Weis, and J. J. Weis. 2014. *Borrelia burgdorferi* arthritis-associated locus *Bbaa1* regulates Lyme arthritis and K/B×N serum transfer arthritis through intrinsic control of type I IFN production. *J Immunol* 193: 6050–6060.

22. Bramwell, K. K. C., Y. Ma, J. H. Weis, X. Chen, J. F. Zachary, C. Teuscher, and J. J. Weis. 2014. Lysosomal β-glucuronidase regulates Lyme and rheumatoid arthritis severity. *J Clin Invest* 124: 311–320.

23. Salazar, J. C., C. D. Pope, T. J. Sellati, H. M. Feder Jr, M. J. Caimano, J. G. Pope, P. J. Krause, and J. D. Radolf. 2003. Coevolution of markers of innate and adaptive immunity in skin and peripheral blood of patients with erythema migrans. *J Immunol* 171: 2660–2670.

24. van der Pouw Kraan, T. C. T. M., C. A. Wijbrandts, L. G. M. van Baarsen, A. E. Voskuyl, F. Rustenburg, J. M. Baggen, S. M. Ibrahim, M. Fero, B. A. C. Dijkmans, P. P. Tak, and C. L. Verweij. 2007. Rheumatoid arthritis subtypes identified by genomic profiling of peripheral blood cells: assignment of a type I interferon signature in a subpopulation of patients. *Ann Rheum Dis* 66: 1008–1014.

25. Wilson, L. E., D. Widman, S. H. Dikman, and P. D. Gorevic. 2002. Autoimmune disease complicating antiviral therapy for hepatitis C virus infection. *Semin Arthritis Rheum* 32: 163–173.

26. Vilcek, J. 2006. Fifty years of interferon research: aiming at a moving target. *Immunity* 25: 343–348.

27. Bramwell, K. K. C., J. H. Weis, C. Teuscher, and J. J. Weis. 2012. High-throughput genotyping of advanced congenic lines by high resolution melting analysis for identificaton of *Bbaa2*, a QTL controlling Lyme arthritis. *Biotechniques* 52: 183–190.

28. Barthold, S. W., D. H. Persing, A. L. Armstrong, and R. A. Peeples. 1991. Kinetics of *Borrelia burgdorferi* dissemination and evolution of disease after intradermal inoculation of mice. *Am J Pathol* 139: 263–273.

29. Brown, J. P., J. F. Zachary, C. Teuscher, J. J. Weis, and R. M. Wooten. 1999. Dual role of interleukin-10 in murine Lyme disease: regulation of arthritis severity and host defense. *Infect Immun* 67: 5142–5150.

30. Wooten, R. M., Y. Ma, R. A. Yoder, P. Jeanette, J. H. Weis, J. F. Zachary, C. J. Kirschning, and J. J. Weis. 2002. Toll-Like receptor 2 is required for innate, but not acquired, host defense to *Borrelia burgdorferi*. *J Immunol* 168: 348–355.

31. Ornstein, K., and A. G. Barbour. 2006. A reverse-transcriptase-polymerase chain reaction assay of *Borrelia burgdorferi* 16S rRNA for highly sensitive quantification of pathogen load in a vector. *Vector Borne Zootonic Dis* 6: 103–112.

32. Sheehan, K. C. F., H. M. Lazear, M. S. Diamond, and R. D. Schreiber. 2015. Selective blockade of interferon-α and -β reveals their non-redundant functions in a mouse model of west nile virus infection. *PLoS One* 10: 1–19.

33. Sheehan, K. C. F., K. S. Lai, G. P. Dunn, A. T. Bruce, M. S. Diamond, J. D. Heutel, C. Dungo-Arthur, J. A. Carrero, J. M. White, P. J. Hertzog, and R. D. Schreiber. 2006. Blocking monoclonal antibodies specific for mouse IFN-α/β receptor subunit 1 (IFNAR-1) from mice immunized by in vivo hydrodynamic transfection. *J Interf Cytokine Res* 26: 804–819.

34. Lee, S. B., J. H. Kim, D.-H. Jin, H.-J. Jin, and Y. S. Kim. 2016. Myostatin inhibitory region of fish (Paralichthys olivaceus) myostatin-1 propeptide. *Comp Biochem Physiol Part B Biochem Mol Biol* 194–195: 65–70.

35. Sonderegger, F. L., Y. Ma, H. Maylor-Hagan, J. Brewster, X. Huang, G. J. Spangrude, J. F. Zachary, J. H. Weis, and J. J. Weis. 2012. Localized production of IL-10 suppresses early inflammatory cell infiltration and subsequent development of IFN-γ− mediated Lyme arthritis. *J Immunol* 188: 1381–1393.

36. Lochhead, R. B., F. L. Sonderegger, Y. Ma, E. Brewster, D. Cornwall, H. Maylor-Hagen, J. C. Miller, J. F. Zachary, J. H. Weis, and J. J. Weis. 2012. Endothelial cells and fibroblasts amplify the arthritogenic type I IFN response in murine Lyme disease and are major sources of chemokines in *Borrelia burgdorferi*-infected joint tissue. *J Immunol* 189: 2488–2501.

37. Meerpohl, H., M. Lohmann-Matthes, and H. Fischer. 1976. Studies on the activation of mouse bone marrow-derived macrophages by the macrophage cytotoxicity factor (MCF). *Eur J Immunol* 6: 213–217.

38. Krutzik, P. O., and G. P. Nolan. 2003. Intracellular phospho-protein staining techniques for flow cytometry: monitoring single cell signaling events. *Cytometry* 55A: 61–70.

39. Miller, J. C., H. Maylor-hagen, Y. Ma, H. John, J. J. Weis, J. C. Miller, H. Maylor-hagen, Y. Ma, J. H. Weis, and J. J. Weis. 2010. The Lyme disease spirochete *Borrelia burgdorferi* utilizes multiple ligands, including RNA, for interferon regulatory factor 3-dependent induction of type I interferon-responsive genes. *Infect Immun* 78: 3144–3153.

40. Ma, Y., K. P. Seiler, K.-F. Tai, L. Yang, M. Woods, and J. J. Weis. 1994. Outer surface lipoproteins of *Borrelia burgdorferi* stimulate nitric oxide production by the cytokine-inducible pathway. *Infect Immun* 62: 3663–3671.

41. Ng, C. T., B. M. Sullivan, J. R. Teijaro, A. M. Lee, M. Welch, S. Rice, K. C. F. Sheehan, R. D. Schreiber, and M. B. A. Oldstone. 2015. Blockade of interferon beta, but not interferon alpha, signaling controls persistent viral infection. *Cell Host Microbe* 17: 653–661.

42. Bolz, D. D., R. S. Sundsbak, Y. Ma, C. J. Kirschning, J. F. Zachary, H. John, and J. J. Weis. 2004. MyD88 plays a unique role in host defense but not arthritis development in Lyme disease. *J Immunol* 173: 2003–2010.

43. Liu, N., R. R. Montgomery, S. W. Barthold, and L. K. Bockenstedt. 2004. Myeloid differentiation antigen 88 deficiency impairs pathogen clearance but does not alter inflammation in *Borrelia burgdorferi*-infected mice. *Infect Immun* 72: 3195–3203.

44. Ivashkiv, L. B., and L. T. Donlin. 2014. Regulation of type I interferon responses. *Nat Rev Immunol* 14: 36–49.

45. Dankbar, B., M. Fennen, D. Brunert, S. Hayer, S. Frank, C. Wehmeyer, D.

Beckmann, P. Paruzel, J. Bertrand, K. Redlich, C. Koers-Wunrau, A. Stratis, A. Korb-Pap, and T. Pap. 2015. Myostatin is a direct regulator of osteoclast differentiation and its inhibition reduces inflammatory joint destruction in mice. *Nat Med* 21: 1085–1090.

46. Hastey, C. J., J. Ochoa, K. J. Olsen, S. W. Barthold, and N. Baumgarth. 2014. MyD88- and TRIF-independent induction of type I interferon drives naive B cell accumulation but not loss of lymph node architecture. *Infect Immun* 82: 1548–1558.

47. Petzke, M. M., R. Iyer, A. C. Love, Z. Spieler, A. Brooks, and I. Schwartz. 2016. *Borrelia burgdorferi* induces a type I interferon response during early stages of disseminated infection in mice. *BMC Microbiol* 16: 1–13.

48. Cervantes, J. L., C. J. La Vake, B. Weinerman, S. Luu, C. O. Connell, P. H. Verardi, and J. C. Salazar. 2013. Human TLR8 is activated upon recognition of *Borrelia burgdorferi* RNA in the phagosome of human monocytes. *J Leukoc Biol* 94: 1231–1241.

49. Love, A. C., I. Schwartz, and M. M. Petzke. 2014. *Borrelia burgdorferi* RNA induces type I and III interferons via toll-like receptor 7 and contributes to production of NF-kB-dependent cytokines. *Infect Immun* 82: 2405–2416.

50. Krupna-Gaylord, M. A., D. Liveris, A. C. Love, G. P. Wormser, I. Schwartz, and M. M. Petzke. 2014. Induction of type I and type III interferons by *Borrelia burgdorferi* correlates with pathogenesis and requires linear plasmid 36. *PLoS One* 9: 1–14.

51. Petnicki-Ocwieja, T., A. S. Defrancesco, E. Chung, C. T. Darcy, R. T. Bronson, K. S. Kobayashi, and L. T. Hu. 2011. Nod2 suppresses *Borrelia burgdorferi* mediated murine Lyme arthritis and carditis through the induction of tolerance. *PLoS One* 6: 1–13.

52. Salazar, J. C., S. Duhnam-Ems, C. La Vake, A. R. Cruz, M. W. Moore, M. J. Caimano, L. Velez-Climent, J. Shupe, W. Krueger, and J. D. Radolf. 2009. Activation of human monocytes by live *Borrelia burgdorferi* generates TLR2-dependent and -independent responses which include induction of IFN-β. *PLoS Pathog* 5: 1–21.

53. Dietrich, N., S. Lienenklaus, S. Weiss, and N. O. Gekara. 2010. Murine toll-like receptor 2 activation induces type I interferon responses from endolysosomal compartments. *PLoS One* 5: 1–10.

54. Petnicki-Ocwieja, T., E. Chung, D. I. Acosta, L. T. Ramos, O. S. Shin, S. Ghosh, L. Kobzik, X. Li, and L. T. Hu. 2013. TRIF mediates toll-like receptor 2-dependent inflammatory responses to *Borrelia burgdorferi*. *Infect Immun* 81: 402–410.

55. Cervantes, J. L., S. M. Dunham-Ems, C. J. La Vake, M. M. Petzke, B. Sahay, T. J. Sellati, J. D. Radolf, and J. C. Salazar. 2011. Phagosomal signaling by *Borrelia*

burgdorferi in human monocytes involves Toll-like receptor (TLR) 2 and TLR8 cooperativity and TLR8-mediated induction of IFN-β. *Proc Natl Acad Sci USA* 108: 3683–3688.

56. Petzke, M. M., A. Brooks, M. A. Krupna, D. Mordue, and I. Schwartz. 2009. Recognition of *Borrelia burgdorferi*, the Lyme disease spirochete, by TLR7 and TLR9 induces a type I IFN response by human immune cells. *J Immunol* 183: 5279–5292.

57. Schreiber, G., and J. Piehler. 2015. The molecular basis for functional plasticity in type I interferon signaling. *Trends Immunol* 36: 139–149.

58. Schreiber, G. 2017. The molecular basis for differential type I interferons signaling. *J Biol Chem* 1–18.

59. Schneider, W. M., M. D. Chevillotte, and C. M. Rice. 2014. Interferon-stimulated genes: a complex web of host defenses. *Annu Rev Immunol* 32: 513–545.

60. Keane, T. M., L. Goodstadt, P. Danecek, M. A. White, K. Wong, B. Yalcin, A. Heger, A. Agam, G. Slater, M. Goodson, N. A. Furlotte, E. Eskin, C. Nellåker, H. Whitley, J. Cleak, D. Janowitz, P. Hernandez-Pliego, A. Edwards, T. G. Belgard, P. L. Oliver, R. E. McIntyre, A. Bhomra, J. Nicod, X. Gan, W. Yuan, L. van der Weyden, C. A. Steward, S. Balasubramaniam, J. Stalker, R. Mott, R. Durbin, I. J. Jackson, A. Czechanski, J. Afonso, G. Assuncao, L. R. Donahue, L. G. Reinholdt, B. A. Payseru, C. P. Ponting, E. Briney, J. Flint, and D. J. Adams. 2011. Mouse genomic variation and its effect on phenotypes and gene regulation. *Nature* 477: 289–294.

61. Yalcin, B., K. Wong, A. Agam, M. Goodson, T. M. Keane, X. Gan, C. Nellåker, L. Goodstadt, J. Nicod, A. Bhomra, P. Hernandez-Pliego, H. Whitley, J. Cleak, R. Dutton, D. Janowitz, R. Mott, D. J. Adams, and J. Flint. 2011. Sequence based characterization of structural variation in the mouse genome. *Nature* 477: 326–329.

62. Sharma, M., C. Mcfarlane, R. Kambadur, H. Kukreti, S. Bonala, and S. Srinivasan. 2015. Myostatin: expanding horizons. *Biochem Mol Bio Int* 67: 589–600.

63. Tang, T. T., L. Zhang, A. Bansal, M. Grynpas, and T. J. Moriarty. 2017. The Lyme disease pathogen *Borrelia burgdorferi* infects murine bone and induces trabecular bone loss. *Infect Immun* 85: 1–13.

64. Hodzic, E., S. Feng, K. J. Freet, and S. W. Barthold. 2003. *Borrelia burgdorferi* population dynamics and prototype gene expression during infection of immunocompetent and immunodeficient mice. *Infect Immun* 71: 5042–5055.

65. Hodzic, E., S. Feng, and S. W. Barthold. 2013. Assessment of transcriptional activity of *Borrelia burgdorferi* and host cytokine genes during early and late infection in a mouse model. *Vector Borne Zootonic Dis* 13: 694–711.

66. Muskardin, T. W., P. Vashisht, J. M. Dorschner, M. A. Jensen, B. S. Chrabot, M. Kern, J. R. Curtis, M. I. Danila, S. S. Co, N. Shadick, P. A. Nigrovic, E. W. St Clair, C. O. Bingham III, R. Furie, W. Robinson, M. Genovese, C. C. Striebich, J. R. O. Dell, G. M. Thiele, L. W. Moreland, M. Levesque, S. L. Bridges Jr, P. K. Gregersen, and T. B. Niewold. 2016. Increased pretreatment serum IFN-β/α ratio predicts non-response to tumour necrosis factor α inhibition in rheumatoid arthritis. *Ann Rheum Dis* 75: 1757–1762.

67. Bray, N. 2015. Targeting myostatin for direct joint defence. *Nat Rev Drug Discov* 14: 1.

Figure 3.1. mAb blocking of IFN-β suppresses *Bbaa1*-Lyme arthritis to the same extent as IFNAR1-blockade. B6.C3-*Bbaa1* mice were infected with 2 x 10^4 *B. burgdorferi* and treated with anti-IFNAR1 (MAR1-5A3), anti-IFN-α (TIF-3C5) or anti-IFN-β (HDβ-4A7) as described in *Materials and Methods* (n = 5 to 6 mice per group). (A) Arthritis was assessed 4 wk post infection, and shown for change in ankle measurement and overall lesion scores. (B) Host defense was assessed by anti-*B. burgdorferi* IgG in the serum and *B. burgdorferi 16S rRNA* transcripts in the joint. Statistical significance for ankle swelling, serum IgG, and bacterial numbers in the joint were determined by 1-way ANOVA followed by Dunnett's multiple comparison test versus isotype, and Mann-Whitney *U* test was used for overall lesion. *$p < 0.05$.

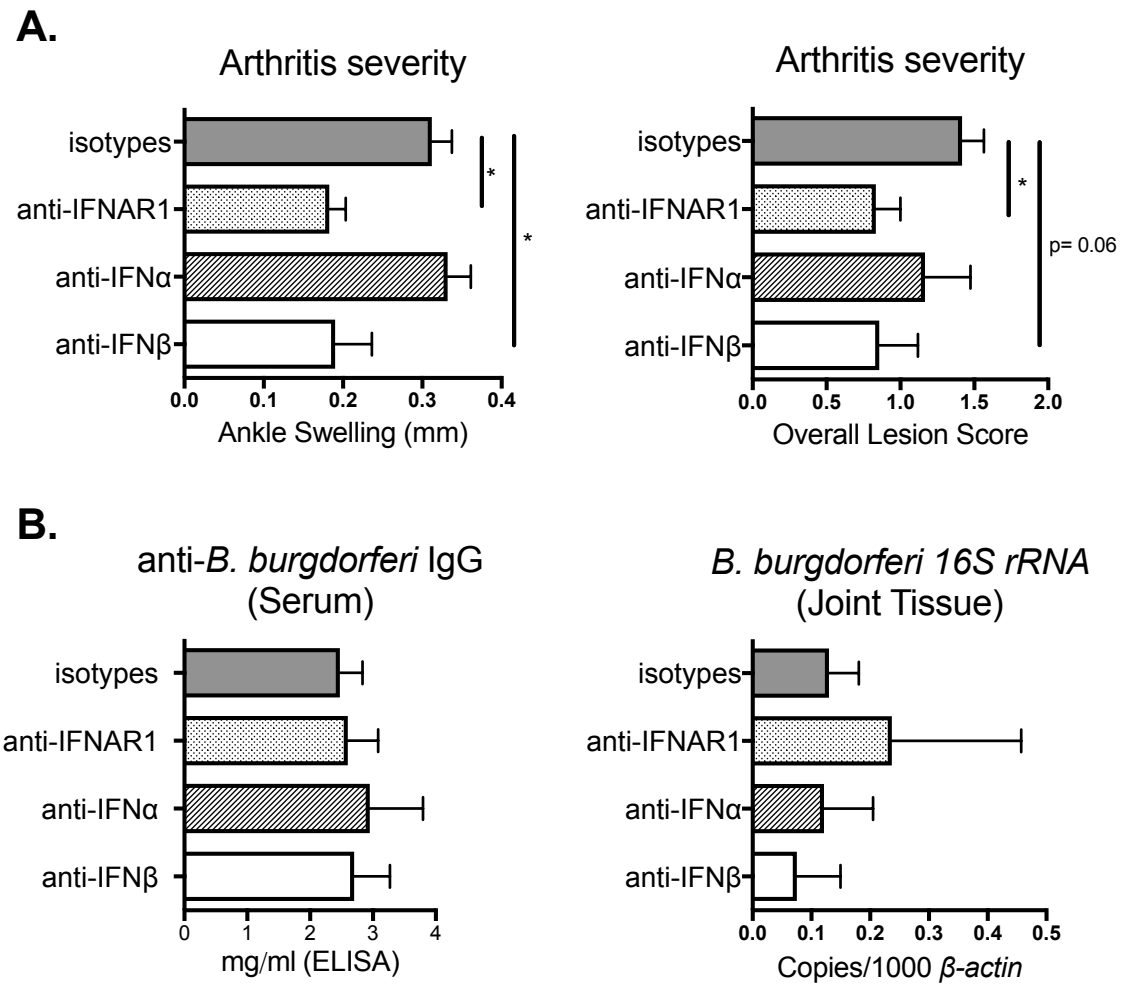
A.
Arthritis severity
isotypes
anti-IFNAR1
anti-IFNα
anti-IFNβ
*
*
0.0
0.1
0.2
0.3
0.4
Ankle Swelling (mm)
Arthritis severity
isotypes
anti-IFNAR1
anti-IFNα
anti-IFNβ
*
p= 0.06
0.0
0.5
1.0
1.5
2.0
Overall Lesion Score
B.
anti-B. burgdorferi IgG
(Serum)
isotypes
anti-IFNAR1
anti-IFNα
anti-IFNβ
0
1
2
3
4
mg/ml (ELISA)
B. burgdorferi 16S rRNA
(Joint Tissue)
isotypes
anti-IFNAR1
anti-IFNα
anti-IFNβ
0.0
0.1
0.2
0.3
0.4
0.5
Copies/1000 β-actin

Figure 3.2. IFN-β drives the type I IFN profile in B6.C3-*Bbaa1* BMDMs in response to *B. burgdorferi*. (A) qRT-PCR analysis of transcripts after 6 hr stimulation with live *B. burgdorferi* (10:1 MOI) and treatment with anti-IFNAR1, anti-IFN-α, or anti-IFN-β (10μg/ml each). Transcript levels for *Oasl2, Gbp2, Cxcl10, Tyki, Iigp,* and *Tnfa* were normalized to *β-actin*. Data are pooled from two experiments conducted on separate days ($n = 4$ per group). Significance determined by 1-way ANOVA followed by Dunnett's multiple comparison test versus media. *$p < 0.05$, **$p < 0.01$, ***$p < 0.001$, ****$p < 0.0001$. (B) Flow cytometric analysis of Stat-1 phosphorylation after 15 hr stimulation with *B. burgdorferi* and treatment with blocking antibodies. Data are representative of three independent experiments.

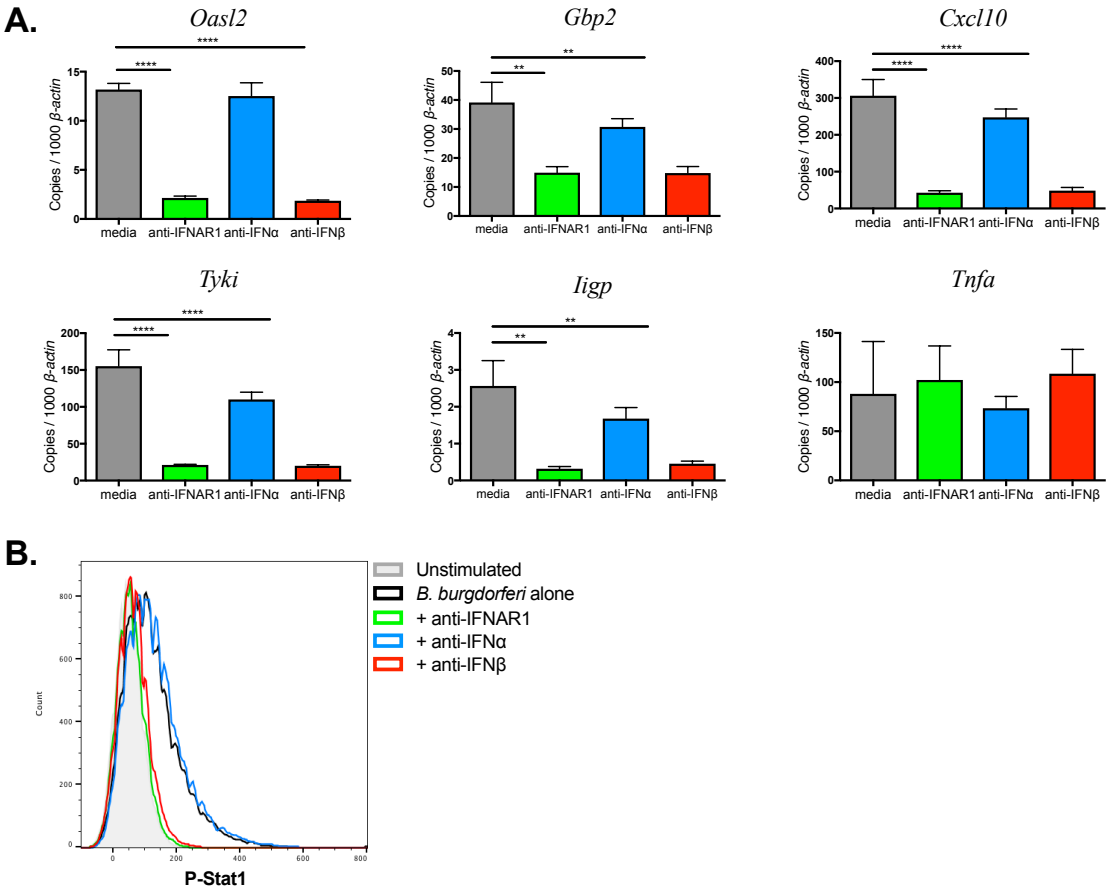
A.
Oasl2
Gbp2
Cxcl10
Tyki
Iigp
Tnfa
Copies / 1000 β-actin
media
anti-IFNAR1
anti-IFNα
anti-IFNβ
B.
Unstimulated
B. burgdorferi alone
+ anti-IFNAR1
+ anti-IFNα
+ anti-IFNβ
Count
P-Stat1

Figure 3.3. Reciprocal radiation chimeras between B6 and B6.C3-*Bbaa1* mice. (A) Experimental design: following a lethal dose of irradiation, B6 mice were reconstituted with B6.C3-*Bbaa1* splenocytes (*Bbaa1*→B6) and B6.C3-*Bbaa1* mice were reconstituted with B6 splenocytes (B6→*Bbaa1*). Autologous transplants (B6→B6 and *Bbaa1*→*Bbaa1*) were also generated for impact of myeloablative radiation. Arrows indicate direction of transplantation from donor to recipient. (B) *Bbaa1* influences arthritis severity through the radiosensitive hematopoietic lineage. Notably, *Bbaa1*→B6 mice developed the full Lyme arthritis phenotype while B6→*Bbaa1* mice were resistant. Arthritis measurements were taken 4 wk post infection with *B. burgdorferi* (n = 8 to 19 mice per group). Statistical significance was assessed between mice of the same recipient genotype by Student t test for ankle swelling and Mann-Whitney U test for overall lesion. $*p < 0.05$. (C) Model depicting the cellular "pass off" between radiosensitive myeloid ($CD45^+$) cells that initiate IFN-β in response to *B. burgdorferi* and radioresistant resident ($CD45^-$) cells that respond to IFN-β and drive arthritis development.

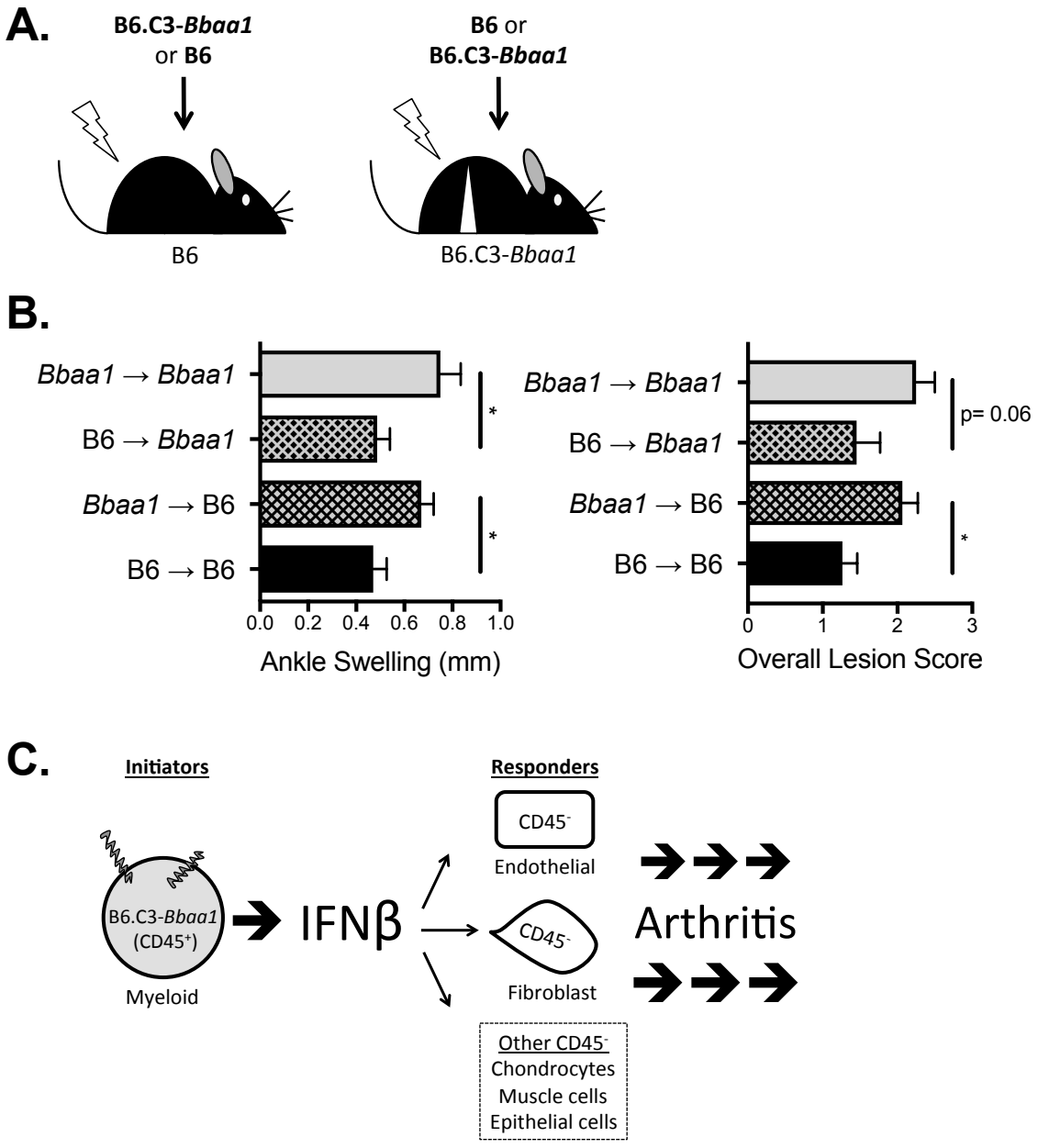
A.
B6.C3-Bbaa1 or B6
B6 or B6.C3-Bbaa1
B6
B6.C3-Bbaa1
B.
Bbaa1 → Bbaa1
B6 → Bbaa1
Bbaa1 → B6
B6 → B6
*
*
0.0 0.2 0.4 0.6 0.8 1.0
Ankle Swelling (mm)
Bbaa1 → Bbaa1
B6 → Bbaa1
Bbaa1 → B6
B6 → B6
p= 0.06
*
0 1 2 3
Overall Lesion Score
C.
Initiators
Responders
B6.C3-Bbaa1 (CD45+)
Myeloid
IFNβ
CD45-
Endothelial
CD45-
Fibroblast
Other CD45-
Chondrocytes
Muscle cells
Epithelial cells
Arthritis

Figure 3.4. Physical boundaries of *Bbaa1* congenic intervals (left) and Lyme arthritis (right) reveal that mice with C3H-derived genes spanning the type I IFN locus have increased arthritis severity compared to B6 mice. Parentheses indicate the exact interval of each congenic line, and rows represent the genetic composition across Chr4, with C3H-derived regions shaded black and B6-derived regions in white. Arthritis shown for ankle swelling measured 4 wk after *B. burgdorferi* infection (n = 10 to 35 mice per group). Significance assessed by 1-way ANOVA followed by Dunnett's multiple comparison test versus B6. *$p < 0.05$, ****$p < 0.0001$.

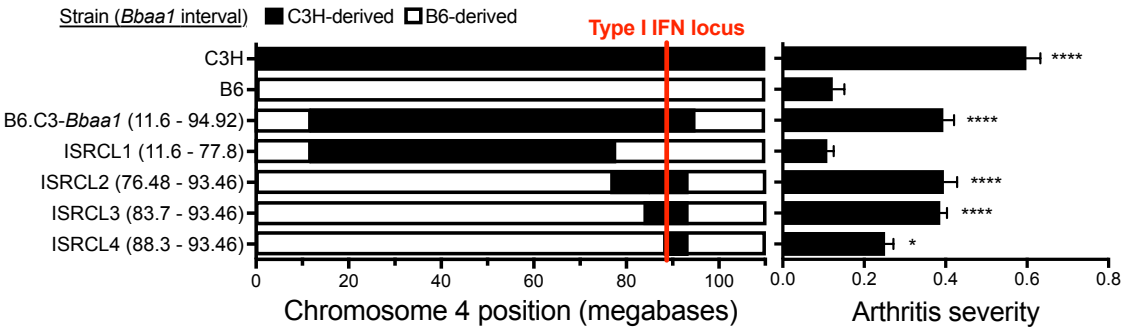
Strain (Bbaa1 interval)
C3H-derived
B6-derived
Type I IFN locus
C3H
B6
B6.C3-Bbaa1 (11.6 - 94.92)
ISRCL1 (11.6 - 77.8)
ISRCL2 (76.48 - 93.46)
ISRCL3 (83.7 - 93.46)
ISRCL4 (88.3 - 93.46)
****
****
****
****
*
0
20
40
60
80
100
0.0
0.2
0.4
0.6
0.8
Chromosome 4 position (megabases)
Arthritis severity

Figure 3.5. BMDMs reveal that *Bbaa1* genes regulating the magnitude of the IFN response to *B. burgdorferi* are retained in the genetic intervals of ISRCL3 and ISRCL4 mice. qRT-PCR analysis of transcripts in BMDMs from B6, B6.C3-*Bbaa1,* ISRCL3, ICRCL4, and C3H mice stimulated with live *B. burgdorferi* for 6 hr (n = 3 to 4 per group). Transcript levels for *Ifnb, Gbp2, Cxcl10, Iigp,* and *Tyki* were normalized to *β-actin*. Significant difference from B6 mice is shown and was determined by Student t test. *$p < 0.05$, **$p < 0.01$, ***$p < 0.001$, ****$p < 0.0001$.

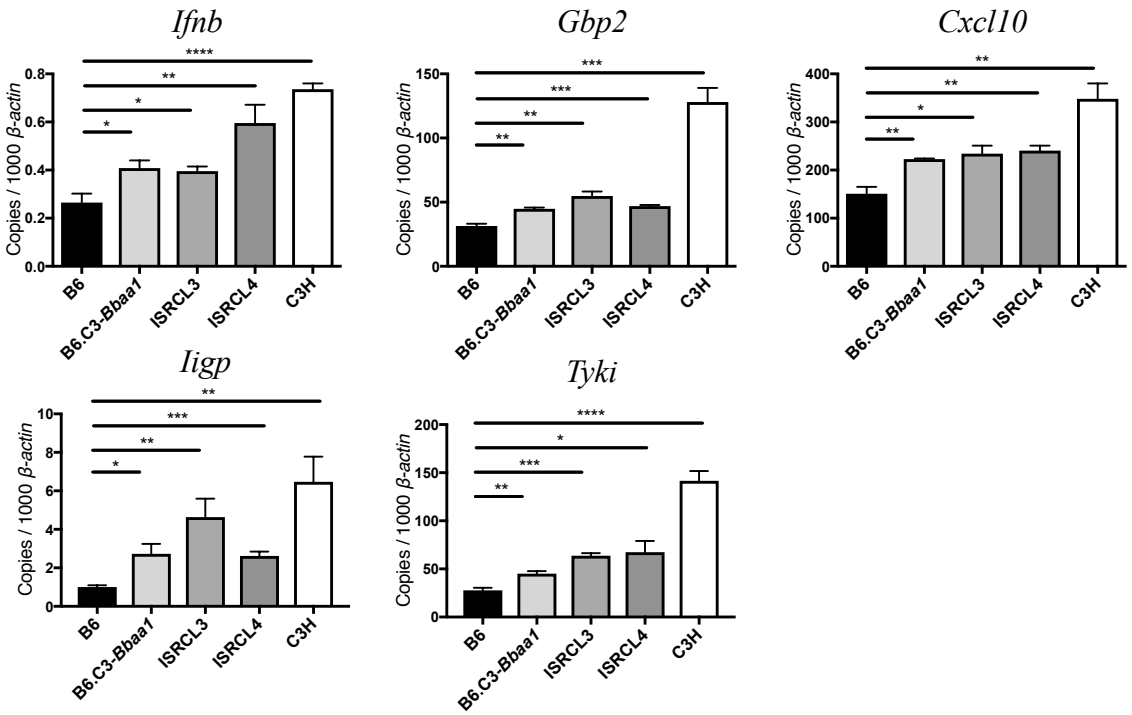
Ifnb
Gbp2
Cxcl10
Iigp
Tyki
Copies / 1000 β-actin
B6
B6.C3-Bbaa1
ISRCL3
ISRCL4
C3H

Figure 3.6. RNA-seq identification of myostatin (*Mstn*) as the strongest candidate for *Bbaa1*-directed Lyme arthritis development. (A) Volcano plot depicts $\log_2$ fold change (*x*-axis) and $-\log_{10}$ adjusted *p*-value (*y*-axis) of genes identified by ISRCL4 vs. B6 RNA-seq comparison. Single genes are plotted as dots, with those achieving significance (*p*-adj <0.05) colored black (*n* = 5 per group). Red and blue dashed lines mark 1.5-fold increase in the congenic or B6, respectively. Circled genes also had ≥1.5-fold change and *p*-adj <0.05 in the ISRCL3 vs. B6 RNA-seq comparison. (B) qRT-PCR confirmation of *Mstn* expression in $CD45^-$ cells isolated from B6, ISRCL4, and ISRCL3 mice that were infected with *B. burgdorferi* for 22 days (*n* = 5 to 6 per group). *Mstn* transcripts were normalized to β-actin and fold change relative to uninfected levels were calculated for each strain. Significance assessed by 1-way ANOVA followed by Dunnett's multiple comparison test versus B6. $^{**}p < 0.01$, $^{***}p < 0.001$

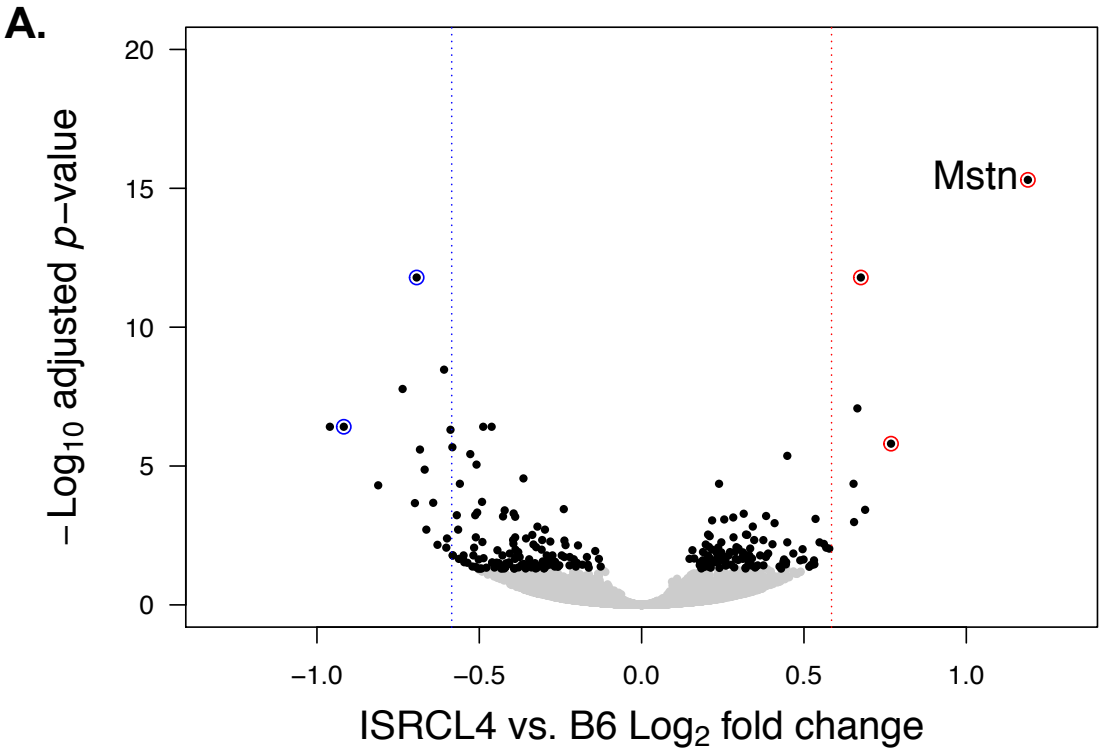
A.
20
15
10
5
0
−Log10 adjusted p−value
Mstn
−1.0
−0.5
0.0
0.5
1.0
ISRCL4 vs. B6 Log2 fold change

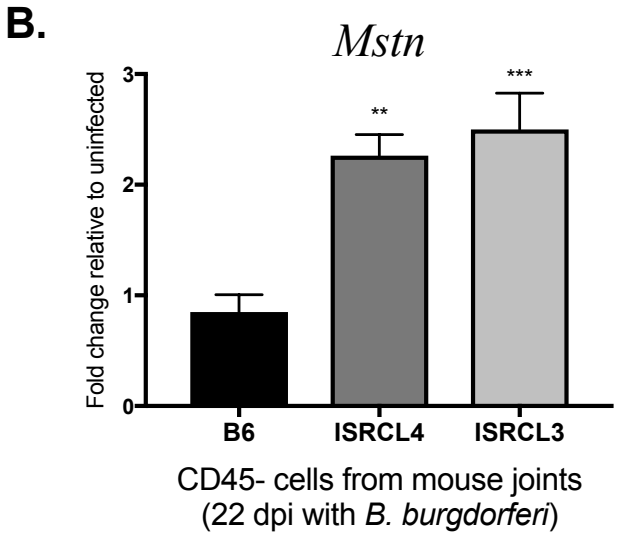
B.
Mstn
Fold change relative to uninfected
3
2
1
0
**
***
B6
ISRCL4
ISRCL3
CD45- cells from mouse joints
(22 dpi with B. burgdorferi)

Figure 3.7. IFN-β and *B. burgdorferi* are both required for the expression of myostatin by CD45$^-$ joint cells during infection and *ex vivo*. (A.) *In vivo* mAb blocking of IFN-β (600μg total) prevents transcriptional upregulation of *Mstn* in CD45$^-$ joint cells from ISRCL4 and ISRCL3 mice 22 days post infection with *B. burgdorferi* (n = 3 to 4 per group). *Mstn* transcripts were normalized to *β-actin* and fold change relative to isotype control was calculated for each strain. Significance determined by unpaired Student t test. *$p < 0.05$, **$p < 0.01$. (B.) *Ex vivo* administration of exogenous IFN-β (100U/ml) in combination with *B. burgdorferi* (10:1 MOI) for 3 hr caused transcriptional upregulation of *Mstn* in CD45$^-$ cells isolated from a naïve B6 mouse joint. Transcripts were normalized to *β-actin* and fold change was calculated relative to media control. Results are pooled data from two experiments using CD45$^-$ cells from 8 or more mice done on separate days (n = 5 wells per group). Significance determined by 1-way ANOVA followed by Dunnett's multiple comparison test versus media. *$p < 0.05$

A.

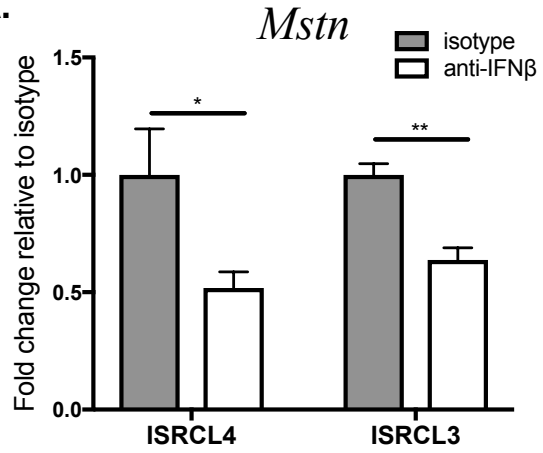

CD45- cells from mouse joints
(22 dpi with *B. burgdorferi*)

B.

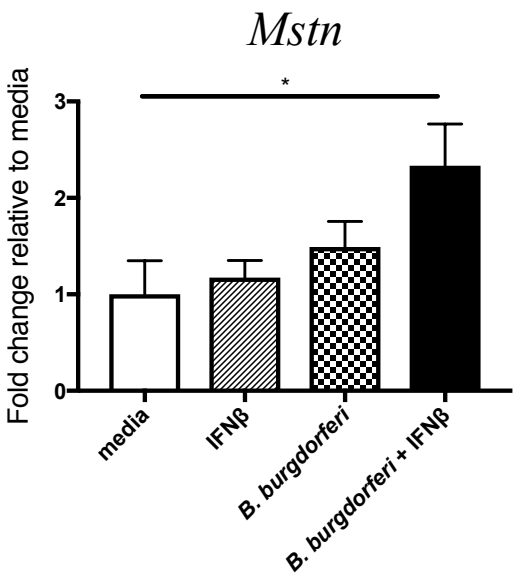

CD45- cells from naïve B6 mouse joints
stimulated *ex vivo*

Figure 3.8. Myostatin inhibition suppresses the development of Lyme arthritis in *Bbaa1* congenic mice. ISRCL4 mice were infected with 2 x 10^4 *B. burgdorferi* and treated with a myostatin inhibitor as described in *Materials and Methods* (n = 3 to 4 mice per group). Arthritis was assessed 4 wk post infection, and shown for change in ankle measurement. Significance was determined by Student t test. ***$p < 0.001$

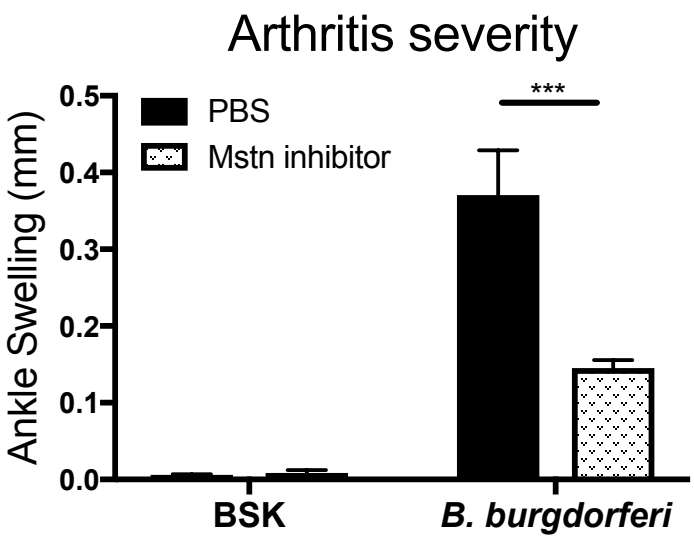
Arthritis severity
Ankle Swelling (mm)
0.5
0.4
0.3
0.2
0.1
0.0
PBS
Mstn inhibitor
***
BSK
B. burgdorferi

Figure 3.S1. Isotype control does not impact the expression of IFN-inducible genes in BMDMs. qRT-PCR analysis of transcripts 6 hr post stimulation with live *B. burgdorferi* (10:1 MOI) and treatment with anti-IFN-β or isotype control (10μg/ml each). Transcript levels for *Tyki, Oasl2, Gbp2,* and *Iigp* were normalized to *β-actin*. Significance was determined by Student *t* test comparison to isotype control. $^{**}p < 0.01$, $^{****}p < 0.0001$.

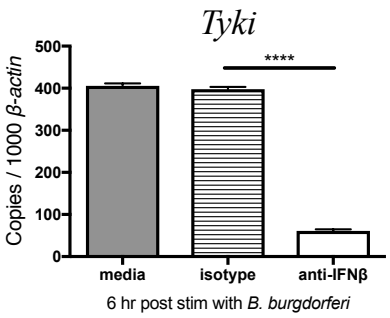
Tyki
Copies / 1000 β-actin
500
400
300
200
100
0
****
media
isotype
anti-IFNβ
6 hr post stim with B. burgdorferi

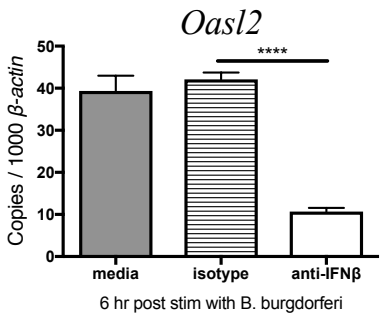
Oasl2
Copies / 1000 β-actin
50
40
30
20
10
0
****
media
isotype
anti-IFNβ
6 hr post stim with B. burgdorferi

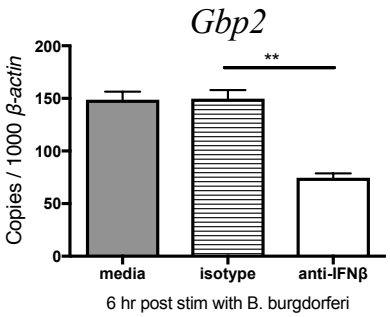
Gbp2
Copies / 1000 β-actin
200
150
100
50
0
**
media
isotype
anti-IFNβ
6 hr post stim with B. burgdorferi

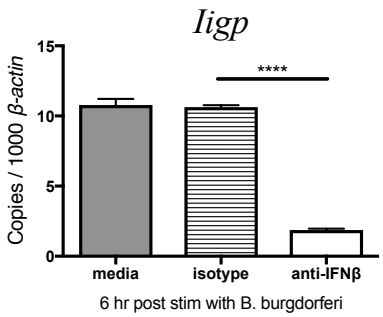
Iigp
Copies / 1000 β-actin
15
10
5
0
****
media
isotype
anti-IFNβ
6 hr post stim with B. burgdorferi

Figure 3.S2. Confirmation of anti-IFN-α functionality. Flow cytometric analysis of Stat1 phosphorylation in BMDMs 15 min post stimulation with exogenous murine IFN-αA alone (3.3ng/ml) or in combination with anti-IFN-α or anti-IFNAR1 (10μg/ml each). Exogenous IFN-αA potently induced Stat1 phosphorylation (black line), isotype control had no effect on induction (dashed line), and anti-IFN-α or anti-IFNAR1 completely blocked phosphorylation of Stat1.

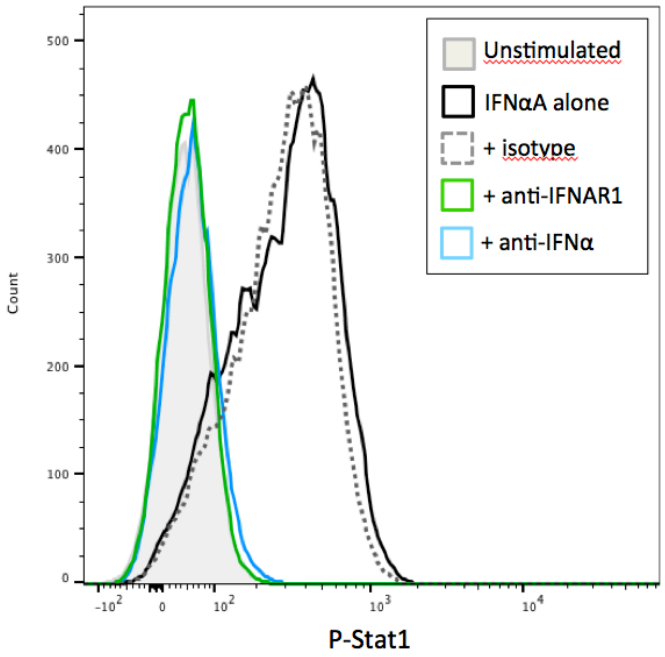
Unstimulated
IFNαA alone
+ isotype
+ anti-IFNAR1
+ anti-IFNα
Count
500
400
300
200
100
0
-10^2
0
10^2
10^3
10^4
P-Stat1

Figure 3.S3. Radiation chimera reconstitution efficiency and impact on host defense. (A) The percentages of donor-derived and recipient-derived cells in mice that were lethally irradiated and reconstituted with splenocytes, 25 days post transplant. Myeloid compartments were sufficiently reconstituted by donor-derived cells (~80%) prior to infection. B and T cells were about 50% donor-derived, but are dispensable for Lyme arthritis development. Statistical significance assessed by Student *t* test. ****$p < 0.0001$. (B) Reconstitution of irradiated mice was adequate for host defense, as measured by anti-*B. burgdorferi* IgG in the serum and *B. burgdorferi 16S rRNA* transcripts in the joint.

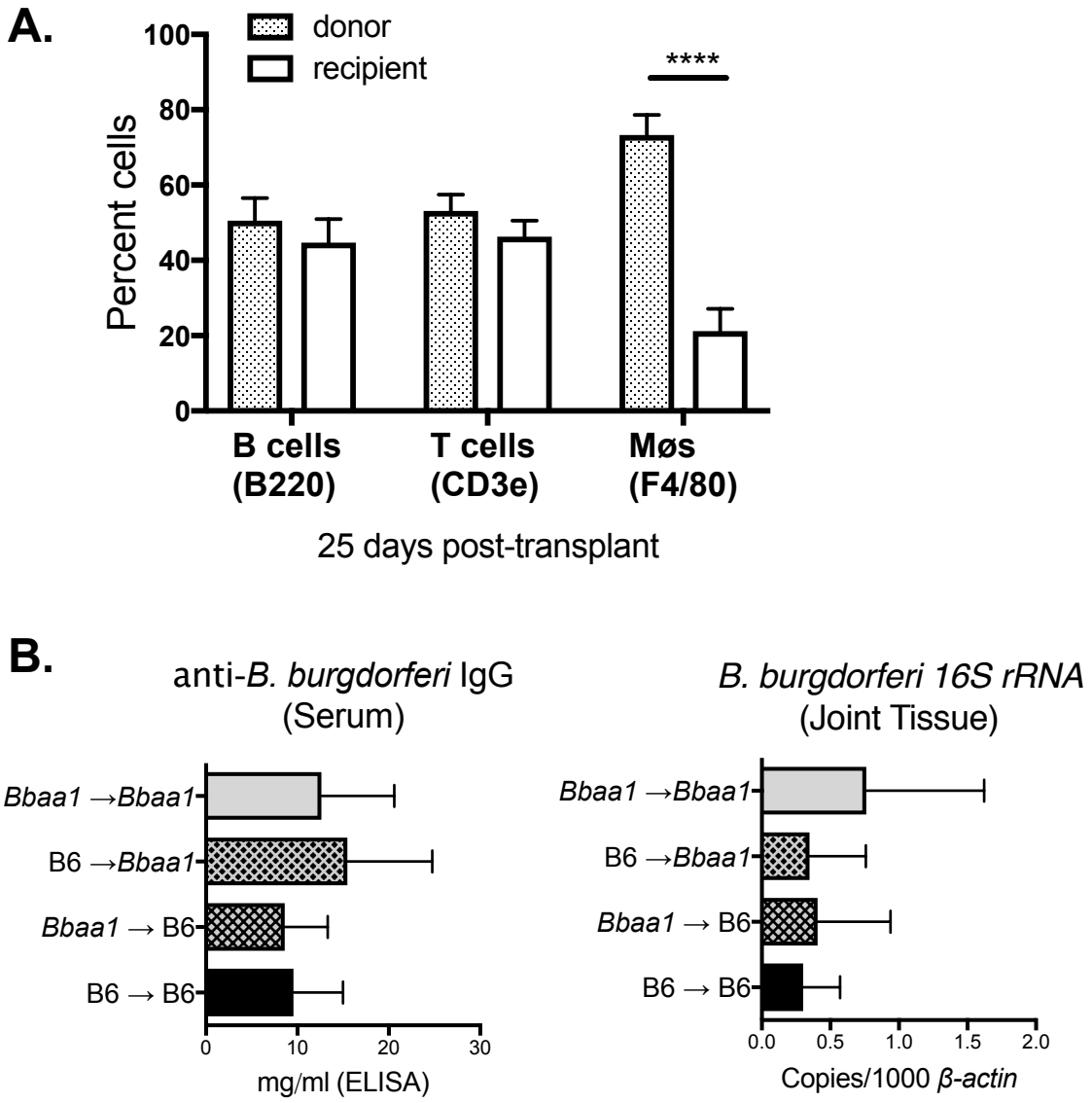
A.
donor
recipient
****
Percent cells
100
80
60
40
20
0
B cells (B220)
T cells (CD3e)
Møs (F4/80)
25 days post-transplant
B.
anti-B. burgdorferi IgG (Serum)
Bbaa1 →Bbaa1
B6 →Bbaa1
Bbaa1 → B6
B6 → B6
0
10
20
30
mg/ml (ELISA)
B. burgdorferi 16S rRNA (Joint Tissue)
Bbaa1 →Bbaa1
B6 →Bbaa1
Bbaa1 → B6
B6 → B6
0.0
0.5
1.0
1.5
2.0
Copies/1000 β-actin

Figure 3.S4. Confirmation of cell viability in CD45$^-$ cells isolated from naïve B6 mouse joint and stimulated *ex vivo*. Administration of exogenous IFN-β (100U/ml) for 3 hr caused transcriptional upregulation of IFN-inducible genes (*Tyki, Cxcl10,* and *Gbp2*), and addition of *B. burgdorferi* (10:1 MOI) for 3 hr induced expression of *Tnfa*. Transcripts were normalized to *β-actin*. Results are pooled data from two experiments using CD45$^-$ cells from 8 or more mice done on separate days (n = 5 wells per group). Significance determined by 1-way ANOVA followed by Dunnett's multiple comparison test versus media. *$p < 0.05$, **$p < 0.01$, ***$p < 0.001$, ****$p < 0.0001$.

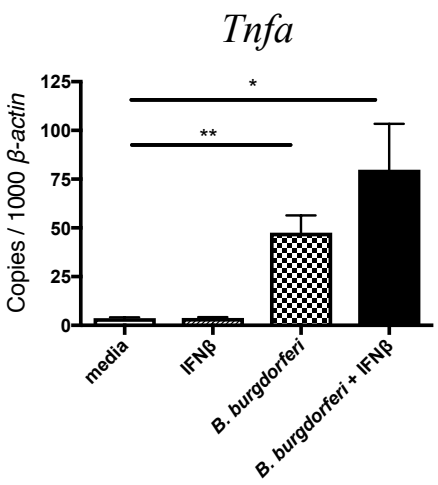
Tnfa
Copies / 1000 β-actin
125
100
75
50
25
0
*
**
media
IFNβ
B. burgdorferi
B. burgdorferi + IFNβ

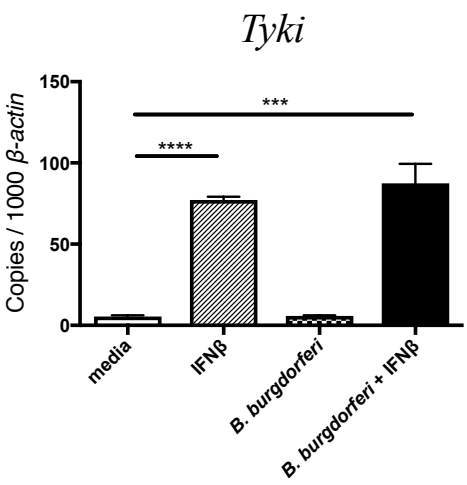
Tyki
Copies / 1000 β-actin
150
100
50
0
***
****
media
IFNβ
B. burgdorferi
B. burgdorferi + IFNβ

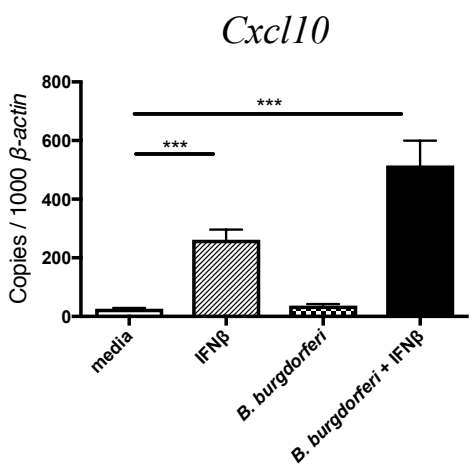
Cxcl10
Copies / 1000 β-actin
800
600
400
200
0
***
***
media
IFNβ
B. burgdorferi
B. burgdorferi + IFNβ

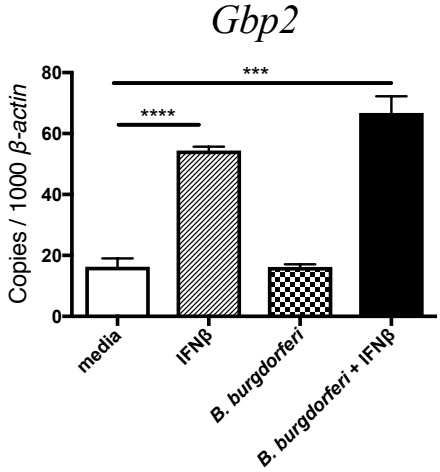
Gbp2
Copies / 1000 β-actin
80
60
40
20
0
***
****
media
IFNβ
B. burgdorferi
B. burgdorferi + IFNβ

Figure 3.S5. Volcano plot of genes identified in ISRCL3 vs. B6 RNA-seq comparisons. Plot depicts $\log_2$ fold change (*x*-axis) and $-\log_{10}$ adjusted *p*-value (*y*-axis). Single genes are plotted as dots, with those achieving significance (*p*-adj <0.05) colored black (*n* = 5 per group). Red and blue dashed lines mark 1.5-fold increase in the congenic or B6, respectively. Circled genes also had ≥1.5-fold change and *p*-adj <0.05 in the ISRCL3 vs. B6 RNA-seq comparison. Myostatin (*Mstn*) was again identified as the most highly induced gene in ISRCL3 mice.

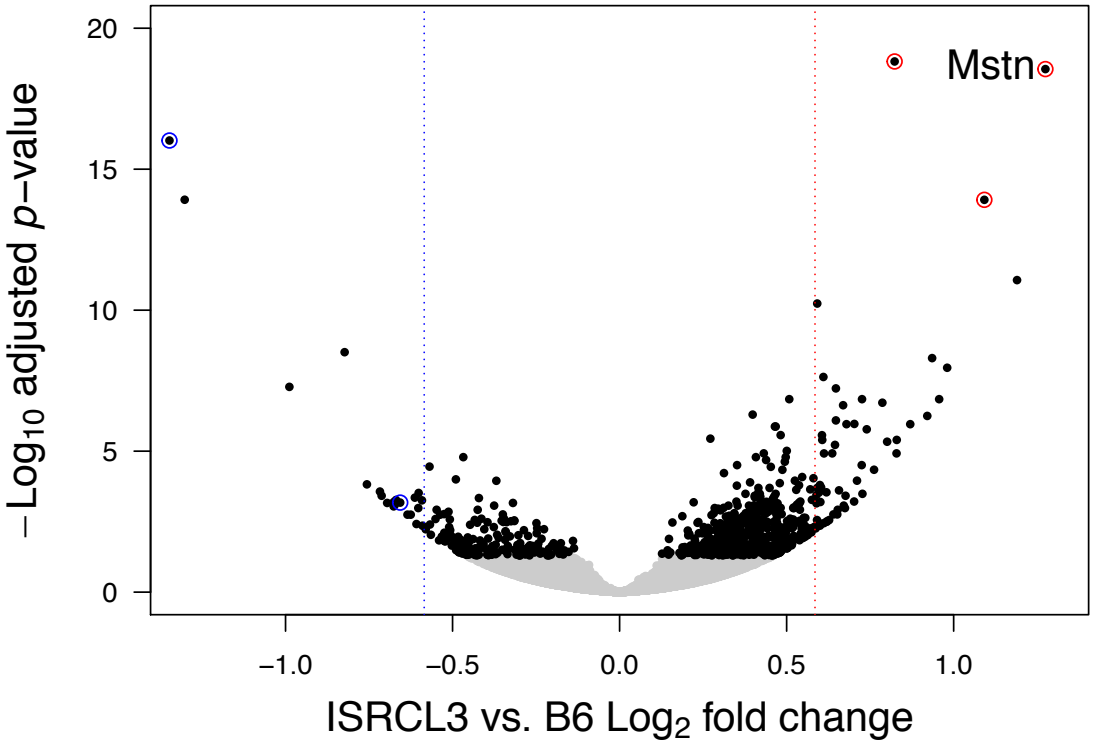
Mstn
20
15
10
5
0
−1.0
−0.5
0.0
0.5
1.0
−Log10 adjusted p−value
ISRCL3 vs. B6 Log2 fold change

CHAPTER 4

DISCUSSION

Overview

Harnessing the power of forward genetics, B6.C3-*Bbaa1* mice allowed for mechanistic interrogation of the *Bbaa1* QTL, independent from the other 5 QTL regulating Lyme arthritis severity on the C3H background (1, 2). The finding that B6.C3-*Bbaa1* mice have increased Lyme arthritis compared to B6 mice, but intermediate to C3H mice, confirmed that *Bbaa1* is one of multiple Lyme arthritis regulators, and is consistent with our previous identification of another major regulator, *Gusb* in the *Bbaa2* QTL (3). Complete suppression of Lyme arthritis in B6.C3-*Bbaa1* mice by anti-IFNAR1 mAb blockade further revealed that their intermediate phenotype is entirely due to pathologic type I IFN production, which is complementary to our previous publications showing that type I IFN drives ~50% of the arthritis phenotype in C3H mice (4, 5). Refined, interval specific recombinant congenic lines (ISRCL1-4) further supported that Lyme arthritis severity is uniquely linked to the C3H allele for the type I IFN locus, and precise treatment of B6.C3-*Bbaa1* mice with anti-IFN-α or anti-IFN-β mAbs established that IFN-β is the sole arthritis-driving factor. Thus, our *Bbaa1* congenic mouse model has provided a unique opportunity to explore all aspects of IFN-β dysregulation on a highly genetically similar B6 background.

Because *Bbaa1* intrinsically controls IFN-β production, reciprocal radiation chimeras between B6.C3-*Bbaa1* and B6 mice allowed *in vivo* identification of the cellular source of pathologic IFN-β, independent from feed-forward amplification. Previously, reciprocal radiation chimeras between C3H and C3H-IFNAR1$^{-/-}$ mice revealed that both radiation-sensitive and radiation-resistant cells in the joint contribute to the proarthritic type I IFN response (5). Now, B6 and B6.C3-*Bbaa1* mice specified that

radiation-sensitive (likely myeloid) cells initiate IFN-β, and radiation-resistant cells responding to IFN-β manifest arthritis in the joint. Identifying this segregation of roles among cell types in the joint milieu, coupled with the generation of refined congenic lines (in which the original 85 Mbp C3-*Bbaa1* locus was reduced to 10 and 5 Mbp in ISRCL3 and ISRCL4 mice, respectively), prompted us to design cell-appropriate RNA-seq experiments to better understand: the mechanism of arthritis development (wherein myostatin was identified, Chapter 3), and the mechanism of IFN-β dysregulation (wherein expressed *Bbaa1* candidates were identified, Appendix). In summary, our utility of unbiased genetic tools throughout this dissertation has allowed us to distinguish key players in *Bbaa1*-directed Lyme arthritis development from start to finish.

Possible Mechanism of IFN-β Dysregulation

It is reasonable to suggest that another gene in the 5-10 Mbp *Bbaa1* interval regulates IFN-β expression because *Ifnb* is identical between B6 and C3H mice (including the well-characterized enhanceosome (6)), and there are only two noncoding SNPs (positioned at 3,000 bps upstream and 1,000 bps downstream) within 10,000 flanking base pairs of the coding sequence (7, 8), neither of which has any connection to IFN-β regulation in the literature. Interestingly, this observation is consistent with the fact that genome-wide association studies (GWASs) and other genetic analyses for systemic lupus erythematosus (a prototypic autoimmune disease with a type I IFN signature) have never identified susceptibility polymorphisms in the actual IFN-α/β genetic sequences, but have identified many genes involved in the IFN signaling pathway (9–13). Although there is not another gene in the *Bbaa1* interval that has been linked to IFN signaling

before, novel mechanisms of IFN-β regulation are continually being discovered (14). Thus, a *Bbaa1* gene that is (1) expressed in the same (myeloid) cell type that initiates *Ifnb,* (2) expressed during or prior to *Ifnb* expression, and (3) polymorphic between B6 and C3H sequences (to explain subsequently differential *Ifnb* expression) may be responsible for this novel function.

Based on the aforementioned criteria, an unbiased RNA-seq experiment was performed, and a list of *Bbaa1* candidates was generated to serve as a starting point for future studies defining this novel mechanism (Appendix). Intriguingly, the list encompasses enzymes (which, as a broad category, are often identified in GWAS studies and majorly impact cell signaling pathways (15)), lincRNAs (which play important gene regulatory roles (16, 17), especially in myeloid cells (18–26), with *lincRNA-Cox2* exemplifying a transcriptional repressor of type I IFN signaling in resting macrophages (26)), and unannotated genes (which is consistent with this being a novel gene function). In summary, the progression of this dissertation has led to a manageable number of exciting *Bbaa1* candidates to be tested in future studies.

Investigations in *Bbaa1* Mice Will Transcend Lyme Disease

Understanding the genetic mechanism of *Bbaa1*-directed IFN-β dysregulation will be highly impactful because a number of human diseases are associated with a pathologic type I IFN signature (27–31), and *Bbaa1* mice provide a natural model for this genetic phenomenon. Although there has not yet been a GWAS for Lyme disease, GWASs for many autoimmune diseases with a type I IFN signature (including systemic lupus erythematosus, type I diabetes, rheumatoid arthritis, Sjögren's syndrome, and systemic

sclerosis) have identified common susceptibility genes (notably *Irf5* and *Ifih1*) involved in type I IFN signaling (15, 32). This highlights that shared genetic polymorphisms (especially those impacting the type I IFN pathway) can manifest as different diseases, and underscores the widespread importance of characterizing the novel *Bbaa1* susceptibility gene.

Additional similarities between our murine model of Lyme arthritis and several human autoimmune diseases further illuminate the power of our *Bbaa1* mouse tool. Specifically, type I diabetes patients display a transient but robust type I IFN profile that precedes active disease (31), similar to the kinetics we observe during Lyme arthritis development in C3H and B6.C3-*Bbaa1* mice (Crandall *et al.* (33) and Chapter 2). IFN-β also seems to be more pathologic than IFN-α in rheumatoid arthritis patients (34), similar to our finding that IFN-β is the proarthritogenic factor in B6.C3-*Bbaa1* mice (Chapter 3). And, patients with idiopathic inflammatory myopathies display a type I IFN signature (35–38) and share susceptibility genes with other autoimmune disorders (39, 40), suggesting that myostatin upregulation in B6.C3-*Bbaa1* mice (Chapter 3) occurs via a shared pathological pathway downstream of a common type I IFN trigger. In conclusion, future studies in *Bbaa1* mice will likely contribute to a global understanding of pathological processes shared among many human diseases.

References

1. Weis, J. J., B. A. McCracken, Y. Ma, D. Fairbairn, R. J. Roper, T. B. Morrison, J. H. Weis, J. F. Zachary, R. W. Doerge, and C. Teuscher. 1999. Identification of quantitative trait loci governing arthritis severity and humoral responses in the murine model of Lyme disease. *J Immunol* 162: 948–956.

2. Ma, Y., J. C. Miller, H. Crandall, E. T. Larsen, D. M. Dunn, R. B. Weiss, M.

Subramanian, J. H. Weis, J. F. Zachary, C. Teuscher, and J. J. Weis. 2009. Interval-specific congenic lines reveal quantitative trait loci with penetrant Lyme arthritis phenotypes on chromosomes 5, 11, and 12. *Infect Immun* 77: 3302–3311.

3. Bramwell, K. K. C., Y. Ma, J. H. Weis, X. Chen, J. F. Zachary, C. Teuscher, and J. J. Weis. 2014. Lysosomal β-glucuronidase regulates Lyme and rheumatoid arthritis severity. *J Clin Invest* 124: 311–320.

4. Miller, J. C., Y. Ma, J. Bian, K. C. F. Sheehan, J. F. Zachary, J. H. Weis, R. D. Schreiber, and J. J. Weis. 2008. A critical role for type I IFN in arthritis development following *Borrelia burgdorferi* infection of mice. *J Immunol* 181: 8492–8503.

5. Lochhead, R. B., F. L. Sonderegger, Y. Ma, E. Brewster, D. Cornwall, H. Maylor-Hagen, J. C. Miller, J. F. Zachary, J. H. Weis, and J. J. Weis. 2012. Endothelial cells and fibroblasts amplify the arthritogenic type I IFN response in murine Lyme disease and are major sources of chemokines in *Borrelia burgdorferi*-infected joint tissue. *J Immunol* 189: 2488–2501.

6. Panne, D., T. Maniatis, and S. C. Harrison. 2007. An atomic model of the interferon-β enhanceosome. *Cell* 129: 1111–1123.

7. Keane, T. M., L. Goodstadt, P. Danecek, M. A. White, K. Wong, B. Yalcin, A. Heger, A. Agam, G. Slater, M. Goodson, N. A. Furlotte, E. Eskin, C. Nellåker, H. Whitley, J. Cleak, D. Janowitz, P. Hernandez-Pliego, A. Edwards, T. G. Belgard, P. L. Oliver, R. E. McIntyre, A. Bhomra, J. Nicod, X. Gan, W. Yuan, L. van der Weyden, C. A. Steward, S. Balasubramaniam, J. Stalker, R. Mott, R. Durbin, I. J. Jackson, A. Czechanski, J. Afonso, G. Assuncao, L. R. Donahue, L. G. Reinholdt, B. A. Payseru, C. P. Ponting, E. Briney, J. Flint, and D. J. Adams. 2011. Mouse genomic variation and its effect on phenotypes and gene regulation. *Nature* 477: 289–294.

8. Yalcin, B., K. Wong, A. Agam, M. Goodson, T. M. Keane, X. Gan, C. Nellåker, L. Goodstadt, J. Nicod, A. Bhomra, P. Hernandez-Pliego, H. Whitley, J. Cleak, R. Dutton, D. Janowitz, R. Mott, D. J. Adams, and J. Flint. 2011. Sequence based characterization of structural variation in the mouse genome. *Nature* 477: 326–329.

9. Sigurdsson, S., G. Nordmark, H. H. H. Goring, K. Lindroos, A.-C. Wiman, G. Sturfelt, A. Jonsen, S. Rantapaa-Dahlqvist, B. Moller, J. Kere, S. Koskenmies, E. Widen, M.-L. Eloranta, H. Julkunen, H. Kristjansdottir, K. Steinsson, G. Alm, L. Ronnblom, and A.-C. Syvanen. 2005. Polymorphisms in the tyrosine kinase 2 and interferon regulatory factor 5 genes are associated with systemic lupus erythematosus. *Am J Hum Genet* 76: 528–537.

10. SLEGEN, J. B. Harley, L. A. Criswell, C. O. Jacob, R. P. Kimberly, K. L. Moser, B. P. Tsao, T. J. Vyse, and C. D. Langefeld. 2011. Genome-wide association scan in women with systemic lupus erythematosus identifies susceptibility variants in ITGAM, PXK, KIAA1542 and other loci. *Nat Genet* 40: 204–210.

11. Ramos, P. S., A. H. Williams, J. T. Ziegler, M. E. Comeau, R. T. Guy, C. J. Lessard, H. Li, J. C. Edberg, R. Zidovetzki, L. A. Criswell, P. M. Gaffney, D. C. Graham, R. R. Graham, J. A. Kelly, K. M. Kaufman, E. E. Brown, G. S. Alarco, M. A. Petri, J. D. Reveille, G. Mcgwin, L. M. Vila, R. Ramsey-goldman, C. O. Jacob, T. J. Vyse, B. P. Tsao, J. B. Harley, R. P. Kimberly, M. E. Alarco, C. D. Langefeld, and K. L. Moser. 2011. Genetic analyses of interferon pathway-related genes reveal multiple new loci associated with systemic lupus erythematosus. *Arthritis Rheum* 63: 2049–2057.

12. Deng, Y., and B. P. Tsao. 2014. Advances in lupus genetics and epigenetics. *Curr Opin Rheumatol* 26: 482–492.

13. Teruel, M., and M. E. Alarcon-Riquelme. 2016. The genetic basis of systemic lupus erythematosus: what are the risk factors and what have we learned. *J Autoimmun* 74: 161–175.

14. Chen, K., J. Liu, and X. Cao. 2017. Regulation of type I interferon signaling in immunity and inflammation: a comprehensive review. *J Autoimmun* In press: 1–11.

15. Kochi, Y. 2016. Genetics of autoimmune diseases: perspectives from genome-wide association studies. *Int Immunol* 28: 155–161.

16. Guttman, M., and J. L. Rinn. 2012. Modular regulatory principles of large non-coding RNAs. *Nature* 482: 339–346.

17. Ulitsky, I., and D. P. Bartel. 2013. lincRNAs: genomics, evolution, and mechanisms. *Cell* 154: 26–46.

18. Li, Z., T. Chao, K.-Y. Chang, N. Lin, V. S. Patil, C. Shimizu, S. R. Head, J. C. Burns, and T. M. Rana. 2014. The long noncoding RNA THRIL regulates TNF-α expression through its interaction with hnRNPL. *Proc Natl Acad Sci USA* 111: 1002–1007.

19. Chan, J., M. Atianand, Z. Jiang, S. Carpenter, D. Aiello, R. Elling, K. A. Fitzgerald, and D. R. Caffrey. 2015. Cutting edge: a natural antisense transcript, AS-IL1 α, controls inducible transcription of the proinflammatory cytokine IL-1α. *J Immunol* 195: 1359–1363.

20. Castellanos-Rubio, A., N. Fernandez-Jimenez, R. Kratchmarov, X. Luo, G. Bhagat, P. H. R. Green, R. Schneider, M. Kiledjian, J. R. Bilbao, and S. Ghosh. 2016. A long noncoding RNA associated with susceptibility to celiac disease. *Science* 352: 91–95.

21. Atianand, M. K., W. Hu, A. T. Satpathy, Y. Shen, E. P. Ricci, J. R. Alvarez-Dominguez, A. Bhatta, S. A. Schattgen, J. D. McGowan, J. Blin, J. E. Braun, P. Gandhi, M. J. Moore, H. Y. Chang, H. F. Lodish, D. R. Caffrey, and K. A. Fitzgerald. 2016. A long noncoding RNA lincRNA-EPS acts as a transcriptional brake to restrain inflammation. *Cell* 165: 1672–1685.

22. Krawczyk, M., and B. M. Emerson. 2014. p50-associated COX-2 extragenic RNA (PACER) activates COX-2 gene expression by occluding repressive NF-κB complexes. *Elife* 3: e01776.

23. Carpenter, S., and K. A. Fitzgerald. 2015. Transcription of inflammatory genes: long noncoding RNA and beyond. *J Interf Cytokine Res* 35: 79–88.

24. Elling, R., J. Chan, and K. A. Fitzgerald. 2016. Emerging role of long noncoding RNAs as regulators of innate immune cell development and inflammatory gene expression. *Eur J Immunol* 46: 504–512.

25. Atianand, M. K., D. R. Caffrey, and K. A. Fitzgerald. 2017. Immunobiology of long noncoding RNAs. *Annu Rev Immunol* 35: 177–198.

26. Carpenter, S., M. Atianand, D. Aiello, E. Ricci, P. Gandhi, L. L. Hall, M. Byron, B. Monks, M. Henry-Bezy, L. A. J. O'Neill, B. Jeanne, M. J. Moore, D. R. Caffrey, and K. A. Fitzgerald. 2013. A long noncoding RNA induced by TLRs mediates both activation and repression of immune response genes. *Science* 341: 789–792.

27. Trinchieri, G. 2010. Type I interferon: friend or foe? *J Exp Med* 207: 2053–2063.

28. Guo, X., B. W. Higgs, A. C. Bay-jensen, M. A. Karsdal, Y. Yao, L. K. Roskos, and W. I. White. 2015. Suppression of T cell activation and collagen accumulation by an anti-IFNAR1 mAb, anifrolumab, in adult patients with systemic sclerosis. *J Invest Dermatol* 135: 2402–2409.

29. Emamian, E. S., J. M. Leon, C. J. Lessard, M. Grandits, E. C. Baechler, P. M. Gaffney, and B. Segal. 2009. Peripheral blood gene expression profiling in Sjögren's syndrome. *Genes Immun* 10: 285–296.

30. Higgs, B. W., Z. Liu, B. White, W. Zhu, W. I. White, C. Morehouse, P. Brohawn, P. A. Kiener, L. Richman, D. Fiorentino, S. A. Greenberg, B. Jallal, and Y. Yao. 2011. Patients with systemic lupus erythematosus, myositis, rheumatoid arthritis and scleroderma share activation of a common type I interferon pathway. *Ann Rheum Dis* 70: 2029–2036.

31. Ferreira, R. C., H. Guo, R. M. R. Coulson, D. J. Smyth, M. L. Pekalski, O. S. Burren, A. J. Cutler, J. D. Doecke, S. Flint, E. F. Mckinney, P. A. Lyons, K. G. C. Smith, P. Achenbach, A. Beyerlein, D. B. Dunger, D. G. Clayton, L. S. Wicker, J. A. Todd, E. Bonifacio, C. Wallace, and A.-G. Ziegler. 2014. Transcriptional signature precedes autoimmunity in children genetically at risk for type 1 diabetes. *Diabetes* 63: 2538–2550.

32. Márquez, A., L. Vidal-Bralo, L. Rodríguez-Rodríguez, M. A. González-Gay, A. Balsa, I. González-Alvaro, P. Carreira, N. Ortego-Centeno, M. M. Ayala-Gutiérrez, F. J. García-Hernández, M. F. González-Escribano, J. M. Sabio, C. Tolosa, A. Suárez,

A. González, L. Padyukov, J. Worthington, T. Vyse, M. E. Alarcón-Riquelme, and J. Martín. 2017. A combined large-scale meta-analysis identifies COG6 as a novel shared risk locus for rheumatoid arthritis and systemic lupus erythematosus. *Ann Rheum Dis* 76: 286–294.

33. Crandall, H., D. M. Dunn, Y. Ma, R. M. Wooten, J. F. Zachary, J. H. Weis, R. B. Weiss, and J. J. Weis. 2006. Gene expression profiling reveals unique pathways associated with differential severity of Lyme arthritis. *J Immunol* 177: 7930–7942.

34. Muskardin, T. W., P. Vashisht, J. M. Dorschner, M. A. Jensen, B. S. Chrabot, M. Kern, J. R. Curtis, M. I. Danila, S. S. Co, N. Shadick, P. A. Nigrovic, E. W. St Clair, C. O. Bingham III, R. Furie, W. Robinson, M. Genovese, C. C. Striebich, J. R. O. Dell, G. M. Thiele, L. W. Moreland, M. Levesque, S. L. Bridges Jr, P. K. Gregersen, and T. B. Niewold. 2016. Increased pretreatment serum IFN-β/α ratio predicts non-response to tumour necrosis factor α inhibition in rheumatoid arthritis. *Ann Rheum Dis* 75: 1757–1762.

35. Niewold, T. B., S. C. Wu, M. Smith, G. A. Morgan, and L. M. Pachman. 2011. Familial aggregation of autoimmune disease in juvenile dermatomyositis. *Pediatrics* 127: 1239–1246.

36. Eloranta, M.-L., S. B. Helmers, A. Ulfgren, L. Ronnblom, G. V Alm, and I. E. Lundberg. 2007. A possible mechanism for endogenous activation of the type I interferon system in myositis patients with anti–Jo-1 or anti–Ro 52/anti–Ro 60 autoantibodies. *Arthritis Rheum* 56: 3112–3124.

37. Greenberg, S. A., J. L. Pinkus, G. S. Pinkus, T. Burleson, D. Sanoudou, R. Tawil, R. J. Barohn, D. S. Saperstein, H. R. Briemberg, M. Ericsson, P. Park, and A. A. Amato. 2005. Interferon-α/β–mediated innate immune mechanisms in dermatomyositis. *Ann Neurol* 57: 664–678.

38. Tezak, Z., E. P. Hoffman, J. L. Lutz, T. O. Fedczyna, D. Stephan, E. G. Bremer, I. Krasnoselska-Riz, A. Kumar, and L. M. Pachman. 2002. Gene expression profiling in DQA1*0501 children with untreated dermatomyositis: a novel model of pathogenesis. *J Immunol* 168: 4154–4163.

39. Ginn, L. R., J.-P. Lin, P. H. Plotz, S. J. Bale, R. L. Wilder, A. Mbauya, and F. W. Miller. 1998. Familial autoimmunity in pedigrees of idiopathic inflammaroty myopathy patients suggests common genetic risk factors for many autoimmune diseases. *Arthritis Rheum* 41: 400–405.

40. Miller, F. W., R. G. Cooper, L. G. Rider, K. Danko, L. R. Wedderburn, I. E. Lundberg, L. M. Pachman, A. M. Reed, S. R. Ytterberg, L. Padyukov, A. S. Callaghan, T. R. D. J. Radstake, D. A. Isenberg, H. Chinoy, W. E. R. Ollier, T. P. O. Hanlon, B. Peng, A. Lee, J. A. Lamb, W. Chen, C. I. Amos, P. K. Gregersen, and the Myositis Genetics Consortium. 2013. Genome-wide association study of

dermatomyositis reveals genetic overlap with other autoimmune disorders. *Arthritis Rheum* 65: 3239–3247.

APPENDIX

RNA-SEQ IDENTIFICATION OF *BBAA1* CANDIDATES THAT ARE EXPRESSED IN BONE MARROW-DERIVED MACROPHAGES FROM B6, ISRCL3, AND ISRCL4 MICE

Table A.1. RNA-seq identification of *Bbaa1* candidates that are expressed in bone marrow-derived macrophages from B6, ISRCL3, and ISRCL4 mice. An unbiased RNA-seq experiment was conducted to identify candidate *Bbaa1* genes regulating IFN-β within the ISRCL3 interval (Chr4: 83.7 – 93.46, green line) and ISRCL4 interval (Chr4: 88.3 – 93.46, yellow line) based on transcriptional activity at or prior to the peak of *Ifnb* expression. Because bone marrow-derived macrophages are an appropriate model for myeloid cells in joint tissue, macrophages from B6, ISRCL3, and ISRCL4 mice were cultured as described previously (Chapters 2 and 3, *Materials and Methods*) and stimulated with live *B. burgdorferi* for 0, 3, or 6 hr (n = 3 to 4 mice per genotype). RNA-seq libraries were prepared using a Ribo-Zero rRNA removal kit in order to retain the maximal number of both coding and noncoding RNA transcripts, and sequenced as described previously (Chapter 3, *Materials and Methods*). Shown is a list of candidate genes arranged in ascending order along Chr4. Genes with SNPs between B6 and C3H sequences are noted, and will be the subject of future investigations determining the consequence of structural changes on IFN-β regulation.

	Gene	SNPs	Gene title	Biotype	Chr4 position
1.	*Ccdc171*		coiled-coil domain containing 171	protein coding	83,525,545 - 83,864,731
2.	*Gm11415*	*	predicted gene 11415	lincRNA	83,884,738 - 83,888,858
3.	*Gm12416*		predicted gene 12416	processed pseudogene	84,104,895 - 84,105,902
4.	*Bnc2*	*	basonuclin 2	protein coding	84,275,095 - 84,675,275
5.	*Gm12421*		predicted gene 12421	processed pseudogene	84,428,818 - 84,429,124
6.	*Gm12420*		predicted gene 12420	processed pseudogene	84,697,863 - 84,698,910
7.	*Cntln*	*	centlein, centrosomal protein	protein coding	84,884,309 - 85,131,921
8.	*Rraga*	*	Ras-related GTP binding A	protein coding	86,575,668 - 86,577,281
9.	*Haus6*	*	HAUS augmin-like complex, subunit 6	protein coding	86,578,855 - 86,612,055
10.	*Scarna8*		small Cajal body-specific RNA 8	scaRNA	86,586,453 - 86,586,570
11.	*Gm12551*	*	predicted gene 12551	unprocessed pseudogene	86,627,075 - 86,631,251
12.	*Plin2*	*	perilipin 2	protein coding	86,648,386 - 86,670,060
13.	*Dennd4c*	*	DENN/MADD domain containing 4C	protein coding	86,748,555 - 86,850,603
14.	*Rps6*	*	ribosomal protein S6	protein coding	86,854,660 - 86,857,412
15.	*Acer2*	*	alkaline ceramidase 2	protein coding	86,874,396 - 86,934,822
16.	*Mllt3*	*	myeloid/lymphoid or mixed-lineage leukemia; translocated to, 3	protein coding	87,769,925 - 88,033,364
17.	*Focad*	*	focadhesin	protein coding	88,094,629 - 88,411,011
18.	*Hacd4*	*	3-hydroxyacyl-CoA dehydratase 4	protein coding	88,396,144 - 88,438,928
19.	***Ifnb1***		**interferon beta 1**	**protein coding**	**88,522,025 - 88,522,794**
20.	*Mrpl48-ps*		mitochondrial ribosomal protein L48 pseudogene	processed pseudogene	88,599,175 - 88,599,810
21.	*Klhl9*	*	kelch-like 9	protein coding	88,718,292 - 88,722,465
22.	*Mtap*	*	methylthioadenosine phosphorylase	protein coding	89,137,122 - 89,181,081
23.	*Gm12606*	*	predicted gene 12606	lincRNA	89,235,699 - 89,273,403
24.	*Cdkn2a*	*	cyclin-dependent kinase inhibitor 2A	protein coding	89,274,471 - 89,294,653
25.	*Cdkn2b*	*	cyclin-dependent kinase inhibitor 2B	protein coding	89,306,289 - 89,311,032
26.	*Gm12609*	*	predicted gene 12609	processed transcript	89,381,957 - 89,399,880
27.	*Gm12610*	*	predicted gene 12610	processed transcript	89,421,848 - 89,463,487
28.	*Gm12634*	*	predicted gene 12634	processed pseudogene	90,368,731 - 90,369,722
29.	*Gm12632*		predicted gene 12632	processed pseudogene	90,856,883 - 90,857,377
30.	*Gm12669*		predicted gene 12669	processed pseudogene	91,805,547 - 91,806,561
31.	*Gm12641*		predicted gene 12641	processed pseudogene	93,106,988 - 93,109,914
32.	*Tusc1*	*	tumor suppressor candidate 1	protein coding	93,334,138 - 93,335,511